

Biogenic synthesis of gold nanoparticles using red and green pear fruit extracts



Simone Caroline Leslie Barry

A mini-thesis submitted in partial fulfilment of the requirements for the degree

Magister Scientiae in Nanoscience

Department of Biotechnology

University of the Western Cape

Supervisor: Prof. Mervin Meyer

Co-supervisor: Dr Marlene du Preez

August 2019

ABSTRACT

Biogenic synthesis of gold nanoparticles using red and green pear fruit extracts

MSc Mini-thesis, Department of Biotechnology, University of the Western Cape

S.C.L. Barry

There has been a growing interest in the design of biocompatible and environmentally affable nanoparticles (NPs) among scientists to develop novel and safe biomaterials for use in various biomedical applications. This can be obtained through the use of plant and/ or fruit-derived phytochemicals that are capable of reducing gold ions into gold nanoparticles (AuNPs). Several studies have shown that different plant and fruit extracts possess different pharmacological properties as a result of their phytochemical profile and are capable of synthesising AuNPs with potential applications in medicine. Pears possess a unique phytochemical profile and these phytochemicals vary in the different parts of the pear and allows pears to exhibit beneficial pharmacological activities such as antioxidant, antimicrobial, anticarcinogenic as well as anti-inflammatory properties. Anthocyanins are important pigments responsible for the colouration of fruits but also have multiple uses in traditional Chinese medicine. Anthocyanins are strong antioxidants and since these molecules are present in pears, they could possibly be able to reduce gold (III) chloride to form NPs. The red-coloured 'Bon Rouge' pear contains higher levels of anthocyanins in comparison to the green-coloured 'Williams Bon Chretien' pear of which it is a mutant bud. A comprehensive study of the capability of the 'Williams Bon Chretien' and 'Bon Rouge' pears as the novel materials for the biogenic synthesis of AuNPs was conducted. Differences in the physicochemical properties of these AuNPs and potential biological applications based on the influence of anthocyanins and other phytochemicals within the pears were also explored. In addition, the effect of reaction temperature and extract concentration as well as kinetics as a function of time on the synthesis of AuNPs were conducted. The synthesized AuNPs were characterised for their size, polydispersity, morphology, crystallinity, active functional groups and *in vitro* stability. The antimicrobial activity was evaluated against Gram-negative and Gram-positive bacterial strains using agar well diffusion assay and cytotoxicity studies against non-cancerous human fibroblast cells (KMST-6) was performed using the WST-1 assay. In this study results showed that the extracts of the peels and flesh of both the 'Williams Bon Chretien' and 'Bon Rouge' pear acted as reducing and capping agents and were capable of reducing gold (III)

chloride to form AuNPs. Mostly spherical AuNPs, with core sizes ranging from 15-20 nm were synthesised. RP-AuNPs, GP-AuNPs, RF-AuNPs and GF-AuNPs were found to have no antimicrobial activity against the tested bacterial strains. These AuNPs also showed no toxicity towards KMST-6 cells which may suggest that these NPs are biocompatible and could be used for biological applications.

August 2019



Biogenic synthesis of gold nanoparticles using red and green pear fruit extracts

Simone Caroline Leslie Barry

KEYWORDS

Anthocyanin

Antimicrobial activity

Cytotoxicity

DLS

FTIR

Gold nanoparticles

Green flesh (GF)

Green peel (GP)

Green synthesis

HRTEM

Nanotechnology

Pear (*Pyrus communis* L.)

Phytochemicals

Red flesh (RF)

Red peel (RP)

UV-Vis Spectroscopy



DECLARATION

I declare that “Biogenic synthesis of gold nanoparticles using red and green pear fruit extracts” is my own work, that it has not been submitted for any degree or examination in any other university, and that all the sources I have used or quoted have been indicated and acknowledged by complete references.

Simone Barry

August 2019

Signed: 



UNIVERSITY *of the*
WESTERN CAPE

ACKNOWLEDGEMENTS

All honour, glory and praise to God for His strength and guidance bestowed upon me throughout this research project.

A special thanks to my mother, Delmary Barry, my greatest supporter. This achievement would not be possible without you. You've shared in all of the highs and lows of this journey. THANK YOU for being my pillar of strength and motivating me to do my best but also be the best version of myself. You're the best!

I would like to express my sincere gratitude and appreciation to my supervisor, Prof. Mervin Meyer for his dedication, commitment and support towards my completion of this degree. I would also like to thank him for his guidance and expertise throughout the study.

I extend my appreciation to my co-supervisor, Dr Marlene du Preez for her guidance, input and encouragement. Your belief in me and commitment to the success of this project has been invaluable. Thank you for keeping an open door policy.

To thank Prof. Abram Madiehe and Dr Dorcas Wusu thank you for your continuous and immediate assistance and support.

I would like to express my deepest thanks to Abdulrahman Mohammed Elbagory, my laboratory advisor and friend for his patience, guidance and mentorship. I have learnt a lot from you.

To Phumuzile Dube, you are a true inspiration. Your silent strength and 'crazy' work ethic has left me in awe. Thank you for your guidance and support and a wonderful friendship filled with laughter. To Zahra Latib, Taahirah Boltman, Vincent Fipaza and Riccarda MacDonald, I would like to express my gratitude for your wonderful friendship and support system.

To all my colleagues in the Biotechnology department, thank you for the talks, the laughs and motivation.

I would also like to express my sincere gratitude to Mrs Valencia Jamalie and Mrs Chyril Abrahams. Thank for all your encouragement, helpfulness and support.

Thank you to the National Nanoscience Teaching and training Platform and Department of Science and Technology for funding this project.

CONFERENCE CONTRIBUTION

S. Barry, M. Meyer, M.G. du Preez. Biogenic synthesis of gold nanoparticles using red and green pear fruit extracts. International Conference on Nanomaterials & Nanotechnology (ICNano-2018), Stockholm, Sweden, 9-12 October 2018, Poster presentation.



UNIVERSITY *of the*
WESTERN CAPE

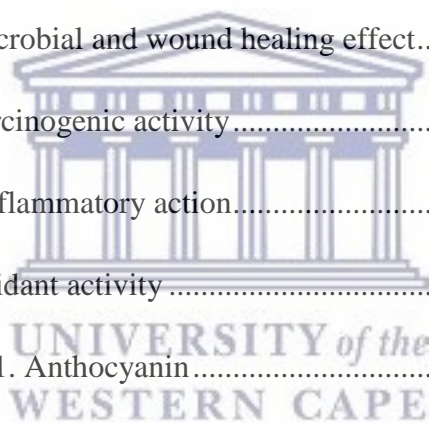
TABLE OF CONTENTS

Abstract	i
Keywords	iii
Declaration	iv
Acknowledgements	v
Conference Contribution	vi
Table of Contents	vii
List of Figures	xi
List of Tables	xiii
List of Abbreviations	xiv

Chapter 1. Literature Review

1.1 Introduction.....	1
1.2. Nanotechnology	4
1.3. Gold nanoparticles (AuNPs).....	6
1.4. Synthesis methods of AuNPs.....	9
1.4.1. Chemical synthesis of AuNPs.....	10
1.4.1.1. Turkevich method	10
1.4.1.2. Brust-Schiffrin method	10
1.4.2. Green synthesis of AuNPs	11
1.4.2.1. Green synthesis of AuNPs using microorganisms.....	13
1.4.2.2. Green synthesis of AuNPs using biomolecules	13
1.4.2.3. Green synthesis of AuNPs using plant and fruit constituents.....	14
1.5. Characterization of AuNPs	17

1.5.1. Ultraviolet Visible (UV-Vis) Spectroscopy analysis	17
1.5.2. Dynamic Light Scattering (DLS) analysis	19
1.5.3. High Resolution Transmission Electron Microscopy (HRTEM) analysis	19
1.5.4. Fourier Transform Infrared (FTIR) spectroscopy analysis	20
1.6. <i>Pyrus communis</i> Linn (<i>Pyrus communis</i> L).....	21
1.6.1. Botanical characteristics of <i>P. communis</i> L.....	21
1.6.2. Pear production in South Africa	22
1.6.3. Chemical composition of <i>P. communis</i> L	23
1.6.4. Pharmacological properties of <i>P. communis</i> L.....	24
1.6.4.1. Antimicrobial and wound healing effect.....	25
1.6.4.2. Anticarcinogenic activity	25
1.6.4.3. Anti-inflammatory action.....	26
1.6.4.4. Antioxidant activity	26
1.6.4.4.1. Anthocyanin.....	27
1.6.4.4.1.1. Pharmacological properties of anthocyanin.....	27
1.7. Research Proposal.....	30
1.7.1. Problem statement.....	30
1.7.2. Aim	30
1.7.3. Objectives of the study.....	31
1.7.4. Primary research questions	31
1.7.5. Hypothesis.....	32



Chapter 2. Materials and methods

2.1. General chemicals and suppliers	33
2.2.. Instruments and suppliers	34
2.3. Stock solutions and buffers.....	35
2.4. Bacterial strain genotype composition.....	35
2.5. Cell line, species, source and media	36
2.6. Preparation of aqueous pear extracts	36
2.7. Synthesis of pear-gold nanoparticles	36
2.7.1. Kinetics of AuNPs formation as a function of time.....	37
2.8. Characterization of pear-gold nanoparticles	37
2.8.1. Ultraviolet-Visible (UV-Vis) Spectroscopy analysis.....	37
2.8.2. Dynamic light scattering (DLS) spectroscopy and zeta potential.....	38
2.8.3. High Resolution Transmission Electron Microscopy (HRTEM) and Energy Dispersive Spectroscopy (EDS) analysis.....	38
2.8.4. Fourier Transform Infrared (FTIR) spectroscopy analysis	38
2.9. <i>In vitro</i> stability testing of pear-gold nanoparticles	39
2.10. Antimicrobial activity pear-gold nanoparticles	39
2.11. Cytotoxicity activity of pear-gold nanoparticles	39
2.12. Statistical analysis.....	40

Chapter 3. The synthesis, characterization and stability of gold nanoparticles synthesized from pear fruit extract

3.1. Introduction.....	41
3.2. Results and discussion	42

LIST OF FIGURES

Chapter 1

Figure 1.1. Applications of nanoparticles (NPs).....	1
Figure 1.2. Types of NPs.....	5
Figure 1.3. Suspension of colloidal gold.....	7
Figure 1.4. Flow diagram displaying the transition from nanotechnology towards green nanotechnology	12
Figure 1.5. Reactions involved in the green synthesis of AuNPs and their applications....	15
Figure 1.6. UV-Vis absorption spectra displaying the SPR band in AuNPs	18
Figure 1.7. DLS distribution curves of AuNPs synthesised from <i>Galenia Africana</i> and <i>Hypoxis hemerocallidea</i> displaying the hydrodynamic diameter	19
Figure 1.8. HTREM image of AuNPs.....	20
Figure 1.9. FTIR spectrum of AuNPs.....	21
Figure 1.10. Photographic images of mature pears from the “Bon Rouge’ pear tree.	22
Figure 1.11. Structure of anthocyanin.....	27

Chapter 3

Figure 3.1. Changes in the colour of the synthesis reaction, indicative of AuNP synthesis	43
Figure 3.2. Effect of temperature on the synthesis of AuNPs from pear fruit extracts at various concentrations	46
Figure 3.3. Comparative UV-Vis spectra of AuNPs synthesised	48
Figure 3.4. Dynamic Light Scattering (DLS) distribution curves of AuNPs.....	50
Figure 3.5. Changes in λ_{max} of synthesised AuNPs as a function of time	52
Figure 3.6. HRTEM images displaying AuNP morphology and sizes	54

Figure 3.7. SAED analysis of AuNPs	55
Figure 3.8. EDS spectra of AuNPs.....	56
Figure 3.9. FTIR spectra of RP, GP, RF, GF and their respective AuNPs	61
Figure 3.10. <i>In vitro</i> stability of AuNPs.....	67
Chapter 4	
Figure 4.1. Antimicrobial activity of the fruit extracts and their respective AuNPs	71
Figure 4.2. The cytotoxic effect of RP-AuNPs, GP-AuNPs, RF-AuNPs and GF-AuNPs against KMST-6 cells as determined by the WST-1 assay.	73



LIST OF TABLES

Chapter 1

Table 1.1. Phytoconstituents of <i>P. communis</i>	24
---	----

Chapter 2

Table 2.1. List of chemicals used in this study.....	33
---	----

Table 2.2. List of instrumentation used in this study	34
--	----

Table 2.3. Stock solutions and buffers prepared in this study.....	35
---	----

Table 2.4. List of bacterial strains used in this study	35
--	----

Table 2.5. Cell line(s) used in this study	35
---	----

Table 2.6. Investigates the effect of pear fruit extract concentration and temperature of AuNP synthesis	37
---	----

Table 2.7. Investigates the kinetics of AuNPs formation as a function of time	37
--	----

Chapter 3

Table 3.1. Optimum concentration (OC), λ_{max} , particle diameter (PD) and polydispersity index (PDI) of the AuNPs synthesised from RP, GP, RF and GF pear extracts at 25 °C, 70 °C and 100 °C	47
--	----

Table 3.2. DLS analysis displaying the average hydrodynamic sizes of RP-AuNPs, GP-AuNPs, RF-AuNPs and GF-AuNPs.....	51
--	----

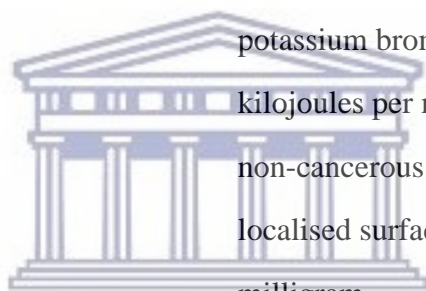
Table 3.3. Major peaks shifts in their position in the pear fruit extracts compared to their respective AuNPs. Shift values (cm ⁻¹) are given as the subtraction of the peak position in the AuNPs from the position in the extract.....	65
---	----

LIST OF ABBREVIATIONS

°C	degree celsius
λ_{\max}	lambda max
Ag	silver
AgNPs	silver nanoparticles
ANOVA	analysis of variance
ATR	attenuated total reference
Au	gold
Au ⁰	gold ions
Au ³⁺	gold atoms
AuCl ₄ ⁻	chloroauric acid
AuNPs	gold nanoparticles
BC	before Christ
BSA	bovine serum albumin
CCD	charge-coupled device
cfu	colony forming unit
cm ⁻¹	reciprocal wavelength (or wavenumber)
CMC	carboxyl methyl cellulose
CO ₂	carbon dioxide
Cu	copper
dH ₂ O	distilled water
DLS	dynamic light scattering
DMEM	Dulbecco's modified eagle medium
DMSO	dimethyl sulfoxide
DNA	deoxyribonucleic acid
EDS	energy-dispersive x-ray spectroscopy
<i>E. coli</i>	<i>Escherichia coli</i>

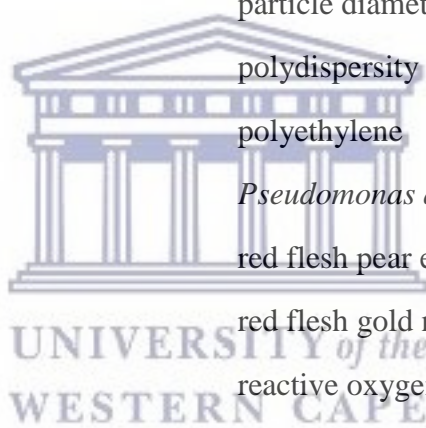


FBS	fetal bovine serum
FEG	field-emission gun
FTIR	Fourier-Transform Infrared
GF	green flesh pear extract
GF-AuNPs	green flesh gold nanoparticles
GP	green peel pear extract
GP-AuNPs	green peel gold nanoparticles
HAuCl ₄	tetrachlorauric acid
HAuCl ₄ ·3H ₂ O	tetrachloroaurate (III) dehydrate
hr(s)	hours
HRTEM	high resolution transmission electron microscopy
KBr	potassium bromide
$\text{kJ}\cdot\text{mol}^{-1}$	kilojoules per mole
KMST-6	non-cancerous human fibroblast cells
LSPR	localised surface plasmon resonance
mg	milligram
mg/kg	milligram per kilogram
mg/ml	milligram per milliliter
MHA	Mueller-Hinton agar
MHB	Mueller-Hinton broth
min(s)	minute(s)
ml	milliliters
mM	millimolar
MO	microorganisms
MRB	Max Red Bartlett
MRSA	Methicillin-resistant <i>Staphylococcus aureus</i>
NB	Nutrient broth
NIR	near-infrared



UNIVERSITY of the
WESTERN CAPE

nm	nanometer
NP(s)	nanoparticle(s)
O	oxygen
OC	optimum concentration
OCH ₃	methoxyl
OD	optical density
OT	optimum temperature
OH	hydroxyl
PBS	phosphate buffered saline
<i>P. communis</i> L.	<i>Pyrus communis</i> Linn
Pd	palladium
PD	particle diameter
PDI	polydispersity index
PEG	polyethylene
<i>P. aeruginosa</i>	<i>Pseudomonas aeruginosa</i>
RF	red flesh pear extract
RF-AuNPs	red flesh gold nanoparticles
ROS	reactive oxygen species
RP	red peel pear extract
RP-AuNPs	red peel gold nanoparticles
rpm	revolutions per minute
RPMI	Roswell Park Memorial Institute
SAED	selected area electron diffraction
<i>S. aureus</i>	<i>Staphylococcus aureus</i>
<i>S. epidermidis</i>	<i>Staphylococcus epidermidis</i>
SPR	surface plasmon resonance
Ti	titanium
TOAB	tetraoctylammonium bromide
UV-Vis	ultraviolet-visible (UV-vis)



w/v

weight by volume

WST-1

water-soluble tetrazolium-1

Zn

zinc



UNIVERSITY *of the*
WESTERN CAPE

Nanotechnology has revolutionised the field of medicine leading to the emergence of a new discipline, Nanomedicine. Due to its tremendous potential of enhancing the bioavailability of drugs with a simultaneous reduction in the toxicity and the side effects of drugs, nanomedicine has attracted the interest of scientists (Balashanmugam *et al.*, 2018). Among various metallic NPs, gold nanoparticles (AuNPs) has been extensively studied due to their unique physicochemical and optoelectronic characteristics when compared to the bulk material of the same composition as well as their ease of synthesis, characterisation and surface modification in the nanoscale range (Sett *et al.*, 2016). Manipulations of their shape and size produce unique properties, which have potential use in various diagnostic, therapeutic and other technological applications (Kumar *et al.*, 2012).

Current physical and chemical methods of AuNPs synthesis involve the use of hazardous compounds such as dimethyl formamide (DMF), hydrazine and sodium borohydride as reducing agents. These processes are energy intensive and may also require expensive equipment. These methods efficiently produce AuNPs, however downstream processing to separate them from the toxic substances is time consuming and expensive (Abdel-Raouf *et al.*, 2017; Krishnaswamy *et al.*, 2014). The employment of these harmful chemicals can limit the use of AuNPs in biomedical applications and may have environmental consequences during large scale up production (Shah *et al.*, 2014). The presence of even a small trace amount of hazardous compounds can make these AuNPs incompatible for biomedical applications (Krishnaswamy *et al.*, 2014).

Researchers in the field are turning to 'Nature' to provide inspiration for innovative and exciting methods of nanomaterial synthesis. This led to the emergence of green nanotechnology. Green nanotechnology integrates the principles of green chemistry and green engineering to produce NPs that are safer and more eco-friendly and limits the use of toxic chemicals in their synthesis protocol (Krishnaswamy *et al.*, 2014). The use of plant extracts for the synthesis of NPs has become an important feature due to the fact that most plants contain a plethora of biomolecules and phytochemicals, and are commonly available and easily accessible. Living organisms are already well-known to synthesise nanostructured composites in the form of gold (Au), silver (Ag), zinc (Zn) and titanium (Ti), palladium (Pd) and copper (Cu) NPs (Singh *et al.*, 2016). Rapid and biosynthesis methods using biological molecules have shown a greater potential for NP synthesis, however, fully understanding the involvement of biomolecules in the synthesis process is yet to be elucidated (Balashanmugam *et al.*, 2018).

Plants and their fruits contain phytochemicals that may exhibit beneficial pharmacological effects, such as anticarcinogenic, antioxidative, antimutagenic and antimicrobial activities (Öztürk *et al.*, 2015). Compounds with antioxidant activity are likely to be involved in the synthesis of NPs, since these compounds have high redox potential and are therefore capable of reducing metal ions (Mittal *et al.*, 2013). This is referred to as the biogenic synthesis of NPs. NPs produced in this way can be considered to be more biocompatible and therefore better suited for applications in biomedicine (Kumar *et al.*, 2012). Such synthesis methods are also considered more environmentally friendly. As the phytochemical constituents of plants and fruits differ, nanomaterials synthesized from different plant and fruit extracts may also vary significantly and so may the potential applications (Elbagory *et al.*, 2016)

The use of plant extracts to mediate solution phase synthesis of AuNPs through the reduction of gold ions (Au^{3+}) to gold atoms (Au^0) has gained profound significance in recent years because of the renewable and biocompatible nature of the plant extracts, eco-friendly aqueous medium and mild reaction conditions. An additional advantage of this method is that the extract itself can act as capping and stabilising agents, without requiring additional stabilisers (Barai *et al.*, 2018). This has led researchers to focus on nanotechnology-based approaches to meet environmental challenges (Das *et al.*, 2009). Even though the synthesis of AuNPs using *Aloe vera* (Chandran *et al.*, 2006), *Maduca longifolia* (Fayaz *et al.*, 2011), *Zizyphus mauritiana* (Sadeghi, 2015), mango or *Mangifera indica* (Philip, 2010), *Anacardium occidentale* (Sheny and Philip, 2011), *Magnolia kobus* and *Diopyrus kaki* leaf extracts (Song *et al.*, 2009), *Cassia auriculata* (Kumar *et al.*, 2011), *Syzygium aromaticum* (Raghunandan *et al.*, 2010) and *Terminalia chebula* (Kumar *et al.*, 2012) have been reported, the potential of other plant extracts, fruits and vegetables as reductant/surfactants for the synthesis of AuNPs is yet to be fully explored (Kumar *et al.*, 2012).

Pears are rich in minerals, nutrients and vitamins and possess phytoconstituents especially phenolics which are important bioactive compounds known for their health benefits. These health benefits are derived from the high antioxidative, anti-inflammatory, antimicrobial and anticarcinogenic properties attributed to pears. Pears have also shown to possess good wound healing properties (Kolniak-Ostek, 2016; Parle and Arzoo, 2016; Kiran *et al.*, 2018). Previous studies have shown that biogenic AuNPs can be synthesised from the golden yellow pear (*Pyrus pyrifolia*) extracts native to China, Korea and Japan. These AuNPs were stable in aqueous buffer solutions and showed biocompatibility with human embryonic kidney 293 cells with potential applications in nanobiotechnology (Ghodake *et al.*, 2010). The 'Bon Rouge'

pear, a South African ‘Williams Bon Chretien’ bud mutant, and a variety of the European pear (*Pyrus communis*) is characterised by its red skinned fruit throughout the growing season and red leaves early in the season, unlike the ‘Williams Bon Chretien’ that remains green in colour (du Preez *et al.*, 2004). The red colour is due to the presence of high levels of anthocyanins. Anthocyanins are water-soluble phenolic compounds that form part of a large and widespread group of plant flavonoids that give plants their distinctive colours but also provide health benefits as they act as strong antioxidants. Anthocyanins are widely distributed in the human diet through crops, beans, fruits, vegetables and red wine (Tsuda *et al.*, 2003). In this study, a comprehensive investigation into the ability of extracts prepared from ‘Williams Bon Chretien’ and its mutant bud ‘Bon Rouge’ as the novel material for the biogenic synthesis of environmentally safe and biocompatible AuNPs was conducted. Differences in the physicochemical properties of the AuNPs and potential biological applications based on the influence of anthocyanins and other phytochemicals within the pears were also explored.

1.2. Nanotechnology

Nanotechnology, a term derived from the Greek word *nannos*, meaning dwarf, is an interdisciplinary field that employs particles in at least one dimension in the size range of 1 to 100 nm (Adams and Barbante, 2013). These nanomaterials possess unique properties and functions as a result of their small size (Hajippour *et al.*, 2012 and Sahoo *et al.*, 2007).

A physicist and Nobel laureate, Richard Feynman envisioned the concept behind nanotechnology during the 1959 American Physical Society meeting in California in his lecture entitled “*There’s Plenty of Room at the Bottom*”. Feynman presented the principles of miniaturisation and atomic-level precision and described a process in which scientists would be able to manipulate and control individual atoms and molecules and use this as a potential tool for future innovation and development (Seigneuric *et al.*, 2010).

With advancements in nanotechnology various new nanomaterials are being produced with the objective of enhancing the properties and performance of existing systems that have been stagnant due to a lack of technological advancement (Liu, 2006; Seigneuric *et al.*, 2010). Nanomaterials can also be synthesised as composite material. The synthesis of NPs that feature an inorganic core surrounded by an organic layer has been described. The versatility of NPs in nanobiotechnology arises from the ability to tailor their shape, size and composition, which categorises them into two groups (Arvizo *et al.*, 2010). These include organic NPs (liposomes,

dendrimers and carbon nanotubes) and inorganic NPs (quantum dots, magnetic NPs, and AuNPs) as illustrated in figure 1.2 (Sanvicens and Marco, 2008).

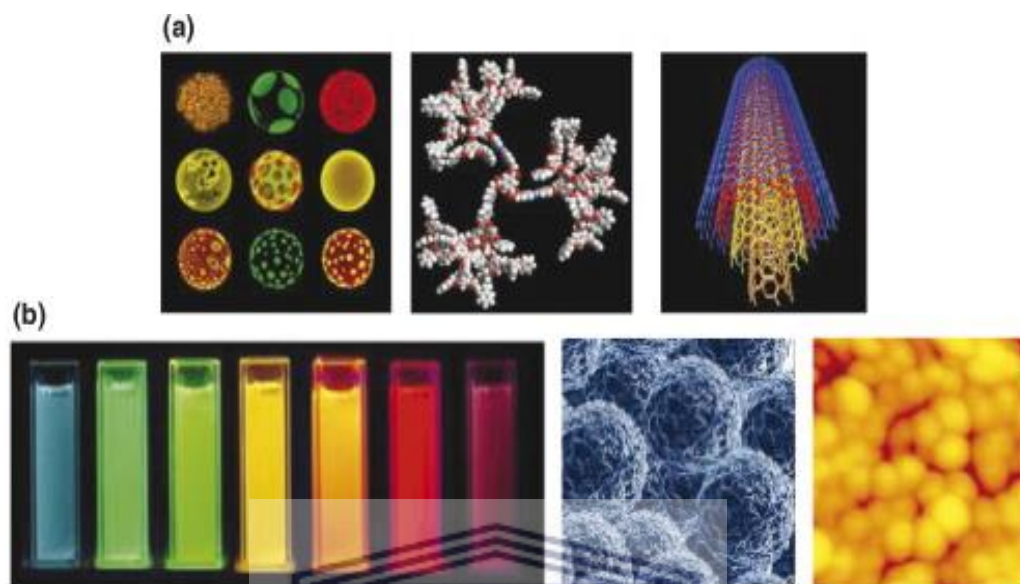


Figure 1.2. Types of NPs. (a) Organic nanoparticles – from left to right: liposomes, dendrimers and carbon nanotubes. (b) Inorganic nanoparticles – from left to right: quantum dots, magnetic nanoparticles and gold nanoparticles (Adapted from Sanvicens and Marco, 2008).

Quantum mechanics exist at the near-atomic scale at which these NPs are synthesized, allowing them to exhibit tuneable physical (magnetic, mechanical, optical and electrical), chemical (melting point and catalytic activity) or biological properties that are dramatically different from the same bulk materials and which accounts for various applications (Liu, 2006; Seigneuric *et al.*, 2010). With slight deviations in the size and shape of the NP, these properties of the NP can be radically affected. As the ratio of the surface area to volume increases, the behaviour of the surface atoms assumes dominance over those in the particle interior. Finally, the organisation of the core material determines the physical properties. (Seigneuric *et al.*, 2010)

Depending on the type of applications, NPs can span different shapes (nanotubes, nanospheres, nanorods, nanowires) and materials (semi-conductors, iron, silica, gold, oxides, polymer- or lipid-based). These characteristics confer NPs high interaction and transport capabilities, making them attractive tools for the design of imaging contrast agents, biosensors and or therapeutic carriers (Seigneuric *et al.*, 2010). For example, semiconductor quantum dots

demonstrate fluorescent properties that are useful for biological labelling and imaging, and the magnetic properties of magnetic NPs provide powerful tools for magnetic resonance induction, cell sorting, magnetic hyperthermia and drug delivery (Singh *et al.*, 2016).

In contrast to the other categories, the application of metal NPs has been an area of intense research interest in recent years because of their applications in diversified areas. These NPs are purely made of metal precursors and as a result of their well-known localised surface plasmon resonance (LSPR) characteristics, possess unique optoelectric properties. NPs of the alkali and noble metals; Cu, Ag and Au have a broad absorption band in the visible zone of the electromagnetic solar spectrum have proven to be the most flexible because of the ease in synthesis and control over shape, size, structure, composition and assembly (Shah *et al.*, 2014; Khan *et al.*, 2017). This results in the fine tunability of their optical properties which forms the basis for their growing applications in various fields like biosensors, bioremediation of radioactive wastes and functional electrical coating. As well as the synthesis of enzyme electrodes and particularly in medicine such as delivery of antigen for vaccination, gene delivery for treatment or prevention of genetic disorder. This has inspired scientists to develop environment friendly procedures for the synthesis of NPs and to avoid use of hazardous chemical, which are traditionally used (Singh *et al.*, 2011). Among the metallic NPs, AuNPs has received more global attention due to their biocompatibility and high potential use in biomedical and physicochemical fields (Noruzi, 2015).

1.3. Gold nanoparticles (AuNPs)

For many years, colloidal gold was highly regarded as the ‘elixir of life’ (Arvizo *et al.*, 2010). Since its discovery, there is no doubt that gold has possessed some value. Aside from its economic value, gold has also been regarded as a medicinal agent (Cornejo-Monroy *et al.*, 2013).

Initial data on gold was retrieved in treatises by Indian, Arabian and Chinese scientists who attempted to attain colloidal gold as early as the fourth to fifth centuries BC (Daraee *et al.*, Dykman and Khlebtsov, 2011). Liquid gold was utilised by the Indians and golden solution by the Chinese for medicinal and other functions (Daraee *et al.*, 2017). During the Middle Ages, soluble gold, a solution containing gold salt, had a reputation for its curative property for various diseases (Daniel and Astruc, 2004). Gold salts possess potent anti-inflammatory properties and have been administered to reduce pain and swelling associated with rheumatoid arthritis and tuberculosis (Shah *et al.*, 2014). Over the years, gold solutions were found to be

used across different parts of the world for treating variety of ailments such as syphilis, alcoholism, and easing suffering in cancer patients (Shah *et al.*, 2014). However, no precautionary measures were taken as to the toxic response of gold, which led to the mortality of some patients. . This initial interest in the applications of gold was further extended by colloidal gold which are sub-micrometer-sized particles of gold in a fluid (Shah *et al.*, 2014).

The beginning of modern gold colloid chemistry, and therefore the emergence of Nanoscience and Nanotechnology date back approximately 150 years with the work of Michael Faraday (Heiligtag and Niederberger, 2013). Faraday was the first to observe and publish the first scientific paper on AuNP synthesis, describing the production of colloidal gold by the reduction of chloroaurate acid (AuCl_4^-) by phosphorous in CS_2 (a two-phase system) and how the colloidal gold solutions have properties that differ from its bulk counterpart (Figure 1.3) (Jain *et al.*, 2012; Giljohann *et al.*, 2010). With advances in various analytical technologies in the 20th century, studies on AuNPs have accelerated. Advanced microscopy methods, such as atomic force microscopy and electron microscopy, have contributed the most to Nanotechnology research (Singh *et al.*, 2016).



Figure 1.3. Suspension of colloidal gold. (a) Faraday's suspension of colloidal gold prepared. (b) High resolution transmission electron microscopic image of individual colloidal gold particles prepared according to Faraday's recipe (Adapted from Das and Marsili, 2010).

Gold is a soft, malleable, transition metal found in group 1B of the periodic table with an atomic number of 197. Common oxidation states of gold metal include +1 (Au^{1+} or aurous compounds) and +3 (Au^{3+} or auric compounds) and is one of the least chemically active elements (Jain *et al.*, 2012; Shah *et al.*, 2014). However, AuNPs possess many interesting properties that make them useful for various applications, specifically biological applications. Though similar applications can also be performed with other metallic NPs, AuNPs possess several unique features such as their biocompatibility, unique physicochemical, optical and biological properties that has allowed them to emerge as a lead candidate in the field of nanotechnology (Sperling *et al.*, 2008).

AuNPs are sub-micrometer-sized particles that exist in a non-oxidized state (Au^0) and are inert to strong acids and alkalis thereby making it biocompatible and one of the least chemically reactive metals known to man (Thakor *et al.*, 2011 and Jain *et al.*, 2012). Thus far, AuNPs has shown no indication of Au particle corrosion and can be easily synthesised and tailored to a desired size from 0.8 to 200 nm. They are colloiddally stable, have low toxicity and they can be easily modified to impart various functionalities and can be readily conjugated with biological molecules without altering the biological activity of the conjugated species (Sperling *et al.*, 2008; Noruzi, 2015). AuNPs possess a surface charge that facilitates their physicochemical stability and further implementation in the cellular process and bioaccumulation. As many previous studies have shown, the level of toxicity assigned to AuNPs is greatly dependent on the particle surface charge which plays a critical role during the fabrication process of nanosystems with potential applications in controlled and targeted drug therapy. AuNPs possess attractive potential for engineering novel nanostructured tools for selective tumour targeting and imaging, emphasising thus their tremendous potential in unconventional cancer diagnosis and treatment (Sengani *et al.*, 2017). As a result of the size-dependent quantum confinement behaviour of metallic NPs, the surface of AuNPs exhibit a peculiar surface plasmon resonance (SPR) phenomenon causing a strong extinction of radiation light wavelength. This unique optical feature present in AuNPs that behaves differently in the bulk material is conferred by the collective oscillation of free conduction electrons within the metal after the interaction with the concerned electromagnetic field. This results in novel nanosystems for unusual challenging optical-related applications (Sperling *et al.*, 2008).

Depending on the particle shape, size, and structure, AuNPs can be visualised with different methods and sensors based on changes of the plasmon resonance (Dykman and Khlebtsov, 2011). The size of the AuNPs is an important aspect towards the development of performing

nanogold-related systems since it is responsible for their bioaccumulation, bioavailability and toxicity in a biological system. AuNPs are considered as one of the most convenient carrier systems, given their enhanced biocompatibility, stability and oxidation resistance. AuNPs has been applied for specific drug delivery carriers, such as doxorubicin, methotrexate and paclitaxel. Thus, colloidal gold is applicable in various medical-related research fields, including biosensing, and bio-detection, catalysis and bioelectronics, drug delivery carriers and macromolecular carriers, bioimaging and photo-hyperthermia (Sengani *et al.*, 2017). AuNPs has also been used for genetic disease detection, tumour detection, angiogenesis, photothermal therapy and photoimaging (Singh *et al.*, 2016). AuNPs also act as radiosensitizer to avoid collateral damage induced by the use of radiotherapy. AuNPs has also been defined as theranostic tools, which combines therapeutic and diagnostic actions. With this nanomedicine strategy, AuNPs are designed to target tumour cells and minimize side effects to enhance conventional therapies or to develop new diagnostic and therapeutic devices (Massard *et al.*, 2018). Different types of AuNPs are already used in many industries, such as medicine and electronics (Jain *et al.*, 2014).

1.4. Synthesis methods of AuNPs

After several decades of intense research effort, it is apparent that a larger number of synthesis approaches to produce a great variety of NPs are available (Heiligtag and Niederberger, 2013). NPs can be fabricated by one of two approaches: top-down or bottom-up approach (Mittal *et al.*, 2013; Shah *et al.*, 2014). The top-down approach involves the breakdown of a bulk material into nanoscale size material without altering the elemental composition of the bulk material. These methods include electron beam lithography and photolithography. The bottom-up approach however, fabricates NPs by collecting, consolidating and fusing individual atoms and molecules to nano-sized particles. Examples of bottom up methods include: nanosphere lithography, electrochemical, sonochemical, chemical, templating, photochemical and thermal reduction techniques. Both these approaches can be used to synthesise AuNPs of various shapes and sizes however, the different approach has some disadvantages such as excessive waste production in the top-down approach and poor monodispersity in the bottom-up approach (Shah *et al.*, 2014)

NP synthesis involves a two-stage process: nucleation and growth (Thanh *et al.*, 2014). Nucleation and growth would ideally be separated in time to achieve a narrow size distribution and possible shape distribution of the produced NPs (Jana *et al.*, 2001). For the reduction of

metal salts to metallic NP, the metal atoms and clusters formed at the initial stages of the reaction have short lifetimes and are extremely reactive.

Based on a studies conducted by Belloni (Belloni, 1996) and Henglein (Henglein 1989 and 1993), it has been established that the redox potentials of coordination compounds containing single metal ions are very negative, and with cluster nuclearity they approach their bulk electrode values. Due to this size dependent redox property, often the chemical reduction of a metal salt is dependent on the conditions of the reaction, as well as the nature of the reaction vessel. This may be the reason that induction periods and anticatalytic reduction kinetics in metal salts reductions are observed (Jana *et al.*, 2001)

1.4.1. Chemical synthesis of AuNPs

Chemical methods are the most popular approach for the production of metallic NPs (Ghodake *et al.*, 2010). Several methods, which include the Turkevich method, Brust-Schiffrin method and numerous green synthesis methods have been described.

1.4.1.1. Turkevich method

The first published method for synthesising colloidal gold was the Turkevich method introduced in 1951 by Turkevich and colleagues and became one of the most commonly used methods for the synthesis of spherical AuNPs in the size range of 10-20 nm (Turkevich *et al.*, 1951). The method employs the citrate reduction of an auric compound or metal salt (tetrachloroauric acid (HAuCl_4)) to yield the non-oxidized state of gold (Au^0) (Jain *et al.*, 2012). The synthesized AuNPs can be further stabilised by various stabilising or capping agents. Several modifications had been made to the original method, which allowed researchers to increase the particle size range. By altering various parameters within the synthesis process, AuNPs of different shapes, sizes and stability can be produced (Shah *et al.*, 2014).

1.4.1.2. Brust-Schiffrin method

The Brust-Schiffrin method, another method used for the synthesis of AuNPs was devised in 1994. This is a two-phase process that employs the transfer of gold salt from an aqueous solution to an organic solvent (such as toluene) by means of transfer agent, tetraoctylammonium bromide (TOAB) (Jain *et al.*, 2012). In the second phase, Au is reduced by sodium borohydride with dodecainethiol as the supplementary agent. The reduction process results in a colour

change of the reaction from orange to brown and the production of 1.5-5.2 nm AuNPs (Giersig and Mulvaney, 1993).

In addition to the aforementioned methods, a multitude of AuNP synthesis methods exists to create stable, monodisperse AuNPs that are commercially available for research purposes (Qureyshi *et al.*, 2016). However, with chemical synthesis of AuNPs, expensive, non-biodegradable toxic reducing and stabilizing agents (sodium dodecyl sulfate, sodium borohydride and sodium citrate) are generally used, that are not the best of choices and poses as a threat to biological systems and the environment (Ghodake *et al.*, 2010; Phull *et al.*, 2016). In such procedures, traces of these reagents remains nonreactive and free in the reaction mixture, which have the potential of entering the environment leading to environmental pollution. These toxic reagents also make it difficult for applications in medicine and biology. To circumvent such concerns, alternative formulations were developed to prepare benign and environmentally friendly AuNPs, which have resulted in the exploration and inception of green nanotechnology (Noruzi, 2015).

1.4.2. Green synthesis of AuNPs

Green nanotechnology integrates the principle of green chemistry and green engineering (figure 1.4) with a strong focus on the synthesis of chemical compounds and chemical engineering processes in industrial applications based on natural materials, thus minimising the application of hazardous materials during reaction and synthesis (Krishnaswamy *et al.*, 2014; Jahangirian *et al.*, 2017). Green nanotechnology is based on designing nanoscale products, enhance nanomaterial production and importantly to evaluate the toxicity of nanomaterials by using rapidly biodegradable reagents, limiting waste products, synthesis at ambient pressure and temperature, and low toxicity of chemical products (Ghodake *et al.*, 2010; Shah *et al.*, 2014).

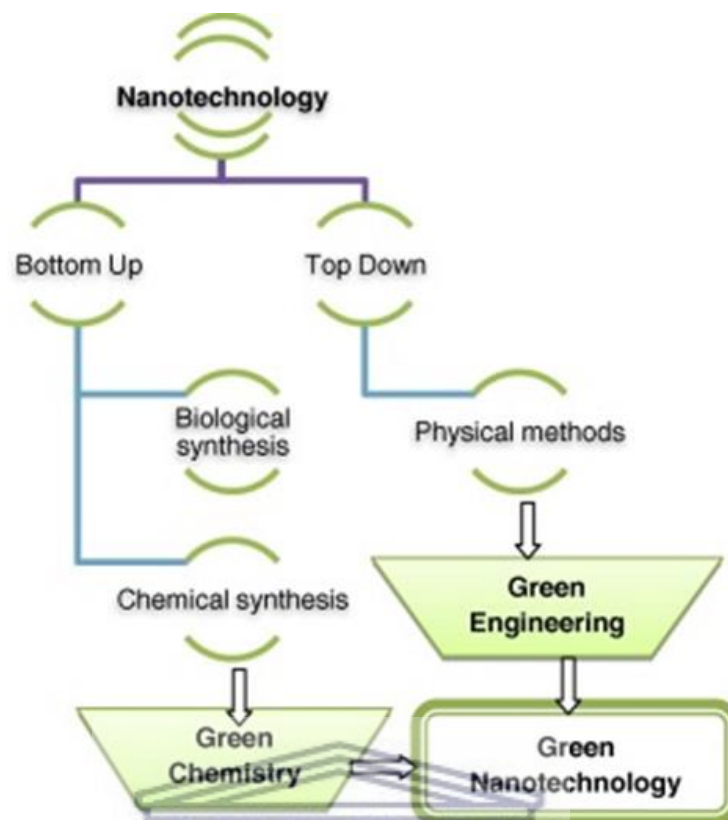


Figure 1.4. Flow diagram displaying the transition from nanotechnology towards green nanotechnology (Adapted by Krishnaswamy *et al.*, 2014).

Green chemical methods are based on the use of pure chemical reagents, which are environmentally friendly. Most of these methods employ the use of natural compounds such as starch, glucose, chitosan, and sucrose and calcium alginate as reducing and/or capping agents. Nontoxic and biodegradable polymers such as polyethylene (PEG) and carboxyl methyl cellulose (CMC) have also been incorporated for the green synthesis of metallic NPs. The NPs produced by these methods are generally spherical (Noruzi, 2015).

The size and shape of AuNPs can be controlled by the use of proper reduction and agitation methods and the choice of suitable types of protecting agents and concentration, as well as synthesis conditions, that is, pH, concentration of reductive biomass, temperature, time and the use of alternative energy sources such as ultrasound and UV light (Sengani *et al.*, 2017). These considerations have resulted in numerous publications suggesting new synthesis routes of AuNPs in which green chemical reduction processes are used. Most of the reducing and capping agents used in these reactions were obtained from plants, bacteria, fungi and algae (Elia *et al.*, 2014).

1.4.2.1. Green synthesis of AuNPs using microorganisms

Microorganisms (MOs) have been shown to be important nanofactories that hold immense potential as eco-friendly and cost-effective tools, avoiding toxic, harsh chemicals and the high energy demand required for physiochemical synthesis. MOs have the ability to accumulate and detoxify heavy metals due to various reductase enzymes, which are able to reduce metal salts to metal NPs with a narrow size distribution and therefore, less polydispersity. Over the past few years, MOs, including yeast, fungi and bacteria (such as actinomycetes) have been studied intra- and extracellularly for the synthesis of metal NPs. An array of biological protocols for NP synthesis has been reported using bacterial biomass, supernatant and derive components. Moreover, metal-resistant proteins, genes, enzymes, peptides, reducing cofactors, and organic materials have significant roles by acting as reducing agents. Furthermore, these help in providing natural capping to synthesise NPs, thereby preventing the aggregation of NPs and helping them to remain stable for a long time, thus providing additional stability. In recent research, bacteria, including, *Bacillus licheniformis*, *Bacillus methylotrophicus*, *Pseudomonas deceptionensis*, *Bhargavaea indica* and *weissella oryzae*, have been explored for AgNPs and AuNPs (Singh *et al.*, 2016). These investigations suggest that the main mechanism of the synthesis of NPs using bacteria depends on enzymes; for instance, the nitrate reductase enzyme was found to be responsible for AgNP synthesis in *B. licheniformis*. When it comes to the synthesis of AuNPs with bacteria, initially *Bacillus subtilis* 168 was used to reduce Au³⁺ ions and octahedral AuNPs were produced having dimensions (5 – 25 nm) within bacterial cells by incubation of gold chloride (Beveridge and Murray, 1980). Reduction of Au³⁺ ions by Fe (III)-reducing bacteria *Shewanella algae* was also reported, which results in the formation of AuNPs with 10 – 20 nm in diameter (Konishi *et al.*, 2004).

1.4.2.2. Green synthesis of AuNPs using biomolecules

Molecules produced by living organisms to catalyse biological functions of the body are known as biomolecules. Biomolecules include nucleic acids, amino acids, lipids and carbohydrates. These molecules possess hydroxyl and carbonyl functional groups which can reduce Au³⁺ ions to Au⁰ neutral atoms. Au⁰ are then capped to form stabilised AuNPs. This method can overcome the problem of biosafety of the reactants used for the synthesis of AuNPs (Shah *et al.*, 2014).

1.4.2.3. Green synthesis of AuNPs plant and fruit constituents

Plants have proven to be excellent candidates for the biosynthesis of AuNPs in a reliable and biofriendly way. There are many articles that report on the biosynthesis of AuNPs using different plants and plant extracts. Some of the benefits of using plant or plant extracts in comparison with microbial synthesis of AuNPs include the use of nontoxic biocomponents as sources of reducing and capping agents for the synthesis of AuNPs; limitation of waste formation and cutting down the need for extra purification steps and time consuming maintenance of microbial cell cultures (Ghodake *et al.*, 2010; Shah *et al.*, 2014; Phull *et al.*, 2016; Pérez *et al.*, 2017; Sengani *et al.*, 2017). Other benefits include increased biocompatibility, simplicity, affordability, easy and cost effective scalability, are environmental friendly, and furthermore, there are no need to use high energy and toxic chemicals are relatively safer to work with and the opportunity to produce massive amounts of NPs at a large industrial scale (Singh *et al.*, 2011).

The plant-mediated synthesis process of AuNPs consists in revaluing the polyphenol-based secondary metabolites such as flavonoids, quinones and phytosterols from plants as efficient reducing agents for metallic precursors. It has been proposed that amino acids, proteins, vitamins organic acid as well as secondary metabolites, such as polyphenols, alkaloids, flavonoids, heterocyclic compounds, terpenoids and polysaccharides, play significant roles in metal salt reduction and furthermore, act as stabilising and capping agents for synthesised NPs.

The identified hydroxyl groups within the plants-derived polyphenols were found to be successfully involved in gold ions reducing process, by encouraging the oxidation reaction and the specific formation of quinone forms as illustrated in [Figure 1.5](#) (Sengani *et al.*, 2017). Shape and size optimisation is possible by adjusting the extract concentration, ion concentration, pH, temperature or quantity. The reaction rate of NP production is dependent on the type of plant and quantity. Recent trends in biosynthesis of NPs include the production of monodispersed particles and pure morphologies (Shah *et al.*, 2014; Sett *et al.*, 2016).

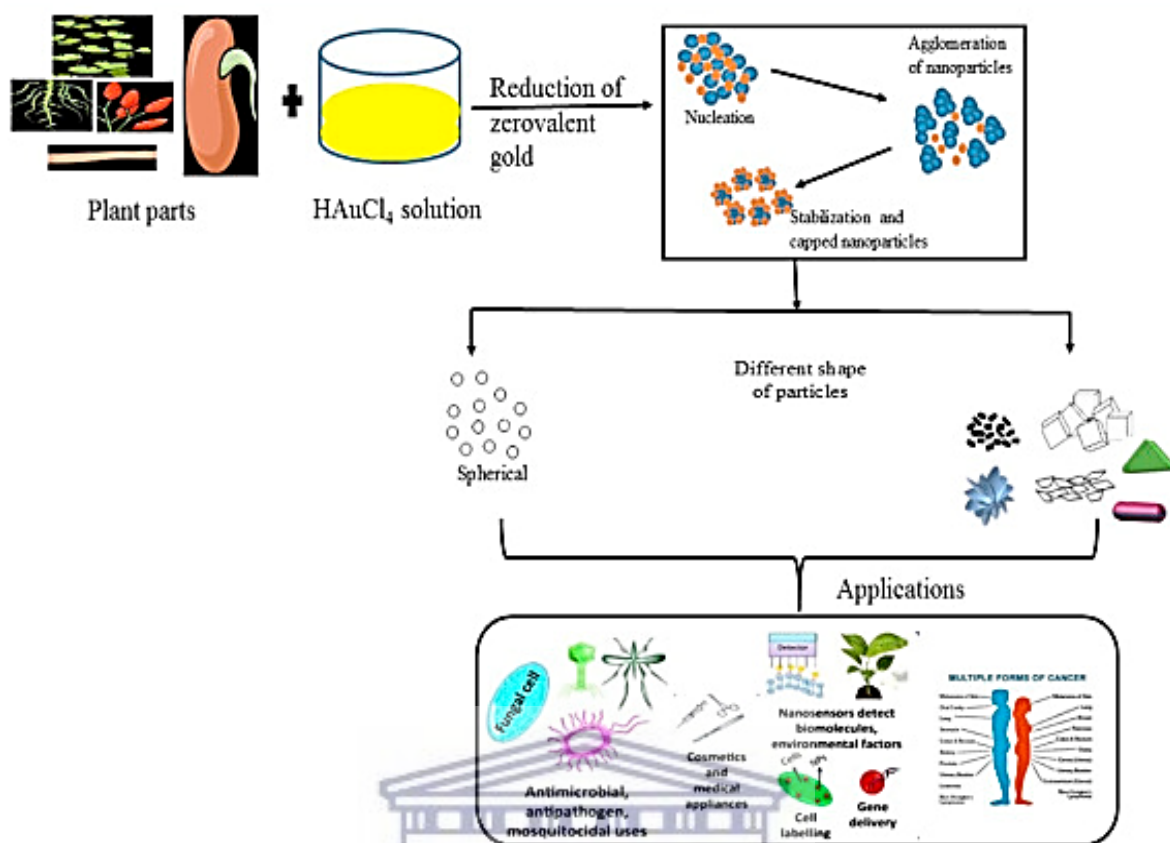


Figure 1.5: Reactions involved in the green synthesis of AuNPs and their applications

Plants and plant products such as fruits and fruit pulps are generally considered to be rich sources of readily available polyphenols. Polyphenols which are the secondary metabolites that are most common and widely found groups of substances in plants. They provide fruits and vegetables with a unique taste and colour. Currently, research trends in natural and, synthetic antioxidant led the screening and identification of new antioxidants from these various plant sources. Polyphenols are also known to possess a significant role in plant defence and human health metabolism. According to reported data, they have shown to exhibit antimutagenic, antioxidative, antiallergenic and anticarcinogenic properties, enzyme inhibiting effects, are antifungal, antimicrobial and display preventative roles against neurodegenerative disorders, diabetes, cataracts, cardiovascular disease and cancer (Sengani *et al.*, 2017). Antioxidant activity in plant extract is due to the redox potential of phytochemicals, which can play an important role in quenching singlet and triplet oxygen, decomposing the peroxides or neutralizing the free radicals. Therefore, it is assumed that higher antioxidant activity of NPs might be due to the preferential adsorption of the antioxidant material from the extract onto the surface of the NPs. Different parameters like surface area,

particle size and surface reactivity determine the toxicity of the NPs in plant extracts (Phull *et al.*, 2016).

These phytochemicals derived from plants not only require shorter periods of incubation with gold salt in order to synthesise AuNPs but also act as capping agents to prevent coalescence of colloidal particles, which are kept apart in solution by electrostatic forces (Nayak *et al.*, 2018). AuNPs synthesis requires a protecting agent, whose role is to adsorb onto the surface of the newly formed AuNPs to prevent further growth and particle agglomeration. It has been suggested that different-shaped polyol and water-soluble heterocyclic components of plant phytochemicals are mainly responsible for the reduction and coating of gold ions (Elbagory *et al.*, 2016). Moreover, the mixture of AuNPs and phytochemicals may possibly result in synergistic biological activities (Noruzi, 2015; Sett *et al.*, 2016).

Recently, a study conducting the synthesis of AuNPs and silver nanoparticles (AgNPs) using the leaf and root extract from the medicinal herbal plant *Panax ginseng* suggested the use of medicinal plants as resources (Singh *et al.*, 2016). El-Kassas and colleague showed that the hydroxyl functional group from polyphenols and the carbonyl group from proteins of *Corallina officinalis* extract could assist in forming and stabilising AuNPs (El-Kassas and El-Sheekh, 2014). Reports also suggested that different mechanisms for synthesising NPs exist in different plant species. For instance, eugenol, the main terpenoid of *Cinnamomum zeylanisum*, was found to have a principal role in the synthesis of AuNPs and AgNPs (Singh *et al.*, 2016). Raghunandan *et al.* (2010) produced irregularly shaped AuNPs using an extract of dried clove (*Syzygium aromaticum*) buds. Reduction and stabilisation of AuNPs were ascribed to the flavonoids present in the extract (Raghunandan *et al.*, 2010). Ghodake and co-workers have obtained AuNPs with different shapes (spherical, hexagonal and triangular) by using the rapid biosynthesis process of metallic Au ions in presence of pear fruit extract (Ghodake *et al.*, 2010). Kasthuri *et al.* (2009) used a dilute phyllanthin containing extract derived from the plant *Phyllanthus amarus*, to produce hexagonal and triangular AuNPs from HAuCl₄. Increasing the concentration of the extract led to the formation of spherical NPs (Kasthuri *et al.*, 2009). Elbagory used various plant extracts in synthesising AuNPs (Elbagory *et al.*, 2016, 2017)

Biological NPs have been applied in many biomedical contexts, including antimicrobial, and anticancer applications due to the higher efficacy of biological NPs compared with physicochemical NPs for biomedical applications (Singh *et al.*, 2016). El-Kassas and

colleague showed the cytotoxic activity of biological AuNPs with the extract of the red seaweed *Corallina officinalis* on the MCF7 human breast cancer cell line (El-Kassas and El-Sheekh, 2014). Nethi *et al.* (2014) developed novel proangiogenic biosynthesised Au nanoconjugates to accelerate the growth of new blood vessels through redox signalling (Nethi *et al.*, 2014). Wang *et al.* (2013) showed the in vivo self-bioimaging of tumours through fluorescent gold nanoclusters that were spontaneously biosynthesized by cancerous cells HepG2 (a human hepatocarcinoma cell line) and K562 (a leukemia cell line) (Wang *et al.*, 2013). Mukherjee *et al.* (2013) demonstrated a biosynthetic approach for the fabrication of gold nano-bioconjugates using *Olax scandens* leaf extract and applied to lung (A549), breast (MCF-7) and colon (COLO 205) cancer cell lines. These results showed the significant inhibition of cancer cell proliferation and fluorescence imaging in A549 cancer cells (Mukherjee *et al.*, 2013). Edison and Sethuraman (2012) used an aqueous extract of *Terminalia chebula* to produce gold nanoparticles with sizes ranging from 6 to 60 nm. These NPs were active against both Gram-positive *S. aureus* and Gram-negative *E. coli* (Edison and Sethuraman, 2012). In a recent finding, Murdoch University researchers have created antibacterial AuNPs from the leaves of *Eucalyptus macrocarpa*. Results showed increased zone of inhibition against *Bacillus subtilis* and *Escherichia coli*. This finding can be used as a new tool to combat the antibiotic-resistant strains of microorganisms (Cui, 2012). Parida *et al.* (2011) reported the synthesis of AuNPs mediated by an extract of *Allium cepa*. The particles had an average size of 100 nm and could be internalized by MCF-7 breast cancer cells via endocytosis (Parida *et al.*, 2011).

1.5. Characterisation of AuNPs

There are several characterisation techniques that can be used to determine various properties of AuNPs (Mittal *et al.*, 2013).

1.5.1. Ultraviolet-Visible (UV-Vis) Spectroscopy analysis

Ultraviolet-Visible (UV-Vis) spectroscopy is a useful tool in studying electronic transition of species that absorb at near infrared through the visible to the UV region of electromagnetic spectrum with transition energy in the approximate range between 10^2 and 10^3 kJ mol⁻¹ (Amendola and Meneghetti, 2009). The optical properties of noble metal NPs have been intensively studied. Metallic NPs, particularly AuNPs, exhibit a strong absorption band in the visible region of the absorption spectra. This absorption band is a result of the coherent oscillation of conduction band free electrons induced by the interaction with the

electromagnetic field of the incident light; this is known as surface plasmon resonance (SPR). This band is characteristic for metallic NPs and is absent in the bulk metal absorption spectra. The position, intensity and shape of the SPR band depend on the size and shape of the particle, interparticle interactions, dielectric properties and the surrounding media such as different solvent or adsorption of a capping agent onto the nanospheres may result in slight variation for the SPR peak position (Hu *et al.*, 2006; Olenic *et al.*, 2016). By varying the NP size and shape, the maximum absorbance of SPR can be tuned anywhere between 520–1000 nm (Olenic *et al.*, 2016). Figure 1.6 shows the UV-Vis spectra of AuNPs at ~532 nm (Kumar *et al.*, 2008). Since the SPR originates an extinction spectrum which depends on the shape, size, and aggregation of AuNPs, UV-Vis spectroscopy is a very useful technique which allows estimation of AuNPs size, concentration, and aggregation level. Morphological feature of AuNPs and their physicochemical environment influence the SPR and the corresponding extinction spectra (Amendola and Meneghetti, 2009). For gold nanospheres about 50 nm in diameter, the SPR peak is positioned at 520 nm, and this peak is responsible for the ruby red colour displayed by conventional gold colloids. Michael Faraday initially observed this spectacular phenomenon (Hu *et al.*, 2006). In addition, aggregation of gold nanospheres will lead to a pronounced colour transition from red to purple. This is due to plasmonic coupling between particles (Hu *et al.*, 2006).

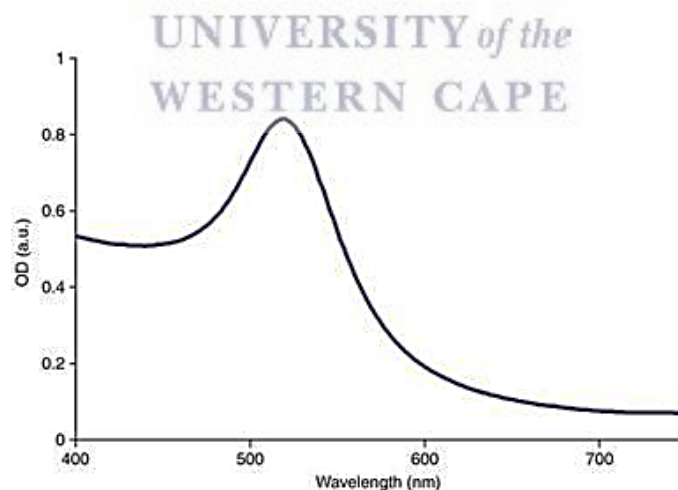


Figure 1.6. UV-Vis absorption spectra displaying the SPR band in AuNPs (Adapted from Kumar *et al.*, 2008).

1.5.2. Dynamic Light Scattering (DLS) analysis

Dynamic light scattering (DLS) technology, also known as photon correlation spectroscopy, can be used to determine the hydrodynamic average particle size, the surface charge and their polydispersity index (PDI) of NPs suspended in a liquid (Mittal *et al.*, 2013). PDI refers to the width parameter, which is derived from the cumulants analyses and provides information about uniformity in NPs size. The PDI value is important to consider, as particles with a value close to 0.7 indicate a very broad size distribution of the sample and is not suitable for DLS measurements (Noruzi, 2015). Figure 1.7 shows the size distribution of AuNPs determined by DLS (Elbagory *et al.*, 2017). DLS instruments measure time-dependent fluctuations of scattering intensities from particles within the sample undergoing Brownian motion, which is based on the Dopplér effect. When a particle is suspended in a solution and illuminated by light, it scatters light given that its index of refraction differs from that of the suspending solvent. Therefore DLS provides information about the size and the size distribution of NPs in solutions. Advantages of using this method include its sensitivity and minimal sample requirement (Laouini *et al.*, 2012).

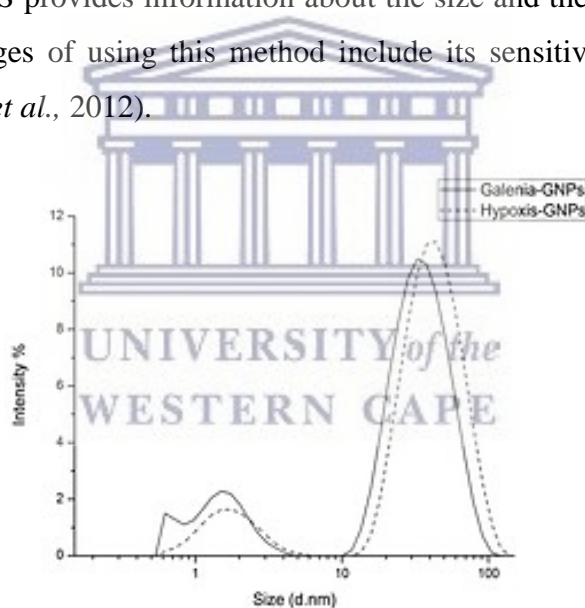


Figure 1.7. DLS distribution curves of AuNPs synthesised from *Galenia Africana* and *Hypoxis hemerocallidea* displaying the hydrodynamic diameter (Adapted from Elbagory *et al.*, 2017).

1.5.3. High Resolution Transmission Electron Microscopy (HRTEM) analysis

High Resolution Transmission electron microscopy (HRTEM) measures the interaction of transmitted electrons as they pass through an ultra-thin specimen. The principle behind HRTEM involves the projection of an electron beam that is primarily focused by a series of magnetic lenses into the specimen deposited onto a small metal grid, where the electrons will

be absorbed and scattered as they interact with the specimen. Subsequently, the transmitted electrons will be focused by the objective lenses and detected by the detector generating an image that can be visualised by the CCD camera. The transmitted electrons will produce an image providing useful information about the morphology of the material. The particle to particle interaction will be conveyed by the agglomeration or dispersion of the particles that make up the specimen (Wang, 2001). HRTEM is one of the most efficient and versatile methods for the characterisation of nanomaterials. This technique analyses the size and size distribution, morphology and topography, composition and crystallography and dispersion of AuNPs (Olenic *et al.*, 2016). **Figure 1.8.** shows a HRTEM image of spherical AuNPs with an average core size of 10 ± 5 nm synthesised from pears (*Pyrus pyrifolia*) obtained in a study conducted by Ghodake and co-workers (Ghodake *et al.*, 2010).

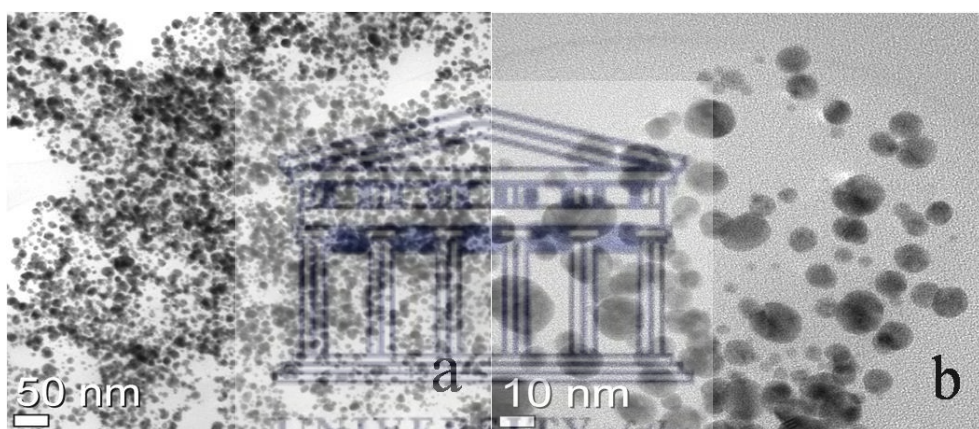


Figure 1.8. HRTEM image of AuNPs (Adapted from Ghodake *et al.*, 2010)

1.5.4. Fourier-Transform Infrared (FTIR) Spectroscopy analysis

FTIR spectroscopy is a technique used to determine and identify the presence of functional groups on the surface of NPs. It give an idea as to which phytochemical(s) may have been involved in the synthesis and also determines how these NPs may react with biomolecules and drugs and how these NPs may react with other NPs (Mittal *et al.*, 2013). **Figure 1.9** shows the FTIR spectra of AuNPs synthesised from *Terminalia chebula* (Kumar *et al.*, 2012). This technique measures the absorption of infrared radiation by the sample material versus wavelength. The infrared absorption bands identify molecular components and structures. Molecules have time-variant dipole moment whose oscillating frequency corresponds to that of incident infrared light to absorb infrared radiation (Lin *et al.*, 2014). When a material is

irradiated with infrared radiation, absorbed infrared radiation usually excites molecules into a higher vibrational state. The wavelength of light absorbed by a particular molecule is a function of the energy difference between the at-rest and excited vibrational states. After the absorption of infrared radiation, the energy is transferred to the molecule which then causes the stretching of a covalent bond, bending or twisting which can be described by a stationary state of molecular vibrational Hamiltonian. An infrared spectrum is therefore then produced which are characteristic of its molecular structure and can function like a molecular fingerprint. Those molecules which lack a dipole moment, for example, O₂ and N₂, do not absorb infrared radiation (Lin *et al.*, 2014). The significant absorption bands which can indicate the role of these compounds are mainly observed in the region 1,000-1,800 cm⁻¹. Stretching vibrations of N-H and O-H groups however, appear between 3,200 and 3,500 cm⁻¹.

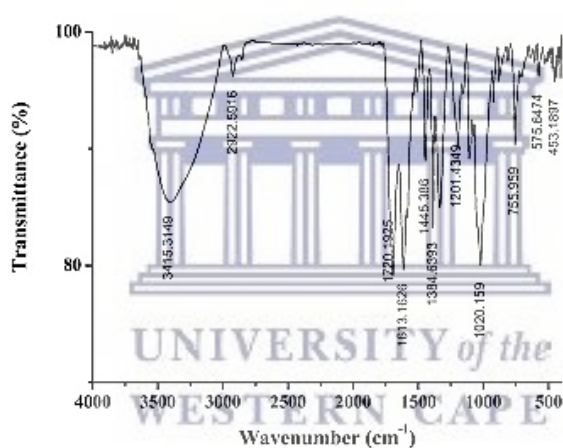


Figure 1.9. FTIR spectra of AuNPs (Adapted from Kumar *et al.*, 2012).

1.6. *Pyrus communis* Linn (*P. communis* L.)

1.6.1. Botanical characteristics of *P. communis* L.

The pear tree belongs to the genus *Pyrus* and has been cultivated for over 3000 years (Silva *et al.*, 2014). *Pyrus* is a member of the Rosaceae family and is comprised of 22 species originating in the temperate regions of Asia, Europe and high-altitude locations in Africa, along with six natural interspecific hybrids. (Thomas *et al.*, 2010). According to the original classification, *Pyrus* is divided into two native groups: Occidental (European) and Oriental (Japanese) pear variety (Bao *et al.*, 2007; Xue *et al.*, 2017). Varieties of the European pear (*P. communis*) can produce pears with both red- and green-skinned fruits, such as the Max Red Bartlett (MRB)

variety and are particularly admired for their unique crispness, taste and flavour (Sharma and Rao, 2015).

1.6.2. Pear production in South Africa

In terms of European pear production, South Africa is ranked seventh in the world following Italy, USA, Argentina, Spain, India and Turkey (Human, 2013). Pears are planted in most of the deciduous fruit producing areas of South Africa, particularly in Ceres. ‘Bon Rouge’, a South African mutant bud of the ‘Williams Bon Chretien’ pear, is a red skinned variety that was discovered by Mr Danie Marais on his farm Ongegund, Simondium as a bud mutation on a ‘Williams Bon Chretien’ tree. ‘Williams Bon Chretien’ itself arose in England in the 1770’s and is also known as ‘Bartlett’. The ‘Bon Rouge’ pear (*Pyrus communis* L.) was evaluated and it was found to be a pear with good qualities in terms of flavour and texture. The pear has also been characterised by high levels of anthocyanins, the pigments responsible for the red leaf and red fruit skin phenotype (Thomas *et al.*, 2010). However, the branches of ‘Bon Rouge’ pear trees that have been planted in the commercial orchards are often inclined to revert to its original green ‘Bon Chretien’ phenotype or manifests sectors (stripes) of red to green on the leaves and in skin of mature ‘Bon Rouge’ pear fruit as shown in figure 1.10 (Jolly, 1993; du Preez *et al.*, 2004).



Figure 1.10. Photographic images of mature pears from the ‘Bon Rouge’ pear tree. (A) Mature green and red pears (B) characteristic stripes of the red to green reversion in the mature ‘Bon Rouge’ pear fruit.

Red leaves and red skinned fruit in the early growing season characterizes ‘Bon Rouge’ pears. However, the loss of red colour in the leaves and fruit skin colour at the ripening stage is the result of the disappearance of anthocyanins when synthesis falls below the rate of pigment turnover (Steyn *et al.*, 2004; Yang *et al.*, 2015). This can be ascribed to response to stress, perhaps the transposable elements within the pear genome (du Preez *et al.*, 2004). The anthocyanins, particularly cyaniding-3-galactoside is responsible for the red colour of ‘Bon Rouge’ and other fruits belonging to a class of flavonoids (Honda *et al.*, 2002). The other pigments that affect the colour of fruit include chlorophyll (green) and carotenoids (yellow) (Holtan and Cornish, 1995; Yang *et al.*, 2015).

1.6.3. Chemical composition of *P. communis* L.

Pear (*Pyrus* spp.) is one of the most important stone fruits that are widely consumed fresh when fully mature and in processed forms. Being high in fiber, low in calorie, *pyrus* is a rich source of alkaloids, tannins, carbohydrates, steroids, amino acids, cardiac and coumarin glycosides, flavonoids and phenolic compounds (Ghodake and Lee, 2011; Kolniak-Ostek, 2016; Kiran *et al.*, 2018). Phytoconstituents are reported in Table 1.1.

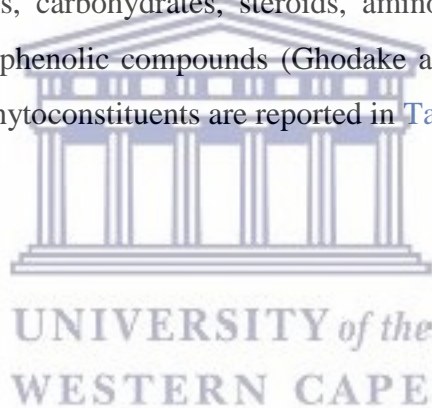


Table 1.1. Phytoconstituents of *P. communis* (Adapted from Parle and Arzoo, 2016; Kiran *et al.*, 2018)

Part	Constituents present in <i>P. communis</i>
Seeds	Minerals (sodium, potassium, magnesium, calcium, phosphorous, copper, iron, zinc, manganese, selenium, fluoride), Carbohydrate , Lipid
Leaves	Glycosides (Arbutin, quercetin, isohamnetin, kaempferol, 3,5-dicafeoylquinic acid, astragaln, pyroside), Phenolic acid (chlorogenic acid gallic acid), Tannins , Coumarin , Triterpenes (ursolic acid)
Bark	Triterpenes (friedelin, epifriedelanol)
Root bark	Phloridzin
Stem bark	Triterpenes (α -amyrin)
Flower	Fatty acid (stearic acid, palmitic acid, arachidic acid), Triterpenes (α -amyrin), Phenolic acid (chlorogenic acid, gallic acid), Sterol (β -sitosterol, saccharostenon),), Flavonoids (Quercetin 3-O- β -D glucopyranoside, Kaempferol 3-O- β -D (6'' –O- α -L-rhamnopyranosyl)-glucopyranoside), Querce 3-O- β -D (6 –O- α -L-rhamnopyranosyl)-glucopyranoside)
Fruit	Glycosides (Arbutin, quercetin, isohamnetin), Flavonoids (Quercetin 3-O- β -D glucopyranoside, Kaempferol 3-O- β -D (6'' –O- α -L-rhamnopyranosyl)-glucopyranoside), Querce 3-O- β -D (6 –O- α -L-rhamnopyranosyl)-glucopyranoside), Vitamins (Vitamin A, Retinol, Vitamin C, Vitamin E, Vitamin K, Vitamin B12 (folate), Vitamin B3 (niacin), Vitamin B5 (pantothenic acid), Choline, Betaine), Polyphenol oxidase , Lipid , Carbohydrate , Tannins , Anthocyanins , Minerals (sodium, potassium, magnesium, calcium, phosphorous, copper, iron, zinc, manganese, selenium, fluoride), Phenolic acid (chlorogenic acid, gallic acid), Alkaloids

1.6.4. Pharmacological properties of *P. communis* L.

Each part of pear tree has high nutritional value and possesses multiple medicinal properties (Parle and Arzoo, 2016). *P. communis* L. also known as Amritphale bears many actions like astringent, febrifuge and sedative activity (Kaur and Arya, 2012). Pears have been used as a traditional folk remedy for more than 2000 years due to their reported anti-inflammatory, antihyperglycemic and diuretic activities. Other traditional uses of pears include use as remedies for relieve of cough, alcohol hangovers and constipation (Reiland and Slavin, 2015). Fruits exhibited anti-diabetic, hypolipidemic, antioxidant and antimicrobial activities (Kiran *et al.*, 2018).

1.6.4.1. Antimicrobial activity and wound healing effect

Arbutin present in pears has been correlated with biochemical processes that operate as a defence mechanism against microbial invasion. Therefore pears act as an antimicrobial agent (Kaur and Arya, 2012). Studies have reported that fresh pear juice and ethyl acetate extracts from pear fruits show antimicrobial activity against *Staphylococcus* and *Escherichia coli* (*E. coli*) as a result of the presence of phytoconstituent arbutin (bacteriostatic), which gets further, converted into hydroquinone in body (Kaur and Arya, 2012; Güven *et al.*, 2006). This hydroquinone also possesses antimicrobial activity, boosts biochemical processes and operates defence mechanisms against bacteria invasion. Jin and Sato also determined that the aqueous extracts from young shoots of the *Pyrus* spp. exhibited strong antimicrobial activity against *Erwinia amylovora* bv. 4. as a result of the substance benzoquinone (Jin and Sato, 2003). Pears have also been shown to be effective in speeding up the healing process for various types of wounds. It aids in several steps of the healing process. Astringent tannins constrict wounds (Ashok and Apadhyaya, 2012). Vitamin C, a powerful antioxidant, helps in tissue repair and stimulates the production of collagen, the primary structural protein in skin and heal wounds (Sarpoooshi *et al.*, 2017). The wound healing activity of ethyl acetate and ethanol extracts of fruits of *P. communis* (EAEPC and EEPC 200 mg/kg) was investigated by various wound healing models in normal rats such as excision, incision and dead space wound model. Results showed that *Pyrus communis* was effective in all the models of wound healing activity by increasing wound contraction, decreased epithelisation and scar area (Chinnasamy and Bhargava, 2014). Other studies have shown that flavonoids endorse wound healing processes primarily owing to their antimicrobial and astringent properties which appear to be responsible for wound contraction and elevated rate of epithelisation (Süntar *et al.*, 2011). Earlier reports have confirmed that proanthocyanins or condensed tannins are a group of biologically active polyphenolic bioflavonoids known to facilitate wound healing (Hupkens *et al.*, 1995; Choudhary, 2008). A phytochemical study confirmed that *Pyrus communis* contains flavonoids, tannins, phenolic compounds and alkaloids. The wound healing potential of the extracts of *Pyrus communis* could be due to the interaction of the mixture of these phytoconstituents with various phases of wound healing (Chinnasamy and Bhargava, 2014).

1.6.4.2. Anticarcinogenic activity

Consumption of pear on a regular basis prevents the danger of oesophageal, bladder and lung cancer (Freedman *et al.*, 2007; Büchner *et al.*, 2009; Linseisen *et al.*, 2007). Pears contain

ursolic acid that inhibits aromatase activity thereby preventing cancer (Yin *et al.*, 2018). Isoquercitrin present in fruit maintains DNA integrity (di Camillo Orfali *et al.*, 2016). Chlorogenic acid is a strong antioxidant in pears and acts as a potential chemopreventative agent and is also an immune system enhancement, possesses anticancer activity and can reduce the toxic side effects of chemotherapy drugs (Öztürk *et al.*, 2015; Li *et al.*, 2016). Thus, consumption of pear on daily basis prevents the danger of cancer, especially in menopausal women (Parle and Arzoo, 2016).

1.6.4.3. Anti-inflammatory action

Pears can be useful in treating inflammation of mucous membranes, colon, chronic gall-bladder disorders, arthritis and gout. Carotene, zeaxanthin and vitamin C are nutrients present abundantly in pear, which lower the concentration of inflammation - causing C-reactive proteins (Parle and Arzoo, 2016).

1.6.4.4. Antioxidant activity

Pears are a rich source of vitamin C, phenolic compounds and copper, which protect cells from damage by free radicals. Fruits (chlorogenic acid, arbutin, epicatechin and quercetin), flowers (chlorogenic acid), leaves (quercetin, coumarin and chlorogenic acid) and root barks (phloridzin) of pear tree help in destroying reactive oxygen species (ROS) thereby exhibiting antioxidant activity (Sharma *et al.*, 2015; Parle and Arzoo, 2016). Chlorogenic acid is the most important antioxidant-active constituent in pears, and acts as a potential chemopreventive agent by promoting the prevention of chronic diseases such as cancer and cardiovascular disease, is also an immune system enhancement, possesses anticarcinogenic activity and can reduce the toxic side effects of chemotherapy drugs (Öztürk *et al.*, 2015; Li *et al.*, 2016; Kiran *et al.*, 2018). Arbutin acts as an antibiotic substance in fire resistance and a specific marker of pear products for the evaluation of product authenticity. The various tissues and organs of a pear, such as the peel, flesh, flower bud or leaf bud possess different levels of phenolics resulting in varied antioxidant capacity (Reiland and Slavin, 2015). Chlorogenic acid and arbutin were detected as a major phenolic compounds in the peel of pear cultivars. Among flavonoids of the leaves and fruits, monomeric and polymeric flavan 3-ols (epicatechin and proanthocyanidins) are also dominant and act as antioxidants or as colouring in the fruit and their products (Fischer *et al.*, 2007; Öztürk *et al.*, 2015; Li *et al.*, 2016). Anthocyanins are correlated to the antioxidant activity in pears (Reiland and Slavin, 2015).

1.6.4.4.1. Anthocyanin

Anthocyanins (Greek: antos, flower and kyanos, blue) are a class of plant constituents sharing the same diphenylpropane skeleton (C₆C₃C₆) and that constitute a subfamily of phenolic compounds collectively known as flavonoids (Kong *et al.*, 2003; Cisowska *et al.*, 2011). Anthocyanins are water-soluble and their spectral properties usually are responsible for blue, purple and red colouring of different plant parts (flowers, fruits, vegetables and other plant tissues). They are particularly abundant in different fruits, especially in almost all types of berries (Cisowska *et al.*, 2011; Huang *et al.*, 2012; Li *et al.*, 2012; Wang *et al.*, 2013). They widely distributed in human diet through crops, beans, fruits, vegetables and wine (Steyn *et al.*, 2004). In pears, cyanidin 3-galactoside and peonidin 3-galactoside are the two main anthocyanin pigments that are responsible for red colouration in pear skins (Dussi *et al.*, 1995).

Anthocyanins are modified by glycosyl and aromatic or aliphatic acyl moieties, resulting in hundreds of anthocyanin molecules that differ in hue and stability (Oren-Shamir, 2009; Cisowska *et al.*, 2011). The basic chemical structure is flavylium cation (2-phenylbenzopyrylium), which links hydroxyl (-OH) and/or methoxyl (-OCH₃) groups, and one or more sugars (Figure 1.11). The sugar-free molecule is called anthocyanidins. The difference between individual anthocyanins relate to the number of hydroxyl groups, the number and nature of the sugars attached to the molecule, the position of this attachment, and the nature and number of the aliphatic or aromatic acids attached to sugars in the molecule. There are 17 known naturally occurring anthocyanidins or aglycones (Kong *et al.*, 2003).

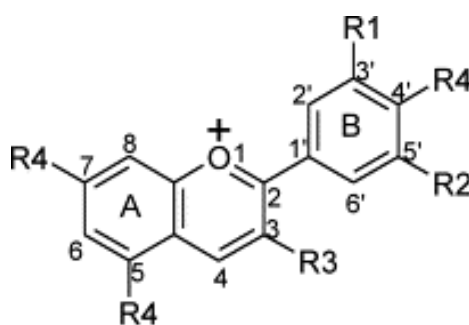


Figure 1.11. Chemical structure of anthocyanin. The flavylium cation. R1 and R2 are H, OH, or OCH₃; R3 is a glycosyl or H; and R4 is OH or a glycosyl (Adapted from Kong *et al.*, 2003).

1.6.4.4.1.1. Pharmacological properties of anthocyanin

Anthocyanins are a rich source of antioxidants known to possess pharmacological properties and are used by humans for therapeutic purposes (Kong *et al.*, 2003; Krishnaswamy *et al.*,

2014; Wang *et al.*, 2013 and Thomas *et al.*, 2010). The beneficial effects of anthocyanins were known at least from the 16th century, when blackberry juice was used in the treatment of mouth and eye infections. Due to numerous studies it is evident that anthocyanins display a variety of biological activities: they act as strong antioxidants, anti-inflammatory, anti-proliferative, anti-carcinogenic, phytoalexins or as antimicrobial agents and free radical scavenging activity (Hamauzu *et al.*, 2007; Cisowska *et al.*, 2011; Amin *et al.*, 2017; Xue *et al.*, 2017). They are also known to protect against cardiovascular diseases; radiation and oxidative DNA damage and prevent cataracts and possess neuroprotective effects by crossing the blood-brain barrier, cancer and atherosclerosis (Adisakwattana *et al.*, 2009; Krishnaswamy *et al.*, 2014; Li *et al.*, 2012). Pears provide antioxidants and are concentrated in flavonols, particularly anthocyanins. Intake of pears is known to prevent type 2 diabetes and stroke (Reiland and Slavin, 2015).

The above mentioned anthocyanin properties were the main reason for the substantially increased interest in the following studies in the last decade. Hamauzu *et al.* (2007) determined the effect of pear procyanidins on gastric lesions induced by HCl/ethanol in rats and found that highly polymerised procyanidins extracted from the pear fruit and administered orally, exhibited a high level of antiulcer capacity. The authors suggested that the antiulcer effect of pear procyanidins may be due to their strong antioxidant activity (Hamauzu *et al.*, 2007). A study conducted by Mink *et al.*, (2007) determined flavonoid intake and cardiovascular disease mortality in postmenopausal women. Individual flavonoid-rich foods associated with significant mortality reduction included pears or apples and coronary heart disease and cardiovascular disease (Mink *et al.*, 2007). Muraki *et al.* (2013) reported that the consumption of specific whole fruits, particularly blueberries, grapes, apples or pears, is significantly associated with lowering risk of type 2 diabetes (Muraki *et al.*, 2013). Anthocyanin extracted from berries have shown to improve cognitive brain function and reduce age associated oxidative stress. They have been shown to prevent learning and memory loss in estrogen-deficient rats (Amin *et al.*, 2017). In a study that tested the effects of anthocyanins on tumours, some anthocyanins were not effective in suppressing tumour growth (Ghiselli *et al.*, 1998). However, an antioxidant activity study of anthocyanin fractions from Italian red wine showed that the anthocyanins was effective in scavenging reactive oxygen species and in inhibiting lipoprotein oxidation and platelet aggregation (Kamei *et al.*, 1998). This result suggests that anthocyanins could be the key component in red wine that protects against cardiovascular disease. Another study on the antitumour activity of anthocyanins shows that the anthocyanin

fraction from red wine suppressed the growth of HCT-15 and AGS cells, which are derived from human colon cancer and human gastric cancer, respectively. The rate of growth suppression by the anthocyanin fraction was significantly higher than that of the other fractions that did not contain anthocyanins (Kamei *et al.*, 1998).

Antimicrobial activity of anthocyanin-containing fruits is likely to be caused by multiple mechanisms and synergies because they contain various compounds including anthocyanins, weak organic acids, phenolic acids, and mixtures of their different chemical forms (Cisowska *et al.*, 2011). Therefore, the antimicrobial effect of chemically complex compounds has to be critically analysed. Pomegranate fruit (*Punica granatum*) known to contain a high proportion of phenolic compounds, such as delphinidin, cyanidin, and pelargonidin were found to be active against Gram-positive (*B. subtilis*, *S. aureus*, *S. epidermidis*, *S. saprophyticus*, *E. faecalis*, *Enterococcus faecium*, *Streptococcus pneumoniae*, and *S. pyogenes*), and Gram-negative (*E. coli*, *P. aeruginosa*, *Salmonella typhi*, *S. paratyphi A and B*, *Shigella dysenteriae*, *S. sonnei*, and *S. flexneriae*) bacterial species. (Naz *et al.*, 2007). Burdulis *et al.* (2009) found that bilberry (*V. myrtillus*) and blueberry (*V. corymbosum*) fruits and their skins possessed inhibitory effects on the growth of Gram-positive (*Listeria monocytogenes*, *Staphylococcus aureus*, *Bacillus subtilis* and *Enterococcus faecalis*) and Gram-negative strains (*Citrobacter freundii*, *E. coli*, *P. aeruginosa*, and *Salmonella enterica ser. Typhimurium*) (Burdulis *et al.*, 2009). Investigation of the antimicrobial properties showed that European cranberry (*Vaccinium oxycoccos*) extracts inhibited the growth of a wide range of human pathogenic bacteria, both Gram-negative and Gram-positive. *L. monocytogenes* and *E. faecalis* strains were the most sensitive, *S. enterica ser. Typhimurium*, and *S. aureus* were found to be of moderate resistance and *E. coli* rods were the least sensitive (Česonienė *et al.*, 2009).

A recent pharmacological study by Amin *et al.* has shown that anthocyanin loaded PLGA@PEG NPs (Anthocyanin-NPs) effectively attenuated A β -induced neurotoxicity in SH-SY5Y cells and showed significant antioxidant, anti-apoptotic, anti-inflammatory and anti-Alzheimer's effects (Amin *et al.*, 2017). In a study conducted by Septiani *et al.*, (2017), it was observed that zinc oxide NPs were successfully synthesised by utilising anthocyanin obtained from Indonesia black rice extract as a capping agent by thermal decomposition of precursor route (Septiani *et al.*, 2017). AuNPs synthesised from the pear (*Pyrus pyrifolia*) showed biocompatibility with human embryonic kidney 293 cells (Ghodake *et al.*, 2010).

1.7. Research Proposal

1.7.1. Problem Statement

An extensive set of NPs have been developed due to the accelerated expansion in the field of nanoscience and nanotechnology. These NPs differ in shape, size, capping layer, charge and stability. However, scientists face major challenges in developing novel NPs that are biocompatible and is produced in an eco-friendly manner without the use of toxic chemicals. Hence, less toxic reducing agents, solvents, and renewable materials are imperative in the production of environmentally affable and biocompatible NPs. Accordingly, the basic aspects of green chemistry can meet the requirements of nontoxic materials when nontoxic or non-poisonous aspects of the plants or fruits are used. This does increase the utilisation value of particular organisms. In particular, plant and fruit extracts are more beneficial than microbial- or fungal-mediated syntheses since they avoid high cost that could be restrained for extensive productions under non-aseptic conditions and avoid time-consuming process of maintaining cells. Various plants and fruit also possess various pharmacological properties as a result of their phytochemical profiles. As the phytochemical constituents differ between plants and fruits, NPs synthesized from different plant and fruit extracts may also vary significantly and so may their potential applications.

1.7.2. Aims

This research aims to assess whether the aqueous extracts of the peel and flesh from the green ‘Williams Bon Chretien’ pear and the peel and flesh from its red mutant bud, ‘Bon Rouge’ pear can be used to synthesise AuNPs in a simple and environmentally friendly way. Previous studies have shown that the yellow *Pyrus pyrifolia* pear is capable of synthesising AuNPs due to the sugars and peptides or proteins of the pear extract, however, no further studies have been documented on the potential biological applications of these pear-AuNPs even though it has shown to be biocompatible. The South African red-coloured ‘Bon Rouge’ pear contains higher levels of anthocyanin than the green-coloured ‘Williams Bon Chretien’ pear. Anthocyanin, a water-soluble phenolic compound has been shown to exhibit pharmacological properties and so have pears. Therefore, this study aims to synthesise AuNPs from the ‘Williams Bon Chretien’ and ‘Bon Rouge’ pears and determine whether there is a difference in the physicochemical properties among these AuNPs due to a difference in the levels of anthocyanin as well as to assess the cytotoxicity and antimicrobial activity of these AuNPs.

1.7.3. Objectives of the study

- To synthesize AuNPs using fresh green peel and flesh from the ‘Williams Bon Chretien’ pear and fresh red peel and flesh from its mutant bud, ‘Bon Rouge’ pear.
- To evaluate the effect of temperature on the synthesis of the AuNPs.
- To determine the kinetics of AuNPs formation as a function of time.
- To characterise the physicochemical properties of the AuNPs using UV-Vis, DLS, HRTEM and FTIR.
- To determine whether there is a difference in the physicochemical properties among the AuNPs due to the influence of anthocyanin levels found in the red and green peel pear extracts and the other phytochemicals in the peels and flesh of these pears.
- To evaluate the in vitro stability of the AuNPs in media and biological buffer solutions.
- To assess the antimicrobial activity of the synthesized AuNPs against Gram negative and Gram positive bacterial strains.
- To evaluate the cytotoxicity of the AuNPs against human non-cancerous fibroblast cells.

1.7.4. Primary Research Questions

- Are the aqueous extracts from the red and green peels and red and green flesh capable of reducing gold (III) chloride to form AuNPs?
- Are the extracts stabilising and capping agents in the synthesis of AuNPs?
- What is the effect of temperature on the synthesis of AuNPs?
- What is the kinetics of AuNPs formation?
- Are the AuNPs stable in media and biological buffer solutions?
- Is there a difference in the physicochemical properties among the various AuNPs synthesised from the various aqueous pear extracts?
- Does the green synthesized AuNPs exhibit antimicrobial activity?
- Is the green synthesized AuNPs toxic?

1.7.5. Hypothesis:

Anthocyanin and other phytochemicals found in the aqueous extracts of the green peel and flesh of the ‘Williams Bon Chretien’ pear and the aqueous extracts of the red peel and flesh of ‘Bon Rouge’ pear may act as reducing, capping and stabilising agents in the bioreduction of gold (III) chloride which will result in the formation of AuNPs with potential biological applications. The phytochemical content of ‘Williams Bon Chretien’ and ‘Bon Rouge’ pears are expected to differ and may therefore produce different AuNPs.



CHAPTER 2

MATERIALS AND METHOD

2.1. General chemicals and suppliers

Table 2.1. List of chemicals used in this study

Chemicals	Suppliers
Ampicillin	Sigma-Aldrich
Bovine Serum Albumin (BSA)	Miles Laboratories
Cell Proliferation Reagent WST-1	Sigma-Aldrich
Tetrachloroauric acid (gold salts)	Sigma-Aldrich
Dimethyl sulphoxide (DMSO)	Sigma
Dulbecco's Modified Eagle Medium (DMEM)	Lonza
Ethanol 99.9%	Kimix
Fetal Bovine Serum (FBS)	Thermo Fisher Scientific
Nutrient Broth (NB)	Merck Biolab
Mueller Hinton Agar (MHA)	Merck
Mueller Hinton Broth (MHB)	Merck
Phosphate Buffered Saline (PBS)	Lonza
Roswell Park Memorial Institute medium (RPMI)	Lonza
Trypsin	Sigma-Aldrich
Trypsin Blue Stain 0.4 %	Gibco

2.2. Instrumentation and suppliers

Table 2.2 List of instrumentation used in this study

Equipment	Supplier	Analysis
Allegra® X-12R	Beckman Coulter, Cape Town, South Africa	Centrifugation of pear extracts
Centrifuge 5417R	Eppendorf AG, Hamburg, Germany	Centrifugation of AuNPs
FreeZone Plus 2.5L Freeze dryer	Labconco, Kansas City, MO, USA	Preparation of pear fruit extracts
Incubator OH-800D	Already Enterprise Inc.	Synthesis of AuNPs
POLARstar Omega microplate reader	BMG Labtech, Cape Town, South Africa	UV-Vis spectra
Malvern Zeta sizer	Malvern Instruments Ltd., Malvern, UK	Hydrodynamic size distribution, polydispersity index
TEM Tecnai G ² F20 X-Twin MAT 200kV Field Emission	FEI Company, USA	Core size distribution, morphology and crystallinity of AuNPs
PerkinElmer spectrum one FTIR spectrophotometer	Waltham, MA, USA	Functional groups
Countess™ automated cell counter	Invitrogen Corporation, San Diego, CA, USA	Cell count of viable cells

2.3. Stock solutions and buffers

Table 2.3 Stock solutions and buffers prepared for this study

Stock solutions and buffers	Composition
Ampicillin antibiotic	100 mg ampicillin was prepared in dH ₂ O, filter sterilized and stored at -20 °C.
Aqua regia	3:1 (v/v) HCl: HNO ₃ .
BSA (0.5 %)	0.5 % (w/v) BSA was prepared in distilled water.
Tetrachloroaurate acid	1 mM stock solution was prepared in distilled water, filter sterilised and stored at 4 °C.
Ethanol (70 %)	70 % (v/v) ethanol in distilled water.
Mueller-Hinton Agar	38 g Mueller-Hinton Agar powder was dissolved into 1 L distilled water. The solution was autoclaved at 121 °C for 20 minutes.
Mueller-Hinton Broth	21 g Mueller-Hinton Broth powder was dissolved into 1 L distilled water. The solution was autoclaved at 121 °C for 20 minutes.
Nutrient Broth	16 g Nutrient broth powder was dissolved into 1 L distilled water. The solution was autoclaved for 20 minutes.

UNIVERSITY of the
WESTERN CAPE

2.4. Bacterial strain genotype composition

Table 2.4. List of bacterial strains used in this study

Bacterial strains	Gram reaction	ATCC number
<i>E. coli</i>	Gram-negative	25,922
<i>P. aeruginosa</i>	Gram-negative	27,853
<i>S. aureus</i>	Gram-positive	29,213
<i>S. epidermidis</i>	Gram-positive	12,228

2.5. Cell line, species, source and media

Table 2.5. Cell line used in this study

Cell line	Species	Source	Media
KMST-6	Human	Fibroblast	Complete DMEM

2.6. Preparation of aqueous pear extracts

Fresh 'Bon Rouge' (red) and 'Bon Chretien' (green) pears were collected in January 2018 from the Agricultural Research Council 'Bien Donne' experimental farm (Cape Town, South Africa). The aqueous extracts were prepared at room temperature. In the preparation of the aqueous extracts (red peel (RP), red flesh (RF), green peel (GP) and green flesh (GF) pear extracts), 40 g of peeled red and green pear flesh and peels were ground in a blender with 400 ml of boiled distilled water respectively. The fruit extracts were filtered through glass wool and centrifuged at 10 000 rpm for 20 minutes. The resultant supernatant was then filtered using Whatman 0.4 micron filter paper and the filtrate was collected and kept at -80 °C overnight and lyophilised using the FreeZone 2.5 L lyophiliser (Labconco, Kansas City, MO, USA). The extracts were stored in a desiccator at room temperature for further experiments.

2.7. Synthesis of pear-gold nanoparticles

To determine the biogenesis of gold nanoparticles (AuNPs), chloroaurate acid (gold salts) was used as precursor salts for the synthesis of AuNPs. To investigate the optimum conditions of AuNP synthesis, NPs were synthesized by adding 500 µl of each plant extract (with varying extract concentrations from 96 to 6 mg/ml) to 2.5 ml of 1 mM sodium tetrachloroaurate (gold salts). The effect of temperature was also studied with glass vials incubated at 25 °C for 24 hours, 70 °C for 1 hour and 100 °C for 30 minutes with shaking at 40 rpm. Table 2.6 summarizes the reaction conditions used in the synthesis of samples RP-, GP-, RF- and GF-AuNPs by various pear fruit extract concentrations on the synthesis of AuNPs at 25 °C, 70 °C and 100 °C. The emergence of a red-purple colour change from yellow was indicative for the synthesis of gold nanoparticles. To remove unbound pear phytochemicals, the synthesized gold nanoparticles were centrifuged at 10,000 rpm for 15 minutes. The biosynthesized AuNPs were purified thrice by washing with distilled water and centrifuged at 10,000 rpm for 10 minutes to obtain nanoparticles in pellet form.

Table 2.6. Investigating the effect of extract concentration and temperature of AuNP synthesis

Sample	Pear Extract (mg/ml)	HAuCl ₄ (mM)	Temperature (°C)
RP	6, 12, 24, 48	1	25, 70, 100
GP	6, 12, 24, 48	1	25, 70, 100
RF	6, 12, 24, 48	1	25, 70, 100
GF	6, 12, 24, 48	1	25, 70, 100

2.7.1. Kinetics of AuNP formation as a function of time

The kinetics of the bioreduction of AuNPs was studied by recording the UV-Vis absorbance at the optimum concentration of the pear fruit extract and optimum temperature as a function of time (0 time, 5 min, 10 min, 20 min, 30 min, 40 min, 1 hr, 3 hrs, 6 hrs and 12 hrs).

Table 2.7. Investigating the kinetics of AuNPs formation as a function of time

Sample	Extract OC (mg/ml)	HAuCl ₄ (mM)	Temperature (°C)	Time
RP	24	1	100	0 mins, 5 mins, 10 mins, 20 mins, 30 mins, 40 mins, 1 hr, 3 hrs, 6 hrs, 12 hrs
GP	48	1	100	
RF	24	1	100	
GF	24	1	100	

2.8. Characterization of pear-gold nanoparticles

The synthesized AuNPs were characterised using various techniques such as UV-Visible (UV-Vis) spectroscopy, Dynamic Light Scattering (DLS), transmission electron microscopy (TEM) and Fourier-Transform Infrared Spectroscopy (FTIR).

2.8.1. Ultraviolet-Visible (UV-Vis) Spectroscopy analysis

The synthesis of AuNPs was characterized by UV-Visible spectroscopy, the primary confirmatory tool for the detection of the surface plasmon resonance (SPR) property of AuNPs. The reduction of the gold ions was monitored from 300-1000 nm on a POLARstar Omega microplate reader (BMG Labtech, Cape Town, South Africa) after a 2-fold dilution of

the samples with deionized water. The recorded spectral data were plotted using Excel and Origin 6.1.

2.8.2. Dynamic light scattering (DLS) spectroscopy analysis

The hydrodynamic size distribution and polydispersity index (PDI) values of freshly synthesized AuNPs were measured at 25 °C using DLS at an angle of 90 ° to the laser beam using the Zetasizer (Malvern Instruments Ltd., UK). Into a 12 mm disposable plastic cuvette, 1 ml of AuNPs was transferred and placed in the instrument. To obtain the averaged corrollogram, 11 runs of 10 seconds' duration was performed. The Z-value as well as the intensity-weight mean value was measured and the average of three measurements was recorded. The intensity-weighted mean value was measured and the average of three measurements taken. The data was analysed with Zetasizer software version 7.11.

2.8.3. High Resolution Transmission Electron Microscopy (HRTEM) and Energy Dispersive Spectroscopy (EDS) analysis

High resolution transmission electron microscopy (HRTEM) was used to characterize the morphology, size and dispersion of the synthesized, optimised AuNPs. A single drop of the biogenic synthesised AuNP solution was loaded onto the carbon-coated copper grid and allowed to dry for several minutes under a Xenon lamp. The grid was analysed under the microscope at an accelerating voltage of 200 kV in bright field mode. HRTEM micrographs were obtained from the FEI Tecnai G² 20 field-emission gun (FEG) HRTEM. Energy dispersive spectra (EDS) were collected using an EDAX liquid nitrogen cooled Lithium doped Silicon detector to confirm the presence of the different elemental composition of the sample.

2.8.4. Fourier Transform Infrared (FTIR) spectroscopy analysis

For FTIR analysis, freeze-dried pear extract samples and air-dried (at room temperature) AuNPs samples from the RP, GP, RF and GF were added to KBr powder, grounded and pressed into a round disk. A pure round disk of KBr was used for background correction. FTIR analysis was conducted by PerkinElmer spectrum one FTIR spectrophotometer (Waltham, MA, USA) with use of the software, Spectrum. The measurements were done using attenuated total reflectance (ATR) accessory.

2.9. *In vitro* stability testing of pear-gold nanoparticles

To evaluate the *in vitro* stability of AuNPs in the presence of various aqueous buffer solutions (water and PBS) and media (Nutrient broth, RPMI, MHB and DMEM supplemented with 10% FBS), 1:1 solution of freshly synthesized AuNPs solution was mixed with aqueous buffer solutions and media respectively and incubated at 37 °C for 24 hours. The stability of the AuNPs were recorded by measuring the UV-Vis spectra and determine whether there were any significant alterations in the surface plasmon wavelength of the samples at 1, 3, 6, 24 and 48 hours.

2.10. Antimicrobial activity pear-gold nanoparticle

The antimicrobial activity of the AuNPs was studied against Gram negative bacterial strains, *E. coli* and *P. aeruginosa* and Gram positive bacterial strains, *S. aureus* and *S. epidermis* on Mueller-Hinton agar (MHA) plates using the agar well-diffusion assay according to the method of Dhand *et al.*, 2016. The assay was used to evaluate the inhibition of bacterial growth by the freshly synthesised AuNPs (RP-AuNPs, GP-AuNPs, RF-AuNPs and GF-AuNPs) and the aqueous pear fruit extracts (RP, GP, RF and GF). Fresh sub-cultures of each of the bacterial strains were prepared by aseptically streaking the frozen stocks with a sterile loop onto Mueller Hinton agar (MHA) plates and maintained overnight at 37 °C. Single colonies were then inoculated into Mueller-Hinton broth (MHB) and incubated at 37 °C with shaking overnight. The number of bacterial cells was determined and adjusted to 0.5 MacFarland using OD₄₅₀ to give a final cell concentration $1 - 2 \times 10^8$ CFU/ml. The cultures were swabbed on the test media with sterile cotton swabs. Six wells of approximately 6 mm were created on each MHA plate with a gel puncture and the wells were treated with 50 µl of each sample in triplicates. Ampicillin was used as a standard antibiotic and was added to a single well on each plate as a positive control in order to demonstrate growth inhibition. A negative control included MHB. The plates were incubated at 37 °C for 24 hours. Antimicrobial activity was evaluated by measuring zone of inhibition (clear zone) against the test organism.

2.11. Cytotoxicity activity of pear-gold nanoparticle

The toxicity of the AuNPs were tested on the non-cancerous human fibroblast cell line (KMST-6). The cells were maintained in DMEM containing 10% FBS in a 37 °C humidified incubator with 5% CO₂ saturation. The viability of the KMST-6 cells was evaluated using the WST-1 assay. The cells were seeded in 96-well microtitre plates at a density of 2×10^4

cells/100 µl/well. The plates were incubated at 37 °C in a humidified CO₂ incubator. After 24 hours, the culture medium was replaced with fresh medium containing the AuNPs at increasing concentrations of 0.125 and 2 mg/ml. As a positive control, cells were treated with 10-15 % DMSO, which is a known inducer of apoptotic cell death. Untreated cells were used as a negative control. All treatments were done in triplicate. After 24 hours, the AuNPs were removed and the wells were washed with PBS to ensure complete removal of AuNPs. Thereafter, 100 µl of WST-1 reagent (prepared from 5.0 mg/ml stock solution and diluted with DMEM medium using a dilution factor of 1:10) were added to each well. The plates were incubated again at 37 °C for 4 h. The WST-1 reagent was then removed and replaced with 100 µl alkaline DMSO. After a 15 minutes incubation period at 37 °C, the absorbance of the samples was measured at 540 nm using the microtitre plate reader. The absorbance at 630 nm was used as a reference wavelength. The percentage of cell viability was calculated using the following equation:

$$\% \text{ cell viability} = \frac{\text{sample absorbance} - \text{cell free sample blank}}{\text{negative control absorbance}}$$

2.12. Statistical analysis

The data presented are means \pm standard deviation (SD) obtained from at least three independent experiments. Differences between the means were considered to be significant if $p < 0.05$ according to Prism's two-way ANOVA.

CHAPTER 3

THE SYNTHESIS, CHARACTERISATION AND STABILITY OF GOLD NANOPARTICLES SYNTHESISED FROM PEAR FRUIT EXTRACT

3.1. Introduction

Plant or fruit capped gold nanoparticles (AuNPs) can be synthesized using green chemistry, where gold ions (Au^{3+}) are reduced to gold atoms (Au^0) in the presence of plant or fruit extract as a reducing agent (Nune *et al.*, 2009). This has become a popular method due to its effectivity, simplicity and low cost (Ghodake *et al.*, 2010; Kumar *et al.*, 2012). In recent years, this method has been improved through altering various parameters in order to improve properties of the synthesised nanoparticles (NPs). Literature suggests that controlling the reaction parameters can influence the quality of the AuNPs (Ghodake *et al.*, 2010; Elbagory *et al.*, 2016). In order to produce AuNPs through chemical synthesis, a reducing agent is commonly added to the gold salt to reduce Au^{3+} and allowing them to grow into AuNPs. The addition of other organic molecules can be done to surround the AuNPs in order to control their growth, prevent their aggregation and increase their stability. The ability of Bon Rouge pear extracts to provide secondary metabolite, not only capable of reducing the gold salts but also able to provide stabilisation (capping) properties, was examined. The shape, distribution, morphology and surface charges of the AuNPs were studied.

The synthesis of small and uniformly sized NPs still remains a challenge, hence this chapter focuses on the synthesis and characterisation of monodispersed and stable red peel-AuNPs (RP-AuNPs), green peel-AuNPs (GP-AuNPs), red flesh-AuNPs (RF-AuNPs) and green flesh-AuNPs (GF-AuNPs) using an eco-friendly approach to be applied in a biological application. Several activities are reported in this chapter, including the (1) synthesis of AuNPs (a) with the effect of temperature, (b) pear extract concentration and (c) the kinetics of the formation of AuNPs and (2) characterisation of AuNPs using Ultraviolet-Visible (UV-Vis) spectroscopy, dynamic light scattering (DLS) analysis, High Resolution Transmission Electron Microscopy (HRTEM), Energy Dispersive X-ray (EDX) Spectroscopy and Fourier-Transform Infrared (FTIR) spectroscopy. This chapter also reports on the stability of the synthesized AuNPs in biological buffer solutions. In this study, reaction parameters such as the temperature of synthesis and the concentration of the pear fruit extract were varied individually to investigate the influence that these parameters have on the size and polydispersity index on the AuNPs.

3.2. Results and discussion

3.2.1. Synthesis of AuNPs

Gold nanoparticles (AuNPs) were synthesized through the direct interaction of hydrogen tetrachloroaurate (III) dehydrate ($\text{HAuCl}_4 \cdot 3\text{H}_2\text{O}$) and extracts of pear peels and flesh. Two varieties of pears, the yellow-green Bon Chretien and red Bon Rouge were used as described in Section 2.7. In these synthesis reactions, $\text{HAuCl}_4 \cdot 3\text{H}_2\text{O}$ was used as the gold precursor, while the fruit extracts was the reducing and stabilising agent for AuNP synthesis. The peel and flesh extracts of Bon Chretien were referred to as green peel (GP) and green flesh (GF), respectively. The peel and flesh extracts of Bon Rouge were referred to as red peel (RP) and red flesh (RF), respectively. The yellow to red-purple colour change as shown in figure 3.1 indicated the formation of AuNPs. Reactions with the RP and GP extracts produced a red colour change, whereas the RF and GF extracts produced a purple colour change. This red-purple colour is a characteristic of colloidal AuNP solutions and is the result of the collective oscillation of free conduction electrons or surface plasmon resonance (SPR). SPR is induced by an interacting electromagnetic field which is not observable in individual atoms or bulk material (Philip, 2010 and Rastogi and Arunachalam, 2012). These optical changes confirmed the presence of AuNPs and that the phytochemicals or/secondary metabolites present in the pear fruit extracts were capable of reducing Au^{+3} ions to Au^0 . These reactions were carried out at three different temperatures (25, 70 and 100 °C). The rate of the colour change varied and was dependent on the temperature of the reaction. At 100 °C and 70 °C, the colour change occurred within 1 hour, while at a lower temperature of 25 °C, the colour changes only occurred after 24 hours.

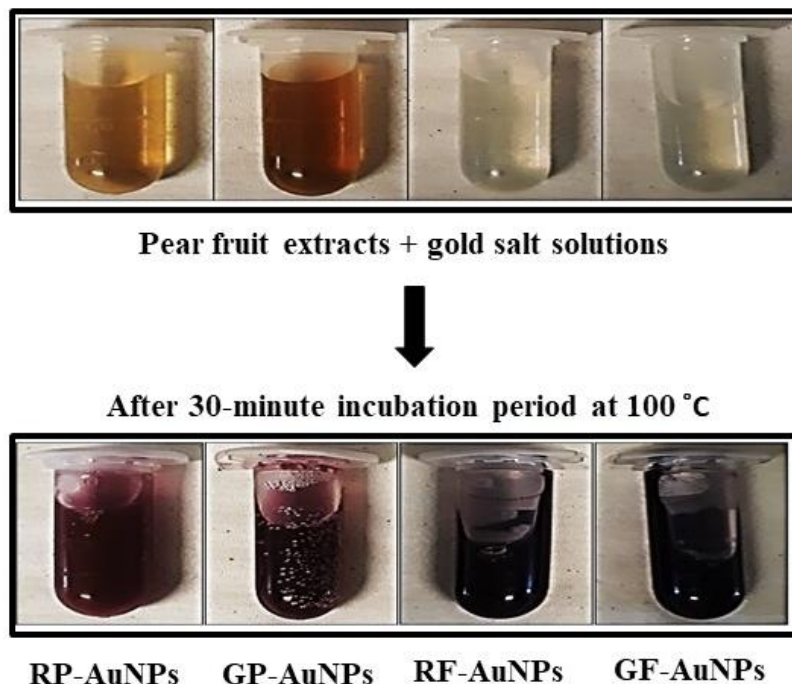


Figure 3.1. Changes in the colour of the synthesis reaction, indicative of AuNP synthesis. Digital photographs displaying a colour change from yellow to red/purple, following the incubation of red peel (RP), green peel (GP), red flesh (RF) and green flesh (GF) extracts with $\text{HAuCl}_4 \cdot 3\text{H}_2\text{O}$ at $100\text{ }^\circ\text{C}$.

3.2.2. UV-Visible (UV-Vis) spectroscopy analysis

Detailed UV-Vis spectroscopy analysis of the red-purple solutions confirmed the formation of AuNPs. Due to the SPR effect, AuNPs display a strong absorption band in the visible region $500 - 600\text{ nm}$ of the electromagnetic spectrum. Observation of an absorption band in the mentioned wavelength is a distinct feature indicating the presence of AuNPs (Link and El-Sayed, 1999). The SPR band, which can be measured by UV-Vis spectroscopy, provides useful information about the shape, size and relative concentrations of the synthesised NPs, since variations in these parameters affects SPR. Lambda max (λ_{max}) refers to the wavelength in the absorption spectrum where maximum absorbance is observed. Increase in particle size results in an increase in λ_{max} (red shift), and the reduction in particle size leads to the decrease in λ_{max} (blue shift). Uniform isotropic AuNPs will produce a narrow SPR band between $500 - 600\text{ nm}$, while isotropic AuNPs will produce a broad and asymmetrical SPR bands. Furthermore, the existence of SPR band in the near infrared (NIR) region can be attributed to longitudinal SPR which indicates the presence of rod-shaped NPs (Noruzi, 2015). An increase in the optical density or absorbance, correlates linearly to the concentration of the AuNPs in

solution. The SPR of AuNPs can be influenced by various factors such as shape, size, free-electron density, inter-particle interactions and the surrounding medium which indicates that UV-Vis spectroscopy can be used to monitor the aggregation or stability of NPs (Amendola and Meneghetti, 2009).

3.2.2.1. Establishing the optimum conditions for AuNPs synthesis

3.2.2.1.1. Effect of pear extract concentration and temperature on AuNPs synthesis

Previous studies have reported on the biogenic synthesis of AuNPs mediated by fruit and plant extracts by mixing fixed concentrations of $\text{HAuCl}_4 \cdot 3\text{H}_2\text{O}$ with extract solutions. The absorption spectra in these studies showed that plant extract concentration and temperature plays an important role in controlling the size and shape of NPs (Ghodake *et al.*, 2010 and Elbagory *et al.*, 2016). To investigate the effect of pear fruit extract concentration and reaction temperature on AuNP synthesis in this study, synthesis was performed at various concentrations of pear fruit extracts (6 mg/ml – 48 mg/ml) and reaction temperatures (25 °C, 70 °C and 100 °C) to determine the optimum concentration (OC) of the extract and optimum temperature (OT) for AuNPs synthesis. The concentration of the $\text{HAuCl}_4 \cdot 3\text{H}_2\text{O}$ (1 mM) however, was kept constant. The OC and OT were considered as the concentration of the plant extract and the reaction temperature at which the smallest and most uniform AuNPs were produced. These conditions were determined based on the SPR (λ_{max}) and the uniformity of the UV-Vis curve and well as the particle diameter (PD) and the polydispersity index (PDI) of the synthesised AuNPs.

Figure 3.2 shows the changes in the UV-Vis spectra observed for AuNPs synthesised at (25 °C, 70 °C and at 100 °C) using increasing concentrations (6 – 48 mg/ml) of the four fruit extracts. Twelve different synthesis conditions (varying fruit extract concentration and temperature) were tested. A SPR band between 500 – 600 nm was observed for all these conditions, suggesting that AuNPs were synthesised. A linear correlation was observed between absorbance (or optical density) and the concentration of the fruit extracts at the different temperatures. However, the absorbance varied significantly between the samples. In general, the SPR bands of AuNPs produced with RP and GP extracts were higher than the AuNPs produced with RF and GF extracts, suggesting that these extracts produced more AuNPs. λ_{max} varied between 530 and 546 nm. It was observed that the SPR band of most AuNP preparations exhibited red shifts as the concentration of the fruit extract increased,

indicating the formation of AuNPs with a larger size. This suggests that by increasing the concentration of the reducing agent (pear fruit extract), particles with larger diameter was being produced (at 100 °C with a concentration of 12 mg/ml, RF and GF produced AuNPs with a λ_{max} of 542 nm and an average diameter of 116.5 nm and 145.7 nm respectively, while at 48 mg/ml RF and GF produced AuNPs with a λ_{max} of 550 nm and 544 nm and an average diameter of 170.3 nm and 182.4 nm respectively). By increasing the concentration of RP, blue shifts were exhibited, producing RP-AuNPs with a smaller diameter (at 6 mg/ml RP produced AuNPs with a λ_{max} of 554 nm and an average diameter of 80.3 nm while at a concentration of 48 mg/ml RP produced AuNPs with a λ_{max} of 546 nm and an average diameter of 55.6 nm at 100 °C). The same was observed for GP-AuNPs synthesised at 100 °C (at 12 mg/ml GP produced λ_{max} of 550 nm with particles of an average diameter of 80.8 nm while at 48 mg/ml GP produced AuNPs with a λ_{max} of 532 nm and an average diameter of 70.6 nm). These changes in the UV-Vis spectra and NP diameter in relation to the changes in concentration of the pear extracts were also observed at 25 and 70 °C. At 25 °C the SPR of the OCs of RP, RF and GF (24 mg/ml) exhibited blue shifts while the red shifts were exhibited for the OC of GP (24 mg/ml) compared to the SPR of the lower concentrations. At 70 °C the SPR of the OCs of RP (48 mg/ml) and RF (24 mg/ml) exhibited blue shifts while the red shifts were exhibited for the OCs of GP (24 mg/ml) and GF (48 mg/ml) compared to the SPR of the lower concentrations. However, at 100 °C, the SPR of the OCs of RP (24 mg/ml) and GP (48 mg/ml) exhibited blue shifts while the red shifts were exhibited for the OCs of RF and GF (24 mg/ml) compared to the SPR of the lower concentrations. The OCs was not only determined based on the SPR (λ_{max}) and the uniformity of the UV-Vis curve but also on the PD and the PDI of the synthesised AuNPs.

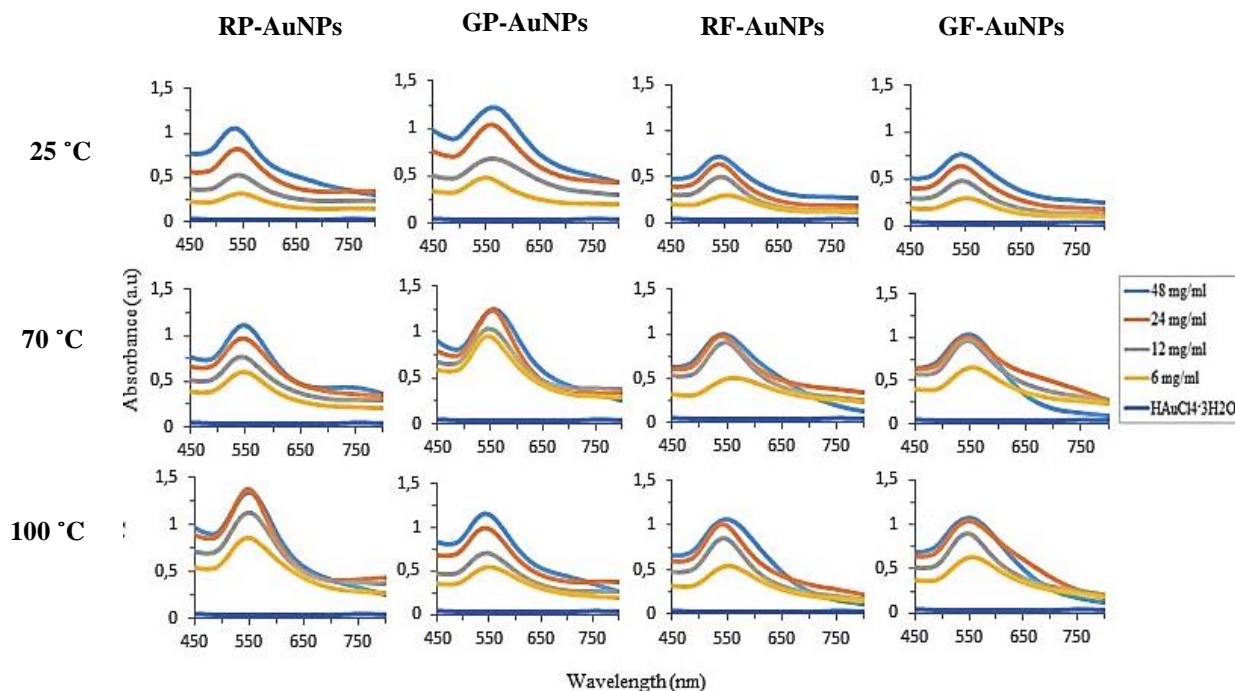


Figure 3.2 Effect of temperature on the synthesis of AuNPs from pear fruit extracts at various concentrations. Synthesis was performed at 25, 70 and 100 °C using increasing concentrations (6 – 48 mg/ml) of red peel (RP-AuNP), green peel (GP-AuNP), red flesh (RF-AuNP) and green flesh (GF-AuNP).

At the OCs of the pear extracts, data from the UV-Vis spectra (Figure 3.2) shows that the λ_{max} of RP-AuNPs, GP-AuNPs, RF-AuNPs and GF-AuNPs synthesised at 25 °C could be observed at 548 nm, 558 nm, 544 nm and 538 nm, respectively. The reaction time for the production of these AuNPs at 25 °C was slow, requiring 24 hours to observe a colour change. When the reaction temperature was raised to 70 °C, λ_{max} for RP-AuNPs, GP-AuNPs, RF-AuNPs and GF-AuNPs was observed at 546 nm, 554 nm, 542 nm and 546 nm, respectively. The reaction time was significantly increased at 70 °C with AuNP formation evident within 1 hour. Increasing the reaction temperature can lead to an increase in NP size, as is evident from the red shifts in the λ_{max} , but this is not true for all fruit samples. The largest absorption peaks were observed at 100 °C after 30 minute synthesis. In addition to faster reaction times, shifts in λ_{max} were also evident, meaning that at a higher temperature of 100 °C, AuNPs in some pear samples became smaller in size. The λ_{max} for RP-AuNPs, GP-AuNPs, RF-AuNPs and GF-AuNPs synthesised at 100 °C could be observed at 546 nm, 532 nm, 540 nm and 544 nm, respectively. Shifts in the peak wavelength when comparing the different temperatures suggest a difference in size and dispersity of the AuNPs. The wavelengths that registered at lower temperatures (25 °C and 70 °C) indicated larger sized RP-AuNPs (95.2 nm at 25 °C; 66.5 nm at 70 °C and 71 nm at 100 °C) and GP-AuNPs (89.6 nm at 25 °C; 78.5 nm at 70 °C and 70.6 at

100 °C) and at a higher temperature (100 °C) yielded smaller particle sizes at higher concentrations of the pear fruit extract. However, smaller sized RF-AuNPs (73.6 nm at 25 °C; 112.9 nm at 70 °C and 168.2 nm at 100 °C) and GF-AuNPs (157.4 nm at 25 °C; 148.1 nm at 70 °C and 181 nm at 100 °C) were produced at lower temperatures and increased in size with an increase in temperature. Table 3.1 summarises the optimum conditions for each pear extract at 25, 70 and 100 °C.

Table 3.1. Optimum concentration (OC), λ_{\max} , particle diameter (PD) and polydispersity index (PDI) of the AuNPs synthesised from RP, GP, RF and GF pear extracts at 25 °C, 70 °C and 100 °C.

	Pear extract	RP	GP	RF	GF
25 °C	OC (mg/ml)	24	24	24	24
	λ_{\max}	548	558	544	538
	PD (nm)	95,2	89,6	73,6	157,4
	Pdi	0,271	0,518	0,51	0,47
70 °C	OC (mg/ml)	48	24	24	48
	λ_{\max}	546	554	542	546
	PD (nm)	66,5	78,5	112,9	148,1
	Pdi	0,477	0,498	0,478	0,53
100 °C	OC (mg/ml)	24	48	24	24
	λ_{\max}	546	532	540	544
	PD (nm)	71	70,6	168,2	181
	Pdi	0,297	0,408	0,355	0,32

Figure 3.3 displays the UV-Vis spectra of AuNPs synthesised under the optimum conditions for RP, GP, FR, and GF pear extracts. This figure displays a comparison of the UV-Vis spectra of the AuNPs synthesised under their optimum conditions. As is clearly seen in all four UV-Vis spectra, RP-AuNPs exhibited a maximum absorbance (λ_{\max}) of 542 ± 2 nm, GP-AuNPs of 532 ± 2 nm, RF-AuNPs of 544 ± 3 nm and GF of 544 ± 4 nm. These wavelength values corresponded to the average values of the peak positions on repeated measurements. The bands generated by RP-AuNPs and GP-AuNPs were more symmetrical and sharper than that of RF-AuNPs and GF-AuNPs which may be indicative of better uniformity in the size distribution. In all four AuNP samples, a minimum absorption tail was shown towards the near infrared

region (NIR) which may be indicative of their stability and/or lack of anisotropic NPs. The same OC (24 mg/ml) was used for RP, RF and GF and 48 mg/ml for GP, however RP-AuNPs generated a band at a higher absorbance intensity than GP-AuNPs, RF-AuNPs and GF-AuNPs. This may be the result of the various peptides and/or proteins from each pear extract which could be attributed as reducing agents and that the rapid reduction of ions facilitated by the pear phytochemicals and the high temperature (i.e., high free energy) are important factors in the rapid formation of nuclei and control of secondary growth (Ghodake *et al.*, 2010). The behaviour of these AuNPs are similar to that reported by Ghodake *et al* (2010).

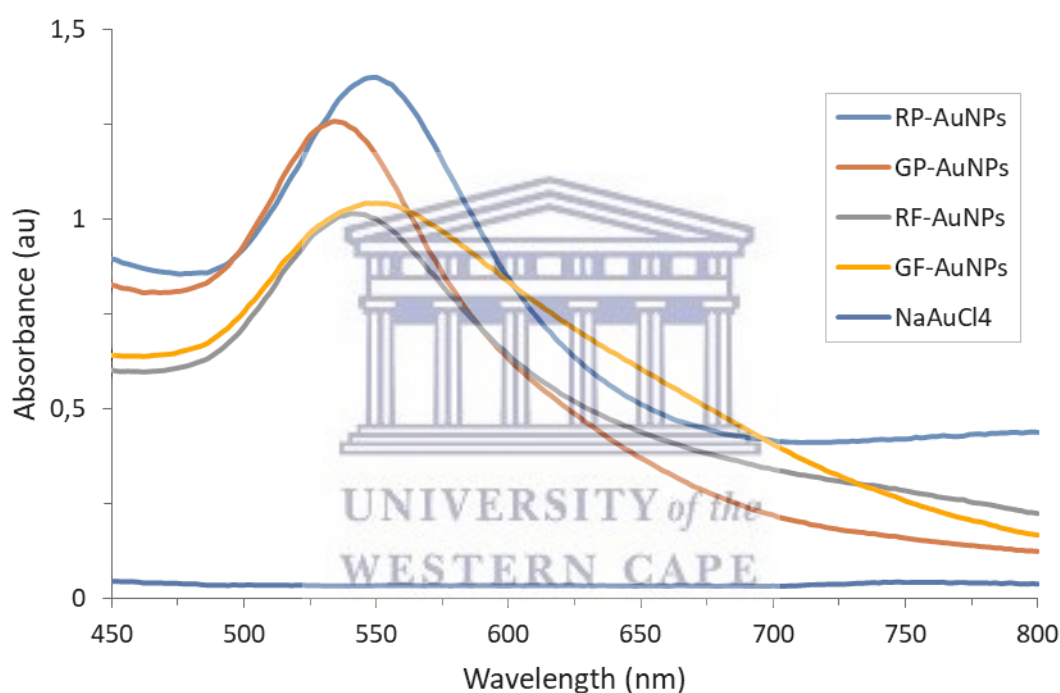


Figure 3.3. Comparative UV-Vis spectra of AuNPs synthesised. UV-Vis spectra of RP-AuNPs, GP-AuNPs, RF-AuNPs and GF-AuNPs synthesized at the optimum conditions (24 mg/ml of red peel, red flesh and green flesh pear extracts and 48 mg/ml of green peel pear extract exposed at 100 °C for 30 minutes) displaying the λ_{max} .

Among the variables, 24 mg/ml of red peel, red flesh and green flesh pear extracts and 48 mg/ml of green peel pear extract exposed at 100 °C for 30 minutes was ideal for AuNP preparation, as figures 3.2 and 3.3 show gold surface resonance occurring between 500 – 600 nm and steadily increased in intensity as a function of temperature and time of reaction without major shift in peak wavelength.

3.2.3. Characterisation of the hydrodynamic diameter and size distribution of AuNPs

Distributions of the hydrodynamic sizes of the AuNPs in the different samples were measured by two different DLS-based techniques; using the Zetasizer (Malvern Instruments Ltd., Malvern, UK). One method was based on size by intensity and the other by the number of AuNPs.

3.2.3.1. Investigating the optimum conditions for AuNPs synthesis

3.2.3.1.1. Effect of pear extract concentration and temperature on AuNPs synthesis

In order to determine the effect of temperature elevation on the synthesis of the AuNPs, the average λ_{max} values, PD and PDI values were calculated. The PDI values in [table 3.1](#) shows that the AuNPs are often more monodispersed when synthesised at 100 °C than at 25 °C or 70 °C. The PDI represents the ratio of particles of different size to total number of particles.

The results are presented in [Figure 3.4A](#), where the scattering intensity is shown as a function of logarithm of the particle diameters. RP-AuNPs and GP-AuNPs displayed bimodal distributions, whereas RF-AuNPs and GF-AuNPs showed multimodal distribution that indicates the anisometric nature of GF-AuNPs compared to the other AuNP samples. In all four cases, the peak intensity of the large particles were higher than the peak intensity of the small particles, which was expected since the particle size distribution based on the light-scattering intensity is greatly influenced by larger particles. On the contrary, the peaks for small particles showed higher intensity in the number-weight based size distribution ([Figure 3.4B](#)), with lower intensities for larger particles as displayed in RF-AuNPs and GF-AuNPs. From [Figure 3.4B](#) it can be observed that the RP and GP were able to synthesize small AuNPs of 10 nm and RF and GF produced AuNPs as small as 50-60 nm in diameter.

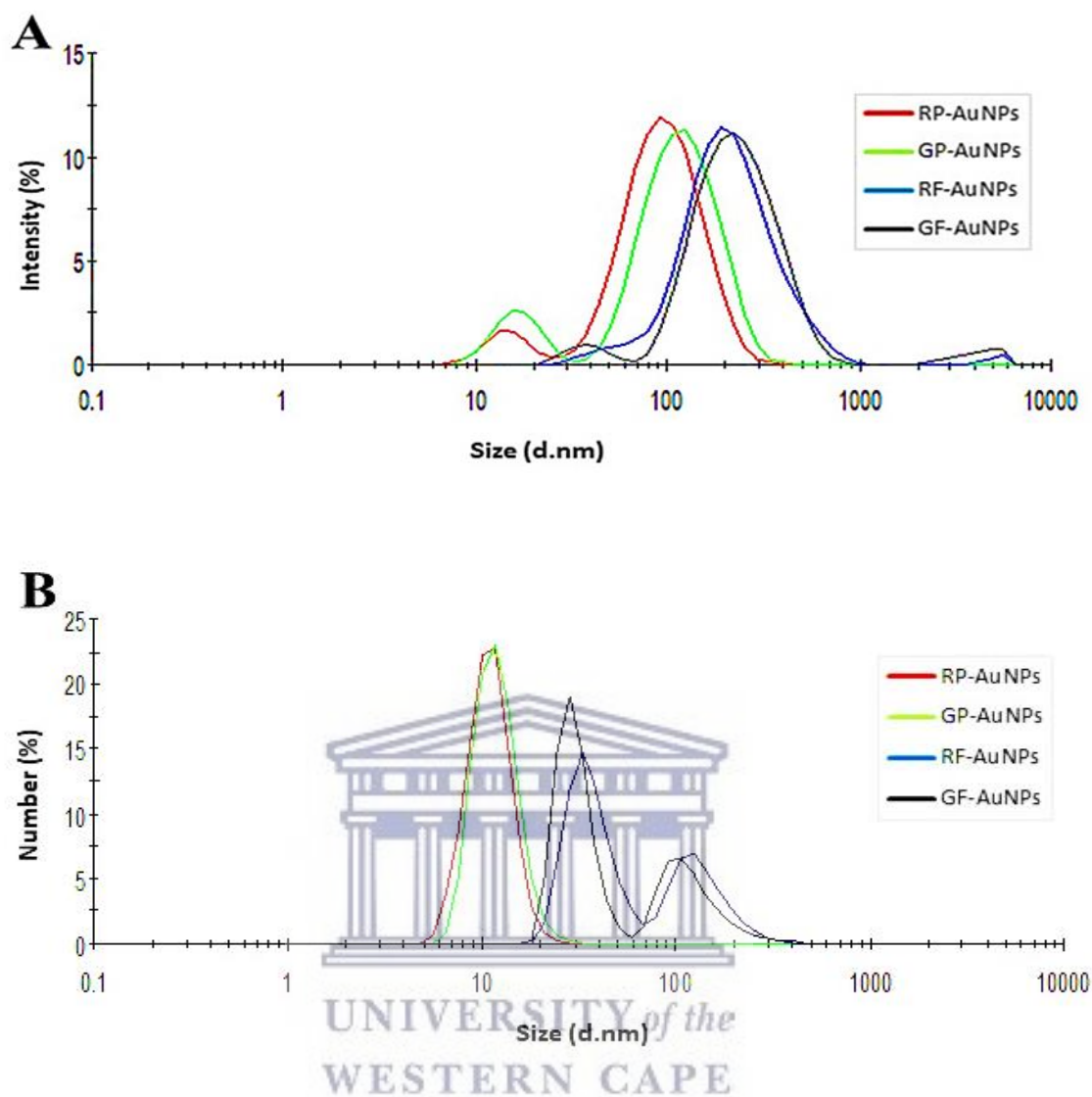


Figure 3.4. Dynamic light scattering (DLS) distribution curve of AuNPs. Distribution curves of RP-AuNPs, GP-AuNPs, RF-AuNPs and GF-AuNPs synthesized at 100 °C displaying the hydrodynamic diameter as a function of (A) intensity and (B) number.

Table 3.2 shows the average diameters of light-scattering intensity peaks shown in Figure 3.4A as well as the Z-average diameter, which is derived from the light-scattering intensity data. In agreement with the distribution to the distribution curves, the Z-average diameter of the RP-AuNPs and GP-AuNPs have a smaller average diameter than RF-AuNPs and GF-AuNP.

Table 3.2. DLS analysis displaying the average hydrodynamic sizes of RP-AuNPs, GP-AuNPs, RF-AuNPs and GF-AuNPs.

Sample	OC (mg/ml)	λ_{\max} (nm)	Small-Particle Size (d.nm)	Large-Particle Size (d.nm)	Z-average (d.nm)	Pdi
RP-AuNPs	4 mg/ml	542 ± 2	13,35 ± 1,6	91.28 ± 1,25	71 ± 1,52	0,295
GP-AuNPs	8 mg/ml	532 ± 2	16,72 ± 0,3	105.7 ± 0,15	70,62 ± 1,13	0,49 ± 0,01
RF-AuNPs	4 mg/ml	544 ± 3	12,74	190.1,4 ± 3,4	168,2 ± 2,5	0,36 ± 0,02
GF-AuNPs	4 mg/ml	544 ± 2	41,81 ± 2	220.2 ± 4,55	180,95 ± 2,15	0,32 ± 0,07

3.2.4. Kinetics of AuNPs formation

Many of the methods used to prepare metallic colloidal particles of uniform size from the growth of metallic seeds are not as successful as they could be due to additional nucleation reactions during the “growth” phase of the synthesis reaction. In the formation of NPs, the kinetics of the reaction plays a vital role as it affects their size (Qureyshi *et al.*, 2016).

To compare the efficiency of AuNP formation between the different pear extracts, the kinetics of AuNPs formation was studied by examining the changes in the λ_{\max} of the AuNPs produced using the different peel and flesh extracts over a time period of 12 hours. The optimum conditions of AuNP synthesis were used in this study. The UV-Vis absorbance was recorded at 24 mg/ml of RP, RF and GF pear extracts and 48 mg/ml of GP pear extract exposed at 100 °C as a function of time (0 time, 5 min, 10 min, 20 min, 30 min, 40 min, 1 hr, 3 hrs, 6 hrs and 12 hrs). An increase in λ_{\max} indicate AuNP synthesis and an increase in the number of the particles. Figure 3.5E clearly shows that the λ_{\max} for NPs synthesised from the peel extracts (RP-AuNP and GP-AuNP) increased before that of the NPs synthesised from the flesh extracts (RF-AuNP and GF-AuNP). For the first 10 minutes of the reactions there was no increase in the λ_{\max} for RF-AuNP and GF-AuNP, while RP-AuNP and GP-AuNP already show an increase. RP-AuNP and GP-AuNP also reached the maximum absorbance at an earlier time point (10 and 20 minutes, respectively) compared to RF-AuNP and GF-AuNP (60 minutes). The delayed increase in λ_{\max} for RF-AuNP and GF-AuNP suggests that AuNP synthesis is much slower and that the reduction power of phytochemicals present in RF and GF extracts are lower than that of the RP and GP extracts. It is possible that RP and GP extracts contain different compounds that have higher reducing power, alternatively RP, GP, RF and

GF extracts contain the same compounds, but RP and GP extracts contain higher concentrations of these compounds.

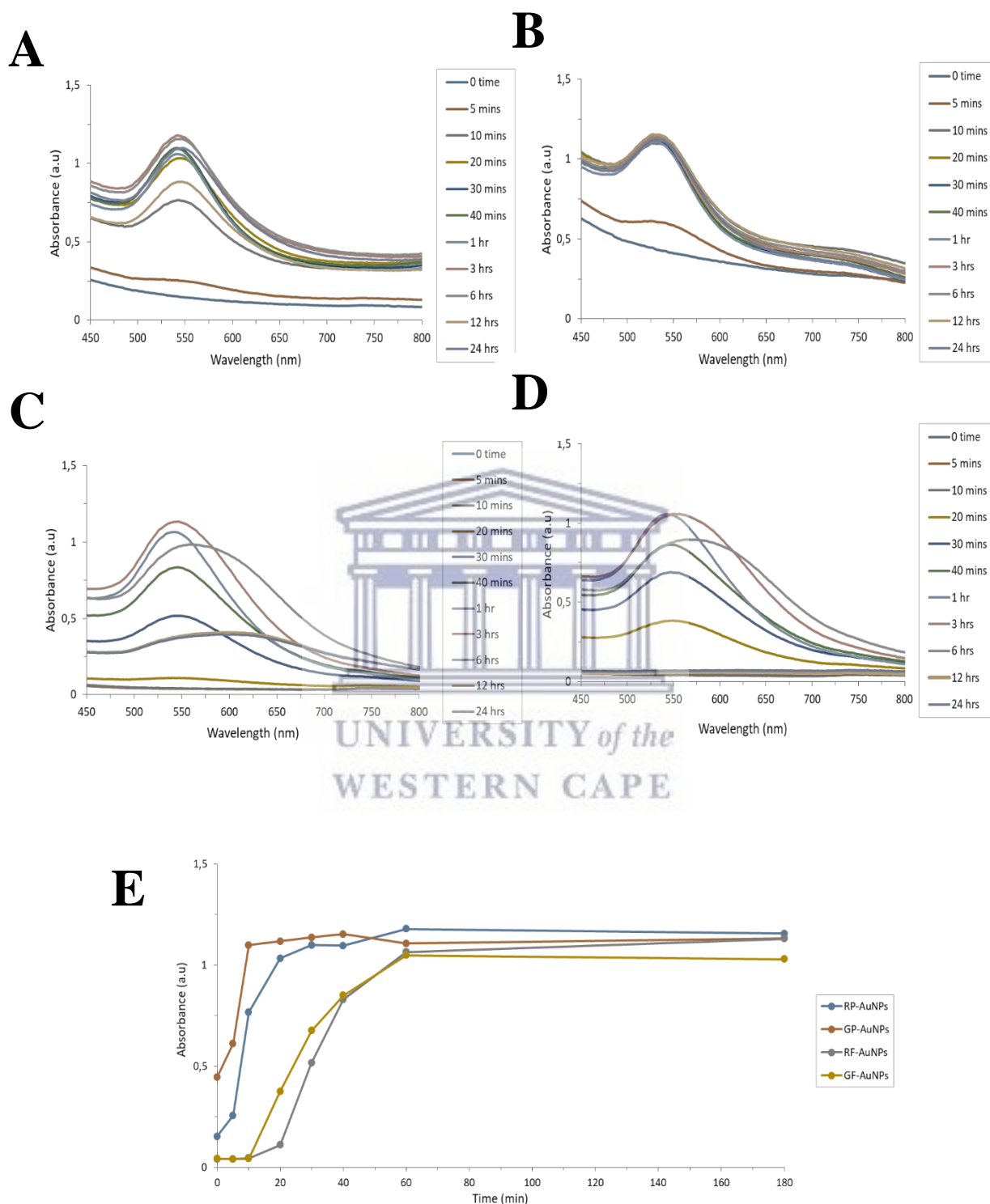


Figure 3.5. Changes in λ_{max} of synthesised AuNPs as a function of time. UV-Vis spectra of (A) RP-AuNPs, (B) GP-AuNPs, (C) RF-AuNPs and (D) GF-AuNPs over 24 hours. (E) displays the changes in λ_{max} values of the four AuNPs samples as a function of time, over the first 180 min.

3.2.5. Characterisation of morphology and size distribution of AuNPs using HRTEM analysis

High resolution transmission electron microscopy (HRTEM) was performed to study the morphology, particle size distribution and crystalline nature of the synthesised AuNPs. A single drop of the biogenic synthesised AuNP solution was loaded onto the carbon-coated copper grid and allowed to dry for several minutes under a Xenon lamp. The grid was analysed under the microscope at an accelerating voltage of 200 kV in bright field mode. HRTEM micrographs were obtained from the FEI Tecnai G² 20 field-emission gun (FEG) HRTEM. Micrograph images of each AuNP sample produced from the pear extracts revealed the existence of particles exhibiting an assortment of geometric shapes, that were mostly spherical and relatively monodispersed with good lattice fringes (Figures 3.7). The smaller detected particles had nearly spherical shapes, while larger particles exhibited various geometrical shape, such as hexagons, pentagons, triangles and truncated triangles. Studies suggest that small sized spherical AuNPs can be synthesised if strong interaction forces between the capping biomolecules and the AuNP surfaces exists which could prevent the nascent AuNPs from sintering (Sujitha and Kannan, 2013). The synthesis of spherical NPs in this study may therefore imply that the capping agents present in the peel and flesh pear extracts exhibit a strong interaction with the newly grown AuNPs and prevent them from developing into other shapes. Yet, some deviations from the spherical shapes were observed in all AuNP samples. This variety of geometrical shapes is typical of AuNPs and has been described in literature (Amendola *et al.*, 2017; Chen *et al.*, 2010; Foss *et al.*, 1994; Kundu *et al.*, 2008).

The particle size distribution of each AuNP was calculated by measuring the circumference of 100 individual particles of the HR-TEM images of RP-AuNPs, GP-AuNPs, RF-AuNPs and GF-AuNPs using Image J software. The particle size range of RP-AuNPs was between 0-30 nm with the largest number of particles between 15-20 nm in diameter. The size range for GP-AuNPs was between 0-20 nm with most of the particles being between 10-12 nm in diameter. The particle size distribution for RF-AuNPs and GF-AuNPs ranged between 0-20 nm and 0-30 nm with the largest number of NPs being 5-10 nm and 10-15 nm in diameter respectively. The core diameters of AuNPs were found to be 15.79 ± 6.02 nm for RP-AuNPs, 10.92 ± 3.6 nm for GP-AuNPs, 12.24 ± 6.77 nm for RF-AuNPs and 18.31 ± 6.91 nm for GF-AuNPs which is reflective of the DLS data (Figure 3.6). Also, the average particle size of RP-AuNPs and GP-AuNPs were smaller than that for RF-AuNPs and GF-AuNPs as obtained by HR-TEM analysis.

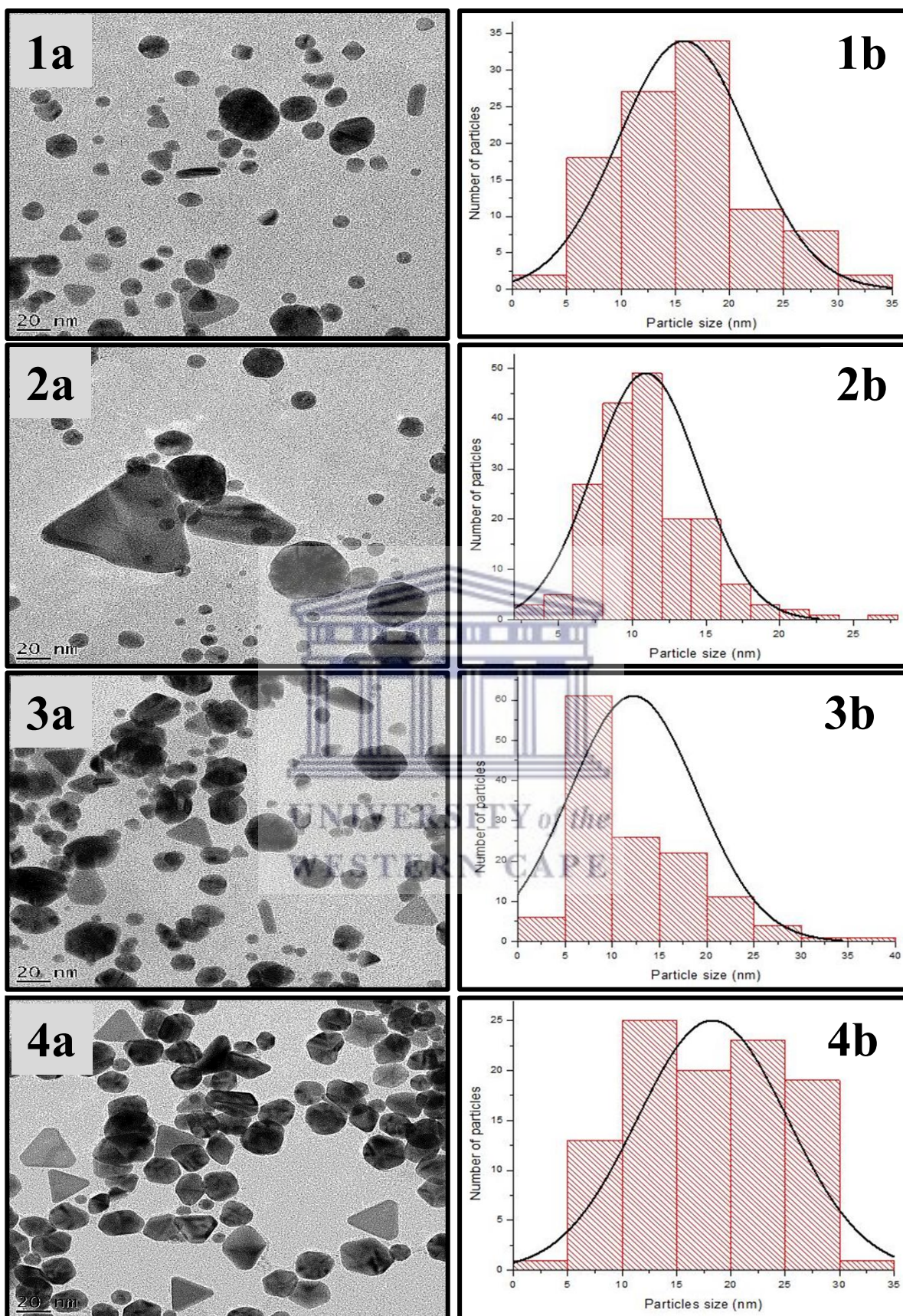


Figure 3.6. HRTEM images displaying AuNP morphology and sizes. (1a), (2a), (3a) and (4a) shows the morphology of RP-AuNPs, GP-AuNPs, RF-AuNPs and RF-AuNPs respectively. (1b), (2b), (3b) and (4b) shows the size distribution of RP-AuNPs, GP-AuNPs, RF-AuNPs and RF-AuNPs respectively.

The crystalline nature of the AuNPs was confirmed by the selected area electron diffraction (SAED). The identified Bragg reflections (bright rings) correspond to the (111), (200), (220), (311) and (222) sets of lattice planes, which can be indexed based in the face center cubic (FCC) structures of gold as aligned by the arrows (Figure 3.7).

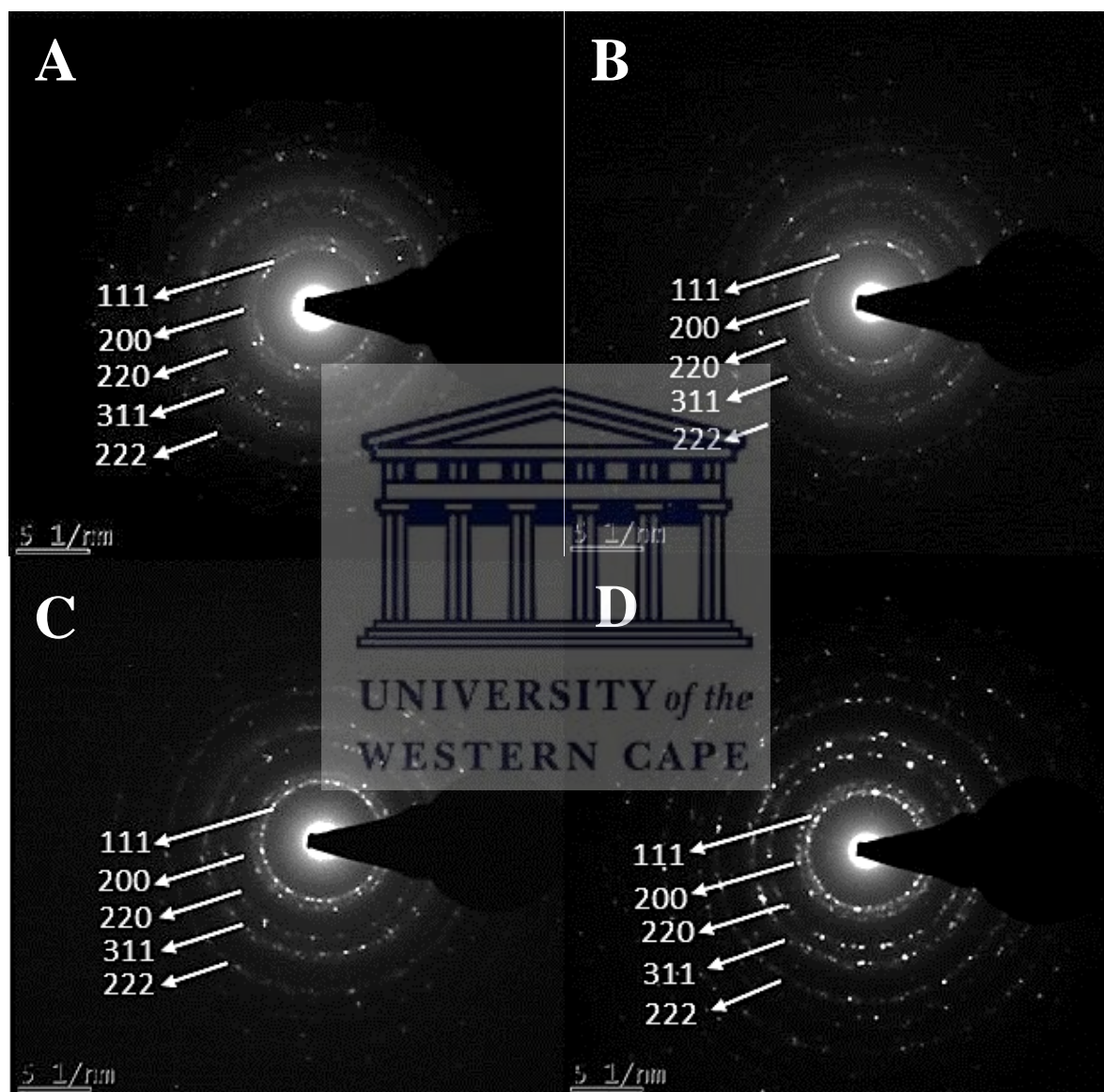
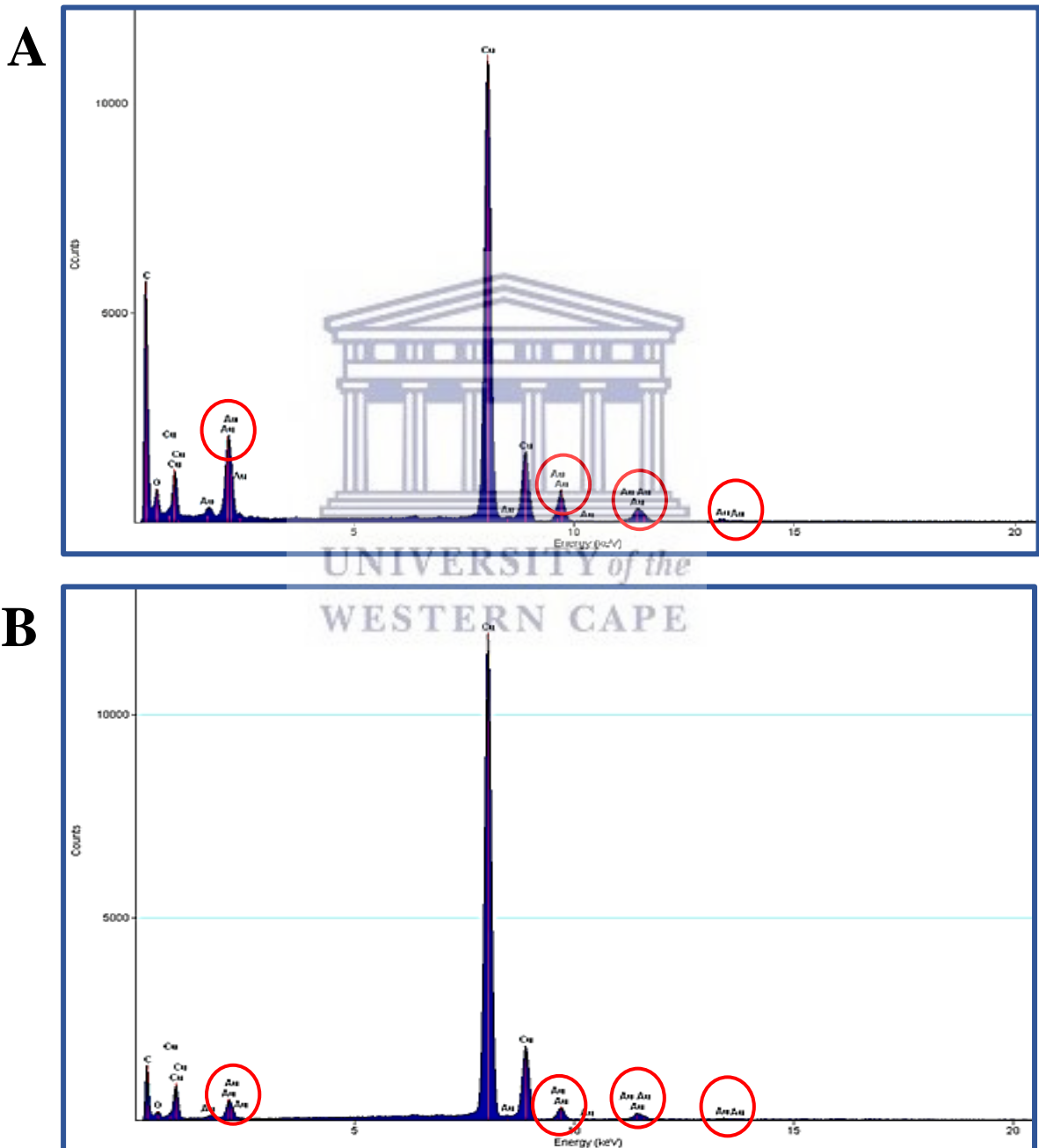


Figure 3.7. SAED analysis of AuNPs. A, B, C and D show analysis of RP-AuNPs, GP-AuNPs, RF-AuNPs and GF-AuNPs respectively.

3.2.6. Elemental composition analysis of AuNPs using Energy Dispersive Spectroscopy (EDS)

The elemental composition of each AuNP was carried out using a field emission (TEC NAI F20 TEM microscope). EDS analysis of RP-AuNPs, GP-AuNPs, RF-AuNPs and GF-AuNPs

show the presence of copper (Cu), carbon (C), oxygen (O) and gold (Au) adsorption peaks (Figure 3.8). Adsorption peaks of gold at 2.3, 9.7 and 11.3 keV are in agreement with previous studies. However, the presence of copper and carbon in the samples is the result of the HR-TEM grid and/or the detector window that the AuNPs were placed on during the analysis. Oxygen peaks were also detected in each AuNP sample which may be attributed to the trace amounts of phytochemicals of the extract capping the AuNPs.



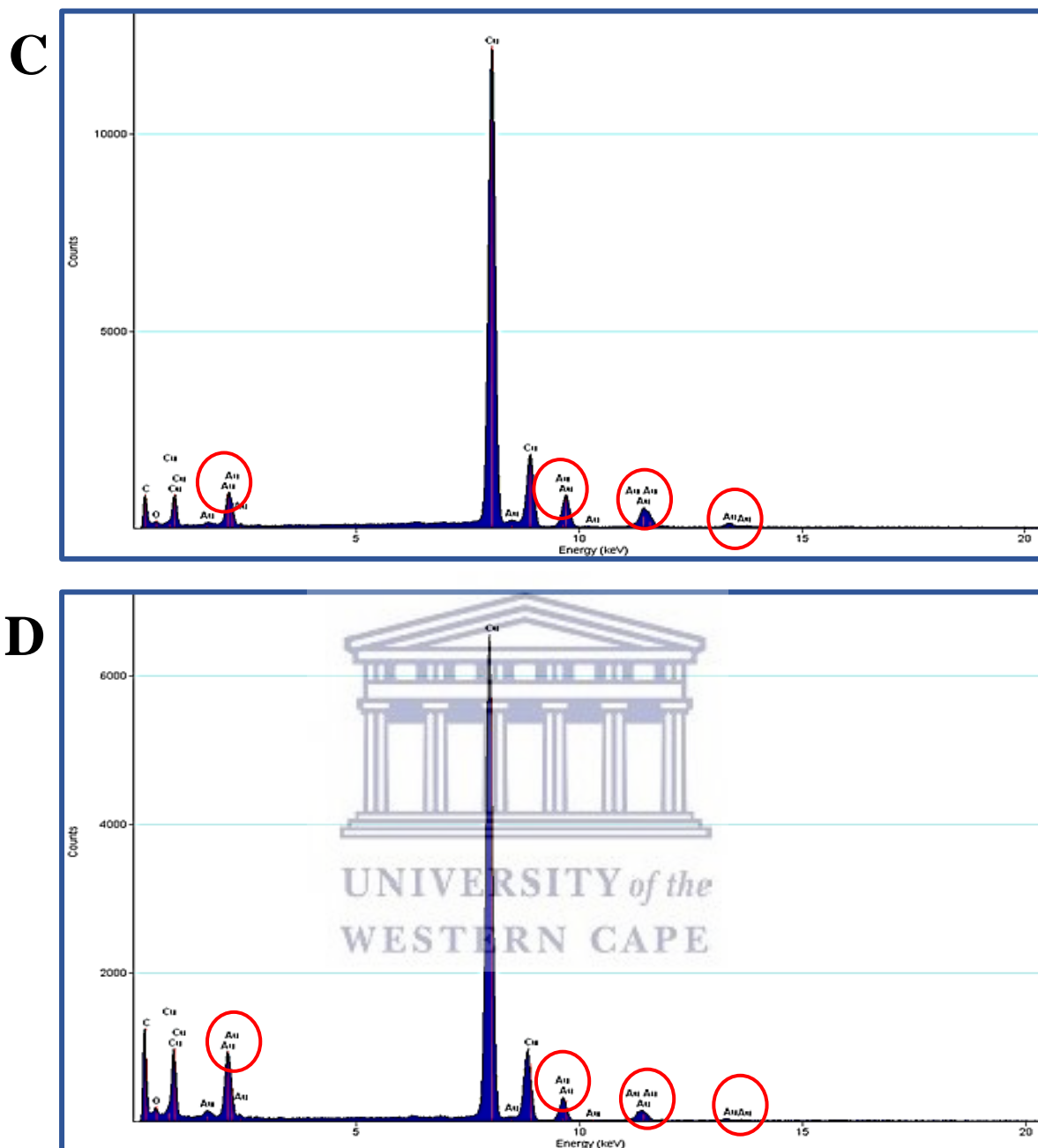


Figure 3.8. EDS spectra of AuNPs. (A) RP-AuNPs (B) GP-AuNPs (C) RF-AuNPs and (D) GF-AuNPs. The circles are indicative of Au peaks.

3.2.7. Characterisation of functional groups present in the pear extracts and the AuNP

Fruits are rich in polyphenolic compounds such as flavonoids, tannins, lignins, phenolic acids and tocopherols (Abdel-Raouf *et al.*, 2017). Some of these molecules play a role in the synthesis and stabilisation of AuNPs (Oueslati *et al.*, 2018). Compounds with antioxidant properties are ideal candidates for the reduction of Au^{3+} to Au^0 and the resultant formation of AuNPs. Fourier Transform-Infrared Spectroscopy (FTIR) is an analytical technique used to identify organic compounds (Faix, 1992).

The functional group region are positioned between $4000 - 1400 \text{ cm}^{-1}$ where the characteristic infrared absorption does not change much from one compound to another. However, in the fingerprint region positioned between $1400 - 600 \text{ cm}^{-1}$, the functional groups are unique and characteristic for the compound as a whole. Peaks in the fingerprint region depend on complex vibrations involving the entire molecule, and it is highly improbable for any two compounds to have precisely the same infrared spectrum.

The FTIR analysis was performed on RP, GP, RF and GF and their respective AuNPs in order to identify the possible functional groups involved in the biosynthesis of AuNPs. This information can be used to identify the phytochemical(s) that may be involved in the reduction of the gold salts and may also determine how these NPs may react with biomolecules and drugs and how these NPs may react with other NPs. The bio-reduction of Au^{3+} using plant extracts continues to be elucidated, despite the increasing attention being given to the biogenic synthesis (Singh *et al.*, 2016). Several studies suggest that various phytochemicals may play a role in the synthesis of AuNPs (Baker *et al.*, 2013). Generally, different chemical classes were found to influence the production of the AuNPs based on the major constituent of each plant extract (Elbagory *et al.*, 2016).

Figure 3.9 displays the FTIR spectra of both the plant extracts and the synthesised AuNPs. The FTIR spectra of RP-AuNPs and GP-AuNPs was similar to the spectra of their corresponding extracts from which they were synthesised. Some peaks were transmitted at similar wavelengths, indicating that the phytochemicals contained in the extract were present on the surface of the AuNPs. However, some bands of the FTIR spectra of the AuNPs appeared to be shifted when compared to the FTIR spectra of the extracts. These shifts were expected and are believed to be caused by the influence of the nearby metal and possibly suggest the involvement of the corresponding functional groups in the AuNP synthesis (Elia *et al.*, 2014). These observed shifts are shown in Table 3.3, which also shows the possible functional groups

involved in the synthesis of AuNPs from the extracts. Some strong peaks were generated in the FTIR spectra of RP-AuNPs and GP-AuNPs indicating that similar functional groups are key players in the synthesis of the AuNPs. The same can be suggested for RF-AuNPs and GF-AuNPs. Strong peaks were generated for both the pear extracts (RP, GP, RF, GF) and the AuNPs (RP-AuNPs, GP-AuNPs, RF-AuNPs, GF-AuNPs) revealing similar broad bands between 3184 and 3333.49 cm^{-1} , which may correspond to the stretching vibration of intermolecular polymeric bonded O-H groups present in alcohol and phenols or N-H groups (1° amines, amides) (Ankamwar *et al.*, 2017). Similarly, sharp peaks observed from 2913.82 to 2931.83 cm^{-1} for all eight samples can be the result of asymmetric stretching of the C-H groups of alkanes (Elbagory *et al.*, 2017). Peaks from 1606.24 to 1636.88 cm^{-1} revealed C=O stretching of flavonoids/phenolic groups and N-H stretching (1° amines, 2° amines) (Ghodake and Lee, 2010). C-N stretching mode from 1411.01 to 1452.62 cm^{-1} , -C-O-H bending, S=O (Sulfones, sulfonates); C-N (Alcohols; carboxylic acid, esters, ethers) and C-H (Alkyl halides) from 1218.27 to 1269.78 cm^{-1} and -C-O-C stretching in ethers, alcohols and polyphenols from 1035.48 to 1052.06 cm^{-1} (Singh *et al.*, 2011; Dorosti and Jamshidi, 2016; Ankamwar *et al.*, 2017; Kumar *et al.*, 2017). The FTIR spectra of RP and GP and their respective AuNPs (RP-AuNPs and GP-AuNPs) revealed the -C-O-C group which is characteristic of monosaccharides from 815.19 to 819.2 cm^{-1} (Abdel-Raouf *et al.*, 2017).

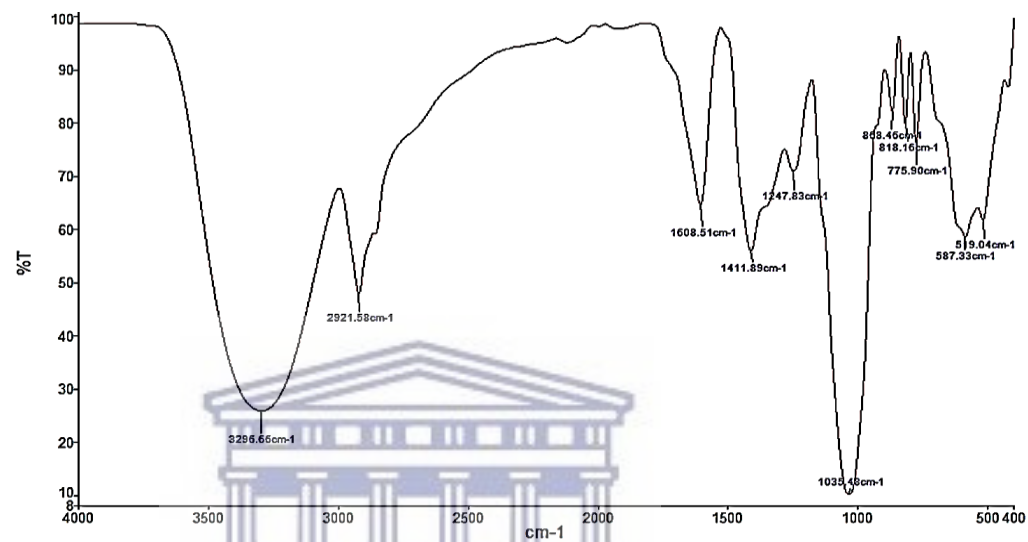
The transmittance of O-H and C-O bands in the FTIR spectra indicates the presence of hydroxyl and carbonyl groups on the AuNPs possibly as a result of the involvement of flavonoids, phenolic compounds, terpenoids and / or carbohydrates in the biosynthesis of the AuNPs (Table 3.3). Researchers in several studies have reported that these hydroxyls and carbonyl containing compounds play a role in the reduction, capping and stabilisation of the AuNPs (Leiva *et al.*, 2009). The carbonyl group forms amino acid residues and peptides of proteins have the stronger ability to bind metal, so that the proteins could most possibly form a coat covering (capping) the AuNPs to prevent agglomeration of the particles and stabilising in the medium. This suggests that the biological molecules could possibly perform the function for the formation and stabilising of the AuNPs in aqueous medium (Abdel-Raouf *et al.*, 2017).

Previous chemical studies have reported that *Pyrus communis* is a rich source of alkaloids, tannins, peptides, carbohydrates, steroids, amino acids, cardiac and coumarin glycosides, flavonoids and phenolic compounds. (Abdel-Raouf *et al.*, 2017). Various functional groups mentioned above are mainly derived from heterocyclic compounds and these are water soluble components of pears. So it is assumed that different water soluble heterocyclic compounds

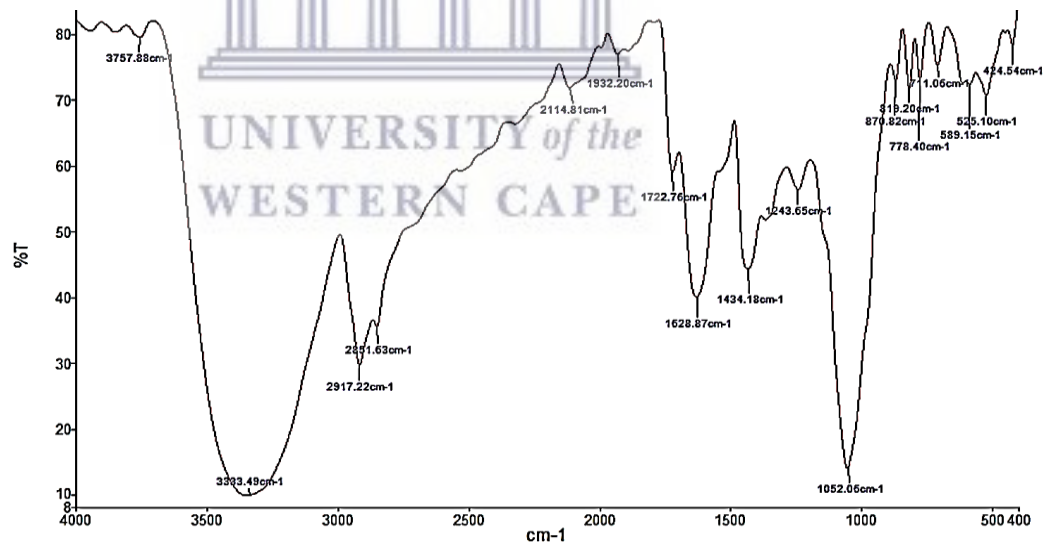
such as alkaloids and flavonoids worked as the capping ligand for the synthesis of AuNPs and the presence of oxygen atoms helped in the stabilisation of AuNPs by facilitating the absorption of heterocyclic compounds on AuNPs (Singh *et al.*, 2011). The phenols, flavonoids, benzophenones and anthocyanins were found to act as reducing agents and accountable for the reduction of the A^{3+} to AuNPs (Sett *et al.*, 2016; Xin Lee *et al.*, 2016). The FTIR spectra of RP-AuNPs, GP-AuNPs, RF-AuNPs and GF-AuNPs showed strong bands at 3333.49, 2917.2 and 1628.87 (RP-AuNPs), 3296.65, 2920.76 and 1636.88 (GP-AuNPs), 3184.85, 2916.36 and 1630.66 (RF-AuNPs) and 3254.11, 2913.32 and 1632.9 (GF-AuNPs) may be assigned to aromatic amines, amide groups of proteins, sugars, secondary alcohols and flavonoid/phenolic groups and arises due to carbonyl stretch and free $-N-H-$ stretch vibrations in the amide linkages of the proteins, respectively. Hence, it is speculated that these bands may be responsible for the reduction, stabilisation and capping of AuNPs (Nadeem *et al.*, 2017; Vijayakumar *et al.*, 2017) However, further tests are required where major compounds can be isolated and tested for the synthesis of the AuNPs in order to identify with certainty the actual functional groups responsible for the synthesis of the AuNPs. This investigation is ongoing.



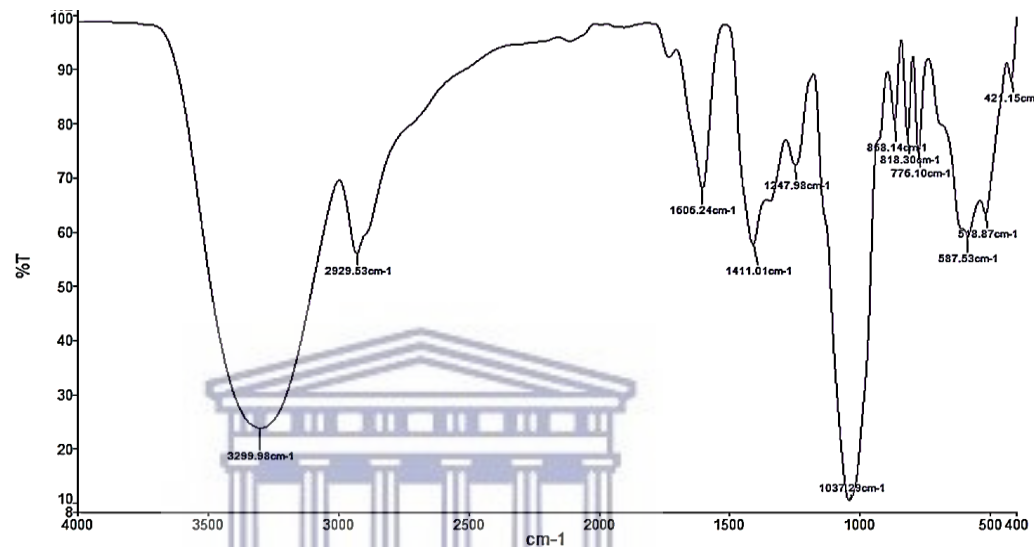
RP pear extract



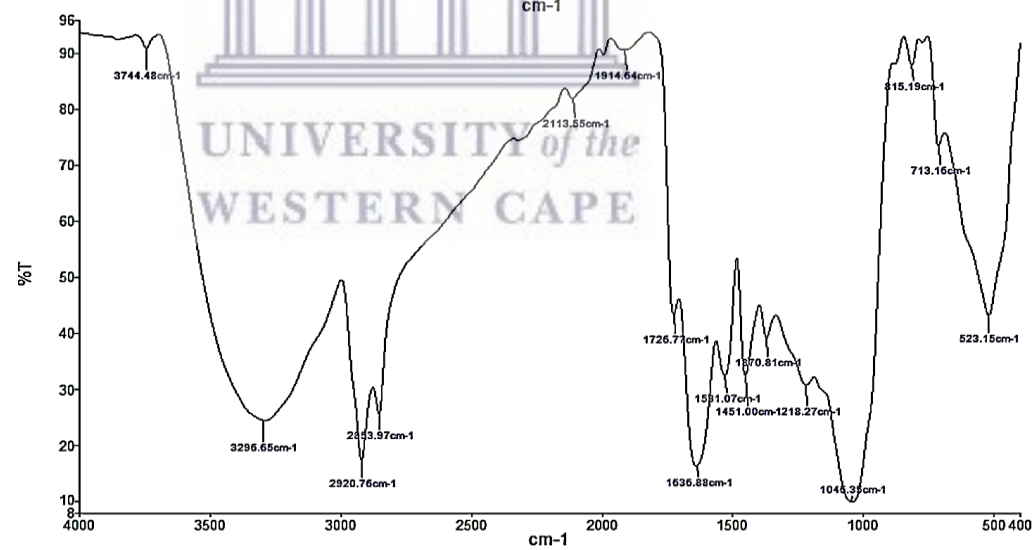
RP-AuNPs



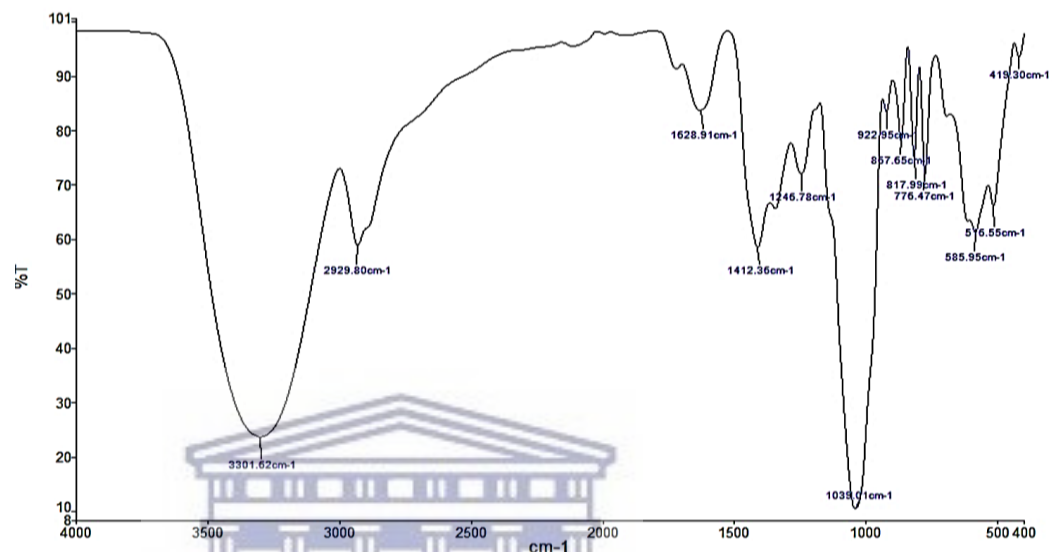
GP pear extract



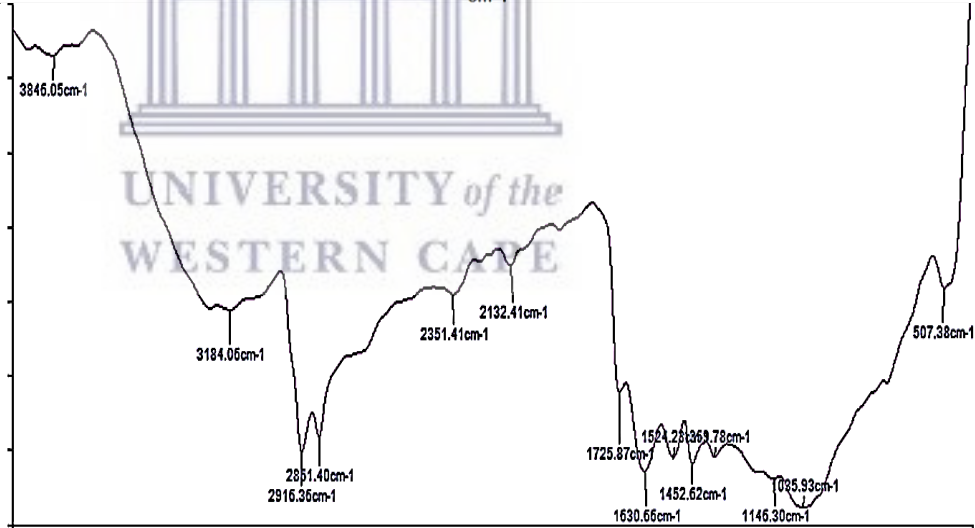
GP-AuNPs



RF pear extract



RF-AuNPs



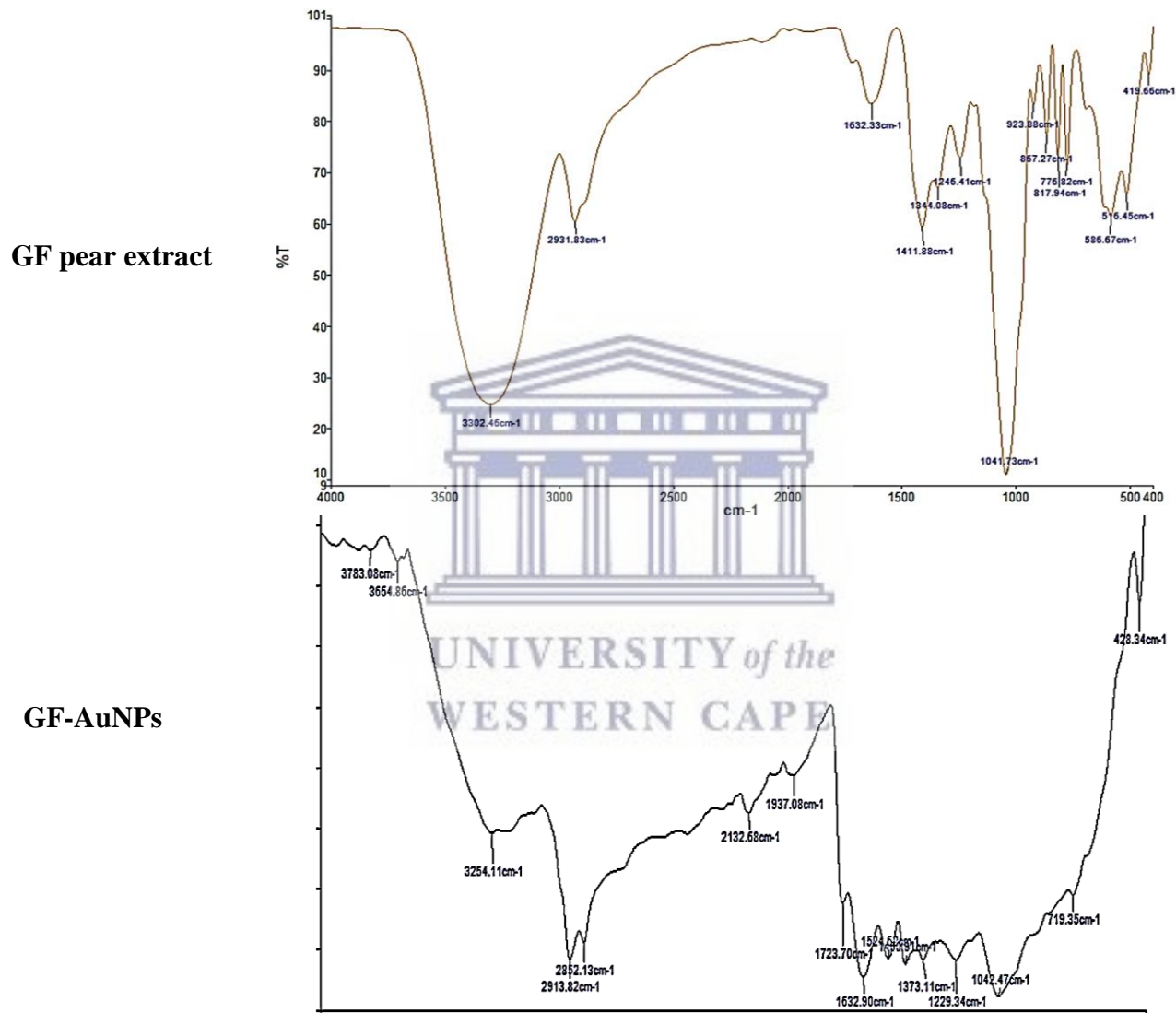


Figure 3.9. FTIR spectra of RP, GP, RF, GF and their respective AuNPs.

Table 3.3. Major peaks shifts in their position in the pear fruit extracts compared to their respective AuNPs. Shift values (cm⁻¹) are given as the subtraction of the peak position in the AuNPs from the position in the extract.

Peak position in RP extract (cm ⁻¹)	Peak position in RP-AuNPs (cm ⁻¹)	Shift in position (cm ⁻¹)	Peak position in GP extract (cm ⁻¹)	Peak position in GP-AuNPs (cm ⁻¹)	Shift in position (cm ⁻¹)	Peak position in RF extract (cm ⁻¹)	Peak position in RF-AuNPs (cm ⁻¹)	Shift in position (cm ⁻¹)	Peak position in GF extract (cm ⁻¹)	Peak position in GF-AuNPs (cm ⁻¹)	Shift in position (cm ⁻¹)	Functional Groups
3296.66	3333.49	-33	3299.98	3296.65	+3.33	3301.62	3184.85	+16.79	3302.46	3254.11	+48.35	O-H (Alcohols, phenols); N-H (1° amines, amides)
2921.58	2917.22	+4.36	2929.53	2920.76	+8.77	2929.8	2916.36	+13.44	2931.83	2913.82	+18.01	C-H (Alkanes)
1608.51	1628.87	-20.36	1606.24	1636.88	-30.64	1628.91	1630.66	-1.75	1632.33	1632.9	-0.57	C=O (Ketones, carboxylic acid, α-, β-unsaturated aldehydes); N-H (1° amines, 2° amines)
1411.89	1434.18	-22.29	1411.01	1451	-39.99	1412.36	1452.62	-40.26	1411.88	1450	-38.12	C-N; C-C (Aromatics)
1247.83	1243.65	+4.18	1247.98	1247.98	+29.27	1246.78	1269.78	-23	1246.41	1229.43	+16.98	C-O-H; S=O (Sulfones, sulfonates); C-N (Alcohols; carboxylic acid, esters, ethers); C-H (Alkyl halides)
1035.48	1052.06	+16.58	1037.29	1046.35	-9.06	1039.01	1035.93	+3.08	1041.73	1042.47	-0.74	C-O-C (Ethers, alcohols, polyphenols)
818.16	819.2	+1.04	818.3	815.19	+3.11							C-O-C (Monosaccharides)
									1344.08	1373.11	-29.03	C-O (Aromatic esters, ethers, carboxylic acids)

3.2.8. *In vitro* stability testing of AuNPs

For AuNPs to be considered for biomedical applications, they need to maintain stability in various buffer solutions. The stability of the AuNPs was measured after incubation in 0.5 % bovine serum albumin (BSA), phosphate buffered saline (PBS), nutrient broth (NB), Mueller Hinton Broth (MHB), Dulbecco's modified eagle medium (DMEM) supplemented with 10 % fetal bovine serum (FBS), Roswell Park Memorial Institute medium (RPMI) and double distilled water. The stability of RP-AuNPs, GP-AuNPs, RF-AuNPs and GF-AuNPs was evaluated by monitoring the changes in the UV-Vis spectra of these NPs in the presence of these buffers over time. When the AuNPs lose their stability, they may precipitate, which can be observed by the significant red shifts and broadening of the UV-Vis bands (Balashanmugam *et al.*, 2018). The AuNPs were incubated in these buffers for 24 hours at 37° C. Figure 3.10 show that there is no change in the UV-Vis spectra of any of these AuNPs in all 7 buffer systems over this period, which suggests that the particles remain monodispersed in the aqueous solution without aggregation. The results confirmed that the AuNPs are intact and thus, demonstrated excellent *in vitro* stability in these buffers (Figure 3.10).

One of the paramount prerequisites of utilising AuNPs for *in vivo* imaging and therapeutic applications is that the NPs can be produced and stabilised in biologically benign media. The stability of AuNPs in physiologic conditions is a very important factor when AuNPs are applied in biology and medicine. The fact that the AuNPs described in this study maintain their stability in various buffer systems makes them suitable for applications in biology and medicine.

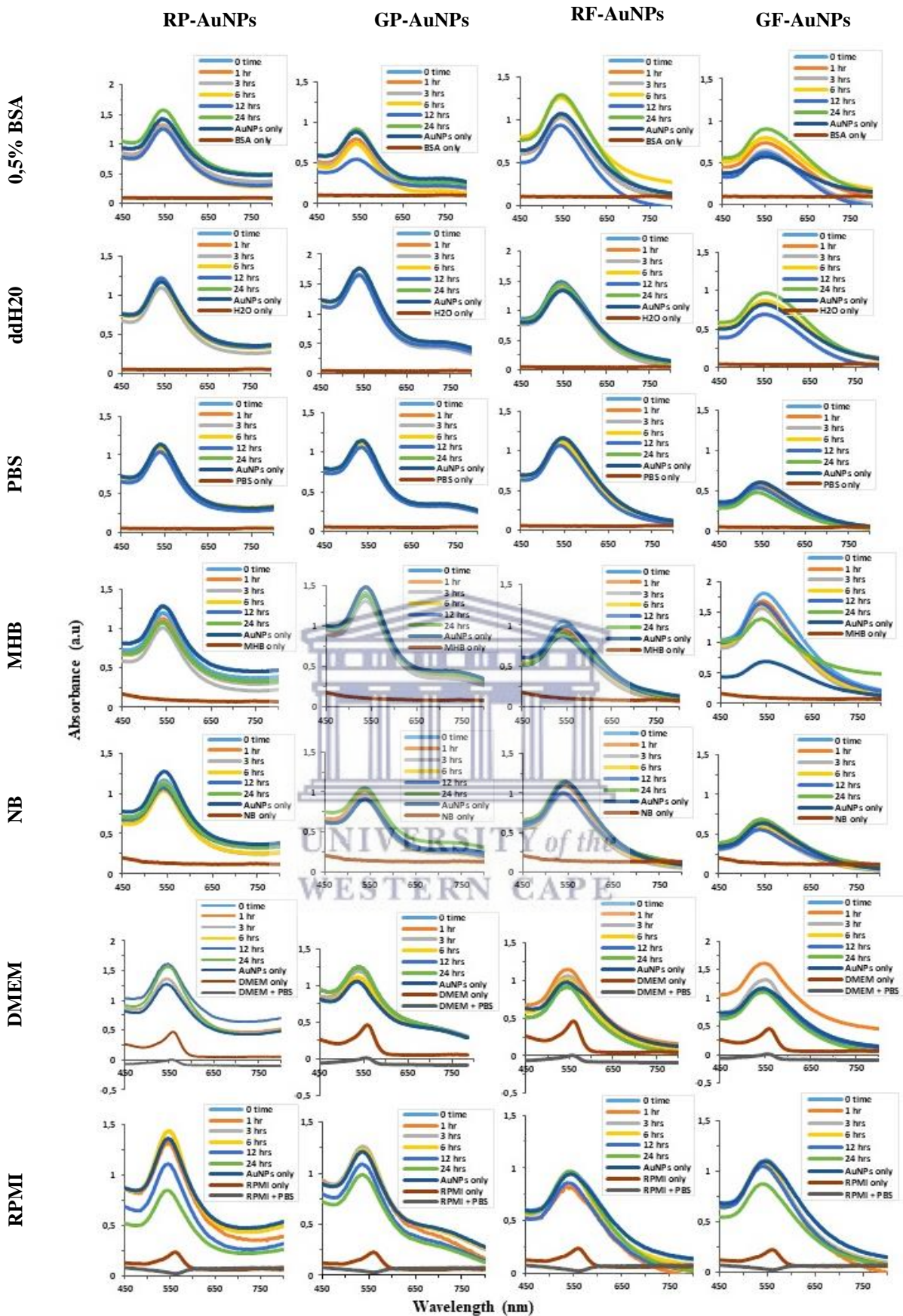


Figure 3.10. *In vitro* stability testing of AuNPs. UV-Vis spectra of RP-AuNPs, GP-AuNPs, RF-AuNPs and GF-AuNPs taken over a 24-hour period in buffers containing 0.5 % BSA, PBS, nutrient broth, Mueller Hinton Broth, DMEM supplemented with 10 % FBS, RPMI and double distilled water.

CHAPTER 4

ANTIMICROBIAL AND CYTOTOXICITY ACTIVITIES OF PEARL-GOLD NANOPARTICLES

4.1. Introduction

In recent years, nanoparticles (NPs) have become a promising and efficient candidate to replace conventional materials with enormous applications in the fields of science and technology. With the unique properties of NPs, such as their higher surface-to-volume ratio and the increased number of active atoms at their outer surfaces, they have proven to be significant materials in the advancement of various novel models and devices that are used in different physical, biological, pharmaceutical and biomedical applications (Shamaila *et al.*, 2016).

Some metallic NPs have been approved as bactericidal and bacteriostatic agents, among those used are silver (Ag), gold (Au), titanium (Ti), copper (Cu), magnesium (Mg) and zinc (Zn), each with different properties and spectrum (Mohamed *et al.*, 2017). These NPs have been under investigation to counter the increase of microbial resistance against the current microbial agents (Elbagory *et al.*, 2017). Gold nanoparticles (AuNPs) in particular, are widely used as a catalyst for gene therapy, medical therapy, biological and diagnostic purposes but apart from their other applications, the antimicrobial activity of AuNPs has been mostly exploited (Nadeem *et al.*, 2017). They pose as a safe and non-toxic antimicrobial agent on a range of several microorganisms due to its functional nature as compared to antibiotics and various other nanomaterials such as silver nanoparticles (AgNPs) (Shamaila *et al.*, 2016).

Researchers have reported that the antimicrobial action of AuNPs is enhanced by their larger total surface area per unit volume, distinctive surface chemistry, size, polyvalent and photothermic nature; therefore allowing AuNPs to possess better antimicrobial action than gold alone (Elbehiry *et al.*, 2018; Nadeem *et al.*, 2017; Shamaila *et al.*, 2016). Gold ions (Au^{3+}) react with SH groups of proteins and play an essential role in bacterial inactivation (Guzman *et al.*, 2012). Reports have also shown that Au^{3+} uncouple respiratory electron transport from oxidative phosphorylation which inhibits respiratory chain enzymes or interferes with membrane permeability to protons and phosphate (Feng *et al.*, 2000). The presence of AuNPs and sulphur in the electron dense granules observed after AuNP treatment in the cytoplasm of bacterial cells suggests an interaction with nucleic acids that probably results in the impairment

of DNA replication. Thus it is reasonable to infer that the biosynthesised AuNPs can be used to manage the disease. Proteomic analysis have also revealed that even a short exposure of nanogold to *E. coli* results in alterations in the expression of a panel of envelope and heat shock protein (Eom *et al.*, 2012). Therefore these particles can penetrate and can disrupt the membranes of bacteria (Abdel-Raouf *et al.*, 2017).

Studies have also shown that the toxicity of AuNPs varies, and is dependent on the nature of the surface coating applied to the NP. Therefore within the same class of NPs, properties change in line with size, geometry, concentration and surface composition. However, not only do AuNP characteristics vary, the experimental conditions also appear to have an effect on the results. The properties of NPs that is, the small size, the geometry, the large surface area, solubility and chemical composition determines the biological response. Consequently, it is imperative to characterise the physiochemical properties of the NP under consideration to correlate them with the biological results (Sanvicens and Marco, 2008).

In the last few decades, green nanoscience and nanotechnology has proven to offer and excel at the opportunities for exploring the effects of metal NPs for antimicrobial activity and environmental issues (Senthilkumar *et al.*, 2017). Generally, the antimicrobial effect of various plant and fruit extracts is well documented and recognised. However, the antimicrobial effect of the biogenic metal NPs produced from such plants and fruit extracts still remains largely unexplored and can prove to be useful in the search for new antimicrobial agents. Biogenic synthesis of AuNPs by the extract of plants or fruits may increase their physiochemical properties at nanoscale and can act as materials for potential application in the field of medicine. Biological molecules have been used to synthesise AuNPs with potent antimicrobial activity. The antimicrobial activity may be due to the synergistic effect of the combination of AuNPs and the extract (Nadeem *et al.*, 2017). Researchers reported the biological activity of AuNPs synthesised by using *Galaxaura elongate* extracts. These NPs showed antimicrobial activity towards *E. coli*, *K. pneumoniae* and *MRSA* (Abdel-Raouf *et al.*, 2017).

Based on published reports on the biogenic synthesis of AuNPs from plants with special pharmacological properties and potential biological applications (section 1.4.2; Elbagory 2016; 2017; Ghodake 2010 and section 1.6. Jin and Sato, 2003; Güven *et al.*, 2006) and given the critical need for new antibiotics, the work in this section of the thesis focuses on evaluating the antimicrobial activity and cytotoxic effects of the pear extracts and their respective AuNPs. The four pear fruit extracts (RP, GP, RF and GF) and their respective AuNPs (RP-AuNPs, GP-

AuNPs, RF-AuNPs and GF-AuNPs) were tested against resistant Gram negative strains, *Escherichia coli* (*E. coli*) ATCC 25922 and *Pseudomonas aeruginosa* (*P. aeruginosa*) ATCC 27853 and Gram positive strains *Staphylococcus aureus* (*S. aureus*) ATCC 29213 and *Staphylococcus epidermidis* (*S. epidermidis*) ATCC 12228 that are known to cause wound infections. Antimicrobial studies were performed using the agar well diffusion assay which is based on the movement of treatment through the agar with the potential of forming zones of inhibition that can be measured following treatment. In order to adequately assess the potential of the synthesised AuNPs as antimicrobials, it was essential to also assess their biocompatibility. The cell proliferation, cell viability and cytotoxicity of the synthesised AuNPs was evaluated against human non-cancerous fibroblast (KMST-6) using WST-1 assay. The principle of the WST-1 assay is based on the cleavage of the tetrazolium salt WST-1 to formazan by cellular mitochondrial dehydrogenases.

4.2. Results and discussion

4.2.1. Antimicrobial activity of AuNPs

Agar well diffusion assays were used to investigate the antimicrobial activity of the pear extracts (RP, GP, RF and GF) and their respective AuNPs (RP-AuNPs, GP-AuNPs, RF-AuNPs and GF-AuNPs) as described in Section 2.10. The results of the agar well diffusion assays in Figure 4.1 clearly shows zones of growth inhibition for the positive control (ampicillin) for all bacterial strains, *E. coli*, *P. aeruginosa*, *S. aureus* and *S. epidermidis* tested in this study. However, no growth inhibition zones were observed around wells containing the crude aqueous pear fruit extracts from the 'Bon Chretien' (GP, GF) and Bon Rouge' (RP, RF), suggesting that the extracts had no antimicrobial activity against these Gram-negative and Gram-positive bacterial strains at their optimum concentration used in the synthesis of AuNPs at 24 mg/ml for RP, RF and GF and 48 mg/ml for GP tested in this study. The biogenic AuNPs (GP-AuNPs, GF-AuNPs, RP-AuNP and RF-AuNPs) synthesized from these extracts also demonstrated no antimicrobial activity at the concentration 2 mg/ml.

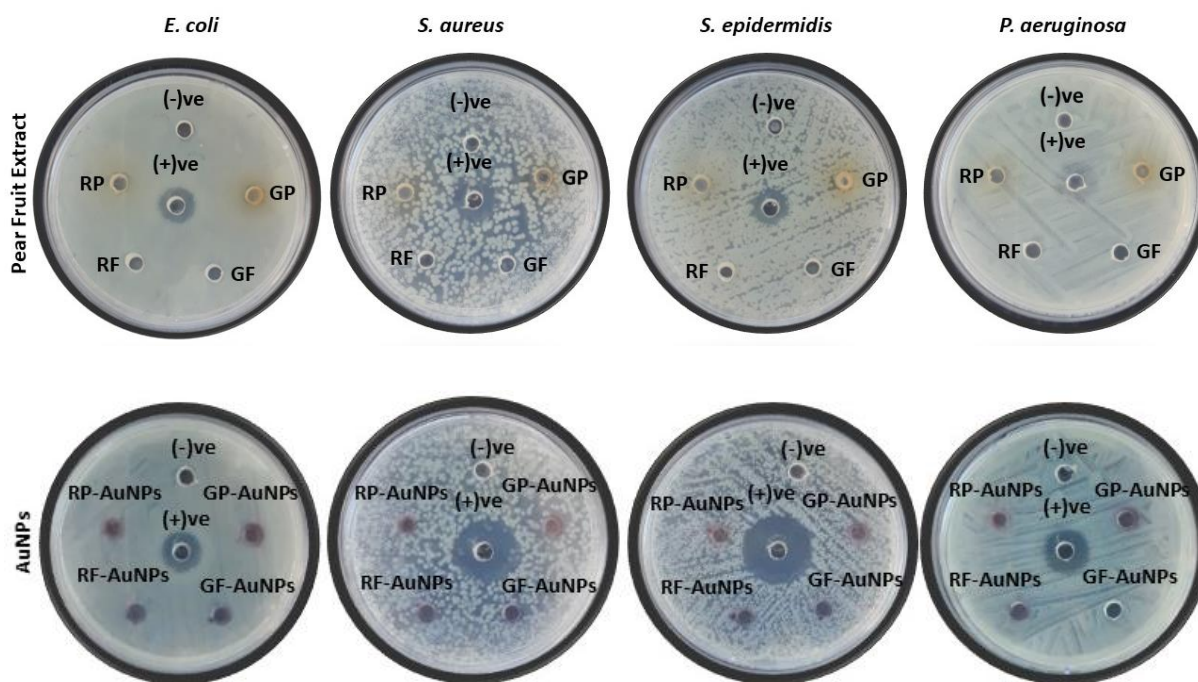


Figure 4.1. Antimicrobial activity of the fruit extracts and their respective AuNPs. *E. coli*, *P. aeruginosa*, *S. aureus* and *S. epidermidis* were exposed for 24hrs to the RP, RF, GF (24 mg/ml) and GP (48 mg/ml) fruit extracts and their respective AuNPs (RP-AuNPs, GP-AuNPs, RF-AuNPs and GF-AuNPs (2 mg/ml)) using the well-diffusion method. (-)ve is indicative of the negative control, Mueller Hinton Broth (MHB). (+)ve is indicative of the positive control, Ampicillin.

These results however exhibited the same growth pattern of bacteria around the well as that of the negative control (Mueller Hinton Broth (MHB)). Even though the AuNPs bind with cytoplasmic membrane, they may not kill the bacterial cell due to its non-toxicity (Gopinath *et al.*, 2014). This contradicts what has been reported in literature, where a previous study has shown that the aqueous extracts of tissue of succulent young shoots of 12 cultivars of European pears (*Pyrus communis*), Chinese pears (*Pyrus pyrifolia*) and Japanese pears (*Pyrus ussuriensis*) exhibited strong antimicrobial activity against gram negative bacterium *Erwinia amylovora* bv. 4. as a result of the benzoquinone (2,5-cyclohexadiene-1,4-dione), found in each extract (Jin & Sato, 2003). We speculate the inhibitory effects absent in the peel and flesh pear extracts of our study may be due to the absence of benzoquinone (2,5-cyclohexadiene-1,4-dione). The study by Jin and Sato have demonstrated that the extracts of the youngest leaves and stems from the shoot tops of the pears showed the strongest activity, however activity decreased with age of the leaves and stem. In our study, the peels and flesh of matured pears were used.

However, in another study Güven *et al.* (2006) reported on the antimicrobial activities of ethyl acetate extract from fruits of *Pyrus communis* subsp. *Communis* (pear) and *Pyrus serikensis* against a number of bacterial (*E. coli*, *S. aureus*, *P. aeruginosa*, *B. cereus*, *K. pneumoniae*) yeast (*R. rubra*, *C. albicans*) and fungal (*P. notatum*, *C. herbarum*, *R. rubra*) strains by means of agar well diffusion assay (Güven *et al.*, 2006). We speculate that the reason for the absence of the antimicrobial activity may be due to the fact that the ethyl acetate extraction of *Pyrus communis* subsp. *Communis* (pear) and *Pyrus serikensis* was used. However, this is the first study that investigated the antimicrobial activity of AuNPs synthesised from the aqueous extracts from the 'Bon Chretien' (GP, GF) and Bon Rouge' (RP, RF) pears.

4.2.2. *In vitro* cytotoxicity assay of AuNPs

A major concern with the synthesis of NPs as antimicrobial agents is their potential toxicity to humans and the environment. It was therefore important to assess the cytotoxicity of the synthesised NPs. Noble AuNPs are generally nontoxic due to their inert nature (Vijayakumar and Ganesan, 2012).

The cytotoxicity was determined using the WST-1 assay which is based on the cleavage of the tetrazolium salt WST-1 to formazan by cellular mitochondrial dehydrogenases that occurs primarily at the cell surface. This bioreduction is largely dependent on the glycolytic production of NAD(P)H in viable cells. Therefore, the amount of formazan dye formed directly correlates to the number of metabolically active cells in the culture. The larger the number of viable cells, the higher the activity of the mitochondrial dehydrogenases, and in turn the greater the amount of formazoan dye formed.

The key parameters in evaluating the biocompatibility of AuNPs are cytotoxicity and cell viability. The development of more effective and biocompatible NPs is incumbent for treating particular diseases as well as manipulating their remediable properties as active drug carriers in cosmetics. To assess the potential cytotoxicity of AuNPs, human fibroblast cells were exposed to various concentrations (0.125 – 2 mg/ml) of AuNPs for 24 hours using the WST-1 assay where the viable cells reduce the dye which can be measured by absorbance spectroscopy. The toxicity of the AuNPs towards the KMST-6 cell line therefore was established using *in vitro* cell culture testing. Control wells were incubated with fresh culture media, and experiments were repeated in triplicates.

Results in Figure 4.1 shows that there was no significant reduction in the percentage viability of KMST-6 after a 24-hour treatment with various concentrations of the RP-AuNPs, GP-AuNPs, RF-AuNPs and GF-AuNPs. RP-AuNPs and RF-AuNPs showed activity against KMST-6 with percentage viability above 90 %. GP-AuNPs followed with percentage viability at 100 % and GF-AuNPs with a percentage viability above 70 % in all concentrations. This indicates the adaption of KMST-6 cells to the various AuNP environment.

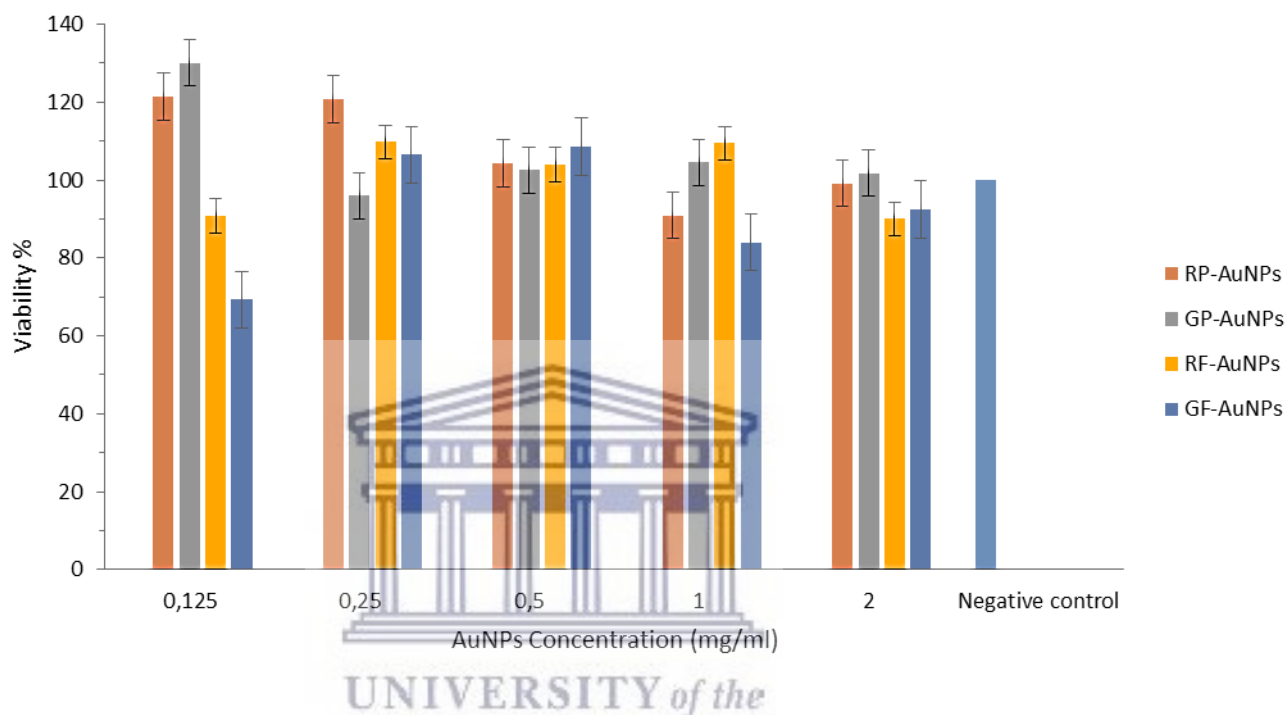


Figure 4.2. The cytotoxic effect of RP-AuNPs, GP-AuNPs, RF-AuNPs and GF-AuNPs against KMST-6 cells as determined by the WST-1 assay.

This preliminary data suggests that these biogenic synthesised AuNPs prepared by this method are not chronically toxic to the cell growth or for their viability and are considered safe for therapeutic use with minimal to no toxicity against human cells. A study by Ghodake *et al.* (2010) shows that a cell viability of pear-AuNPs were biocompatible with human embryonic kidney 293 cells (Ghodake *et al.*, 2010). The capability of pear phytochemicals to efficiently reduce chloroaurate ions to biocompatible AuNPs has now been demonstrated. This single-step biogenic synthesis uses pear extract for both the production and subsequent nontoxic biomimetic coating of AuNPs.

CHAPTER 5

CONCLUSION AND FUTURE WORK

The objectives of this study were to synthesize AuNPs using fresh green peels and flesh from the ‘Williams Bon Chretien’ pear and fresh red peels and flesh from its mutant bud, ‘Bon Rouge’ pear. To determine the optimum conditions of synthesis by evaluating the effect of temperature and extract concentration on the synthesis of the AuNPs as well as determining the kinetics AuNPs formation as a function over time, characterize the physicochemical properties of the AuNPs, determine the influence of different pigmentation on these physicochemical properties, assess the antimicrobial activity against *E. coli*, *S. aureus*, *S. epidermidis* and *P. aeruginosa* and assess the cytotoxicity of the AuNPs against human non-cancerous fibroblast cells (KMST-6).

Previous studies have demonstrated a competent biosynthetic route for the production of AuNPs using from the extracts of *Pyrus* spp. and HAuCl_4 in an aqueous medium (Ghodake et al., 2010). Studies have also shown that *Pyrus communis* has antimicrobial activity. This led to the hypothesis that the aqueous extracts of the peels and flesh of the ‘Williams Bon Chretien’ pear and the ‘Bon Rouge’ pear are capable of reducing gold (III) chloride to form AuNPs that may exhibit antimicrobial activity and may also be biocompatible. The AuNPs were successfully synthesized from the pear extracts using a bioreduction method under the optimum conditions of 100 °C for 30 minutes. Synthesis using all 4 extracts produced a colour change from yellow to red-purple for RP-AuNPs, GP-AuNPs, RF-AuNPs and GF-AuNPs. This red-purple colour was the initial indication of successful AuNP synthesis and is a characteristic of colloidal AuNP solutions.

The AuNPs were characterized using different spectroscopic and microscopic techniques such as UV-Vis, DLS analysis, HRTEM, SAED, EDS and FTIR. UV-Vis was used to confirm the synthesis of AuNP production. λ_{max} absorbance peaks were recorded between 530 and 548 nm, which is a distinctive characteristic of AuNPs. The size of the AuNPs was determined using HRTEM and DLS. These two methods provide different sizes for the AuNPs. However, the principle of the two methods is very different and this could explain the difference in size. The core diameters of AuNPs were found to be 15.79 ± 6.02 nm for RP-AuNPs, 10.92 ± 3.6 nm for GP-AuNPs, 12.24 ± 6.77 nm for RF-AuNPs and 18.31 ± 6.91 nm for GF-AuNPs by using HRTEM analysis. HRTEM shows that the AuNPs exhibited an assortment of geometric shapes, but was mostly spherical. A previous study found that the z-average size could only be

considered an accurate measure of the hydrodynamic size if the NP sample under investigation is monomodal and/ or monodispersed (Lim et al., 2013). The hydrodynamic size was 71 ± 1.52 nm for RP-AuNPs, 70.62 ± 1.13 nm for GP-AuNPs, 168.2 ± 2.5 nm for RF-AuNPs and 180.95 ± 2.15 nm for GF-AuNPs. The size determined by DLS analysis was greater than that of HRTEM, as DLS measures the hydrodynamic diameter whereas HRTEM measures the core diameter. The size determined by DLS analysis, takes into account the capping agent of the AuNPs whereas in HRTEM, carbon based materials are transparent to the electron beam. The crystalline nature of the synthesized AuNPs was confirmed with SAED that showed that the synthesized AuNPs corresponded with gold and the elemental composition by EDS confirmed the presence of gold.

To compare the efficiency of AuNP formation between the different pear extracts, the kinetics of AuNPs formation was studied by examining the changes in the λ_{max} of the AuNPs produced using the different peel and flesh extracts over a time period. RP-AuNP and GP-AuNP was found to reach the maximum absorbance at an earlier time point compared to RF-AuNP and GF-AuNP. The delayed increase in λ_{max} for RF-AuNP and GF-AuNP suggests that AuNP synthesis was much slower and that the reduction power of phytochemicals present in RF and GF extracts were lower than that of the RP and GP extracts. It is possible that RP and GP extracts contain different compounds that have higher reducing power, alternatively RP, GP, RF and GF extracts contain the same compounds, but RP and GP extracts contain higher concentrations of these compounds.

The FTIR data suggested that the presence of polysaccharides, peptides or proteins flavonoids/phenolic groups of RP-AuNPs, GP-AuNPs, RF-AuNPs and GF-AuNPs might be responsible for the biogenic synthesis of the AuNPs. In vitro stability studies showed that all four AuNPs were stable when incubated in various biological buffers and culture media (0.5 % BSA, PBS, Nutrient broth, MHB, DMEM, RPMI and double distilled water), respectively.

The four pear extract samples as well as their respective AuNPs were evaluated for antimicrobial activity against four bacterial strains (*E. coli*, *P. aeruginosa*, *S. aureus* and *S. epidermidis*) whilst quantitatively characterizing the cytotoxic effects of the said NPs to human fibroblast cells. Although no antimicrobial activity was observed for both the extracts and NPs against the four pathogens, it is important to note that these NPs also did not produce any toxic effects against the non-cancerous human fibroblast cell line (KMST-6).

Based on the data in this study, there were little to no differences found in the characteristics of the AuNPs synthesized from the red peel of the 'Bon Rouge' pear and the green peel from the 'Williams Bon Chretien' pear as a result of the levels of anthocyanins found within these extracts.

However, differences (such as the size, shape, synthesis reaction time, bands on the FTIR spectra) were discovered between the AuNPs synthesized from the peel and those synthesized from the flesh. The objectives of this study were therefore successfully achieved.

Due to the biocompatibility of the NPs synthesized in this study, further studies can be conducted on potential theranostic applications.



REFERENCES

Abdel-Raouf N, Al-Enazi NM and Ibraheem IBM (2017). Green synthesis of gold nanoparticles using *Galaxaura elongata* and characterization of their antibacterial activity. *Arabian Journal of Chemistry*, 10, 3029-3039.

Adams FC and Barbante C (2013). Nanoscience, nanotechnology and spectrometry. *Spectrochimica Acta Part B*, 86, 3-12.

Adisakwattana S, Charoenlertkul P and Yibchok-anun S (2009). α -Glucosidase inhibitory activity of cyanidin-3-galactoside and synergistic effect with acarbose. *Journal of Enzyme Inhibition and Medicinal Chemistry*, 24, 1, 65-69.

Ali DM, Thajuddin N, Jeganathan K and Gunasekaran M (2011). Plant extract mediated synthesis of silver and gold nanoparticles and its antibacterial activity against clinically isolated pathogens. *Colloids and Surfaces B*, 85, 360-365.

Amendola V and Meneghetti M (2009). Size evaluation of gold nanoparticles by UV-vis spectroscopy. *The Journal of Physical Chemistry C*, 113, 4277-4285.

Ankamwar B, Salgaonkar M and Sur UK (2017). Room temperature green synthesis of anisotropic gold nanoparticles using novel biological fruit extract. *Inorganic and Nano-metal Chemistry*, 47, 9, 1359-1363.

Arvizo R, Bhattacharya R and Mukherjee P (2010). Gold nanoparticles: opportunities and challenges in nanomedicine. *Expert Opinion on Drug Delivery*, 7, 6, 753-763.

Ashok PK and Upadhyaya K (2012). Tannins are astringent. *Journal of Pharmacognosy and Phytochemistry*, 1, 3, 45-50.

Balashanmugam P, Mosachristas K and Kowsalya E (2018). *In vitro* cytotoxicity and antioxidant evaluation of biogenic synthesized gold nanoparticles from *Marsilea*

quadrifolia on lung and ovarian cancer cells. *International Journal of Applied Pharmaceutics*, 10, 5, 153-158.

Baker S, Rakshith D, Kavitha KS, Santosh P, Kavitha HU, Rao Y and Satish S (2013). Plants: Emerging as nanofactories towards facile route in synthesis of nanoparticles. *BioImpacts*, 3, 111-117.

Bao L, Chen K, Zhang D, Cao Y, Yamamoto T and Teng Y (2007). Genetic diversity and similarity of pear (*Pyrus L.*) cultivars native to East Asia revealed by SSR (simple sequence repeat) markers. *Genetic Resources and Crop Evolution*, 54, 959-971.

Barai AC, Paul K, Dey A, Manna S, Roy S, Bag BG and Mukhopadhyay C (2018). Green synthesis of *Nerium oleander*-conjugated gold nanoparticles and study of its in vitro anticancer activity on MCF-7 cell lines and catalytic activity. *Nano Convergence*, 5, 1.

Belloni J (1996). Metal colloids. *Current Opinion in Colloid & Interface Science*, 1, 184-196.

Beveridge TJ and Murray RG (1980). Sites of metal deposition in the cell wall of *Bacillus subtilis*. *Journal of Bacteriology*, 141, 2, 876-887.

Büchner FL, Bueno-de-Mesquita HB, Ros MM, Kampman E, Egevad L, Overvad K, Raaschou-Nielsen O, Tjønneland A, Roswall N, Clavel-Chapelon F, Boutron-Ruault MC, Touillaud M, Chang-Claude J, Kaaks R, Boeing H, Weikert S, Trichopoulou A, Lagiou P, Trichopoulos D, Palli D, Sieri S, Vineis P, Tumino R, Panico S, Vrieling A, Peeters PH, van Gils CH, Lund E, Gram IT, Engeset D, Martinez C, Gonzalez CA, Larrañaga N, Ardanaz E, Navarro C, Rodríguez L, Manjer J, Ehrnström RA, Hallmans G, Ljungberg B, Allen NE, Roddam AW, Bingham S, Khaw KT, Slimani N, Boffetta P, Jenab M, Mouw T, Michaud DS, Kiemeneij LA, Riboli E (2009). Consumption of vegetables and fruit and the risk of bladder cancer in the European Prospective Investigation into Cancer and Nutrition. *International Journal of Cancer*, 125, 11, 2643-51.

Burdulis D, Šarkinas A, Jasutienė I, Stackevičienė E, Nikolajevs L and Janulis V. (2009). Comparative study of anthocyanin composition, antimicrobial and antioxidant activity in bilberry (*Vaccinium myrtillus* L.) and blueberry (*Vaccinium corymbosum* L.) fruits. *Acta Poloniae Pharmaceutica – Drug Research*, 66, 399-408.

Česonienė L, Jasutiene I and Šarkinas A (2009). Phenolics and anthocyanins in berries of European cranberry and their antimicrobial activity. *Medicina (Kaunas)*, 45, 992-999.

Chandran SP, Chaudhary M, Pasricha R, Ahmad A and Sastry M (2006). Synthesis of gold nanotriangles and silver nanoparticles using *Aloe vera* plant extract. *Biotechnology Progress*, 22, 577-583.

Chen R, Wu J, Li H, Cheng G, Lu Z and Che C-M (2010). Fabrication of gold nanoparticles with different morphologies in HEPES buffer, *Rare Metals*, 29, 2, 180-186.

Chinnasamy VM and Bhargava A (2014). Wound healing activity of various extracts of fruit of *Pyrus communis* L. in normal rats. *Journal of Pharmaceutical and Scientific Innovation*, 3, 2, 148-153.

Choudhary GP (2008). Wound healing activity of the ethanol extract of *Terminalia bellirica* Roxb. fruits. *Natural Product Radiance*, 1, 19-21.

Cornejo-Monroy D, Acosta-Torres LS, Moreno-Vega AI, Saldana C, Morales-Tlalpan V and Castana VM (2013). Gold nanostructures in medicine: past, present and future. *Journal of Nanoscience Letters*, 3, 25.

Cui Y (2012). The molecular mechanism of action of bactericidal gold nanoparticles on *Escherichia coli*. *Biomaterials*, 33, 2327-2333.

Daniel M and Astruc D (2004). Gold nanoparticles: assembly, supramolecular chemistry, quantum-sized-related properties, and applications towards biology, catalysis, and nanotechnology. *Chemical Reviews*. 104, 293-346.

Daraee H, Eatemadi A, Abbasi E, Aval SF, Kouhi M and Akbarzadeh A (2014). Application of gold nanoparticles in biomedical and drug delivery. *Artificial Cells, Nanomedicine, and Biotechnology*, 1-13.

Das SK, Das AR and Guha AK (2009). Gold nanoparticles: microbial synthesis and application in water hygiene management. *Langmuir*, 25, 8192-8199.

di Camillo Orfali G, Duarte AC, Bonadio V, Martinez NP, Melo Branco de Araújo ME, Priviero FBM, Carvalho PO and Priolli DG (2016). Review of anticancer mechanisms of isoquercetin. *World Journal of Clinical Oncology*, 7, 2, 189-199.

Dorosti N and Jamshidi F (2016). Plant-mediated gold nanoparticles by *Dracocephalum kotschyi* as anticholinesterase agent: synthesis, characterization, and evaluation of anticancer and antibacterial activity. *Journal of Applied Biomedicine*, 14, 235-245.

du Preez MG, Labuschagne IF and Rees DJG (2004). Differential display gene expression patterns for red and green phenotypes of Bon Rouge pear trees, *Pyrus communis* L. *Acta Horticulturae*, 663, 299-305.

Dussi MC, Sugar D and Wrolstad RE (1995). Characterizing and quantifying anthocyanins in red pears and the effect of light quality on fruit color. *Journal of American Society for Horticultural Science*, 120, 785-789.

Dykman LA and Khlebtsov NG (2011). Gold nanoparticles in biology and medicine: recent advances and prospects. *Acta Naturae*, 3, 2, 34-55.

Edison T and Sethuraman M (2012). Instant green synthesis of silver nanoparticles using *Terminalia chebula* fruit extract and evaluation of their catalytic activity on reduction of Methylene Blue. *Process Biochemistry*, 47, 1351–1357.

Elbagory AM, Cupido CN, Meyer M and Hussein AA (2016). Large scale screening of Southern African plant extracts for the green synthesis of gold nanoparticles using microtitre-plate method. *Molecules*, 7, 417.

Elbagory AM, Meyer M, Cupido CN and Hussein AA (2017). Inhibition of bacteria associated with wound infection by biocompatible green synthesized gold nanoparticles from South African plant extracts. *Nanomaterials*, 21, 1498.

Elbehiry A, Al-Dubaib M, Marzouk E and Moussa I (2018). Antibacterial effects and resistance induction of silver and gold nanoparticles against *Staphylococcus aureus*-induced mastitis and the potential toxicity in rats. *Microbiology Open*, 8, 4.

Elia P, Zach R, Hazan S, Porat Z and Zeiri Y (2014). Green synthesis of gold nanoparticles using plant extracts as reducing agents. *International journal of Nanomedicine*, 9, 4007-4021.

El-Kassas HY and El-Sheekh MM (2014). Cytotoxic activity of biosynthesised gold nanoparticles with an extract of the red seaweed *Corallina officinalis* on the MCF-7 human breast cancer cell line. *Asian Pacific Journal of Cancer Prevention; APJCP*, 15, 10, 4311-4317.

Eom SH, Kim YM and Kim SK (2012). Antimicrobial effect of phlorotannina from marine brown algae. *Food and Chemical Toxicology*, 50, 3251–3255.

Faix, O (1992). Fourier transform infrared spectroscopy. *Methods in Lignin Chemistry*, 83-109.

Fayaz AM, Girilal M, Venkatesan R and Kalaichelvan (2011). Biosynthesis of anisotropic gold nanoparticles using *Maduca longifolia* extract and their potential in infrared absorption. *Colloids and Surfaces B: Biointerfaces*, 88, 1, 287-291.

Feng QL, Wu J, Chen GQ, Cui FZ, Kim TN, Kim TN and Kim JO (2000). A mechanistic study of the antibacterial effect of silver ions on *E. coli* and *Staphylococcus aureus*. *Journal of Biomedical Materials Research*, 52, 662–668.

Fischer TC, Gosch C, Pfeiffer J, Halbwirth H, Halle C, Stich K and Forkmann G (2007). Flavonoid genes of pear (*Pyrus communis*). *Tree*, 21, 521-529.

Foss CA, Hornyak GL, Stockert JA and Martin CR (1994). Template-synthesized nanoscopic gold particles: optical spectra and the effects of particle size and shape. *The Journal of Physical Chemistry*, 98, 11, 2963-2971.

Francis FJ (1970). Anthocyanins in pears. *Horticulture Science*, 5, 42.

Freedman ND, Park Y, Subar AF, Hollenbeck AR, Leitzmann MF, Schatzkin A and Abnet CC (2007). *International Journal of Cancer*, 121, 12, 2753-2760.

Ghodake G and Lee DS (2010). Green synthesis of gold nanostructures using pear extract as effective reducing and coordinating agent. *Korean Journal of Chemical Engineering*, 28, 2329-2335.

Ghodake G, Eom CY, Kim SW and Jin ES (2010). Biogenic nano-synthesis; towards the efficient production of the biocompatible gold nanoparticles. *Bulletin of the Korean Chemical Society*, 31, 10.

Giersig M and Mulvaney P (1993). Preparation of ordered monolayers by electrophoretic deposition. *Langmuir*, 9, 3408-3413.

Giljohann DA, Seferos DS, Daniel WL, Massich MD, Patel PC and Mirkin CA (2010). Gold nanoparticles for biology and medicine. *Angewandte Chemie International Edition*, 49, 19, 3280-3294.

Gopinath K, Gowri S, Karthika V and Arumugam A (2014). Green synthesis of gold nanoparticles from fruit extract of *Terminalia arjuna*, for the enhanced seed germination activity of *Gloriosa superba*. *Journal of Nanostructure in Chemistry*, 4, 115.

Güven K, Yücel E and Cetintaş F (2006). Antimicrobial activities of fruits of *Crataegus* and *Pyrus* species. *Pharmaceutical Biology*, 44, 2, 79-83.

Guzman M, Dille J and Godet S (2012). Synthesis and antibacterial activity of silver nanoparticles against gram-positive and gram-negative bacteria. *Nanomedicine: Nanotechnology, Biology and Medicine Journal*, 8, 37-45.

Hajippour MJ, Fromm KM, Ashkarran AA, Jimenez de Aberasturi D, de Larramendi IR, Rojo T, Serpooshan V, Parak WJ and Mahmoudi M (2012). Antibacterial properties of nanoparticles. *Trends in Biotechnology*, 30, 10, 499-511.

Hamazu Y, Forest F, Hiramatsu K and Sugimoto M (2007). Effect of pear (*Pyrus communis* L.) procyanidins on gastric lesions induced by HCl/ethanol in rats. *Food Chemistry*, 100, 255-263.

Heiligtag FJ and Niederberger M (2013). The fascinating world of nanoparticle research. *Materials Today*, 16.

Henglein A (1989). Small-particle research: physicochemical properties of extremely small colloidal metal and semiconductor particles. *Chemical Reviews*, 89, 8, 1861-1873.

Henglein A (1993). Physicochemical properties of small metal particles in solution: "microelectrode" reactions, chemisorption, composite metal particles, and the atom-to-metal transition. *The Journal of Physical Chemistry*, 97, 21, 5457-5471.

Honda C, Kotoda N, Wada M, Kondo S, Kobayashi S, Soejima J, Zhang Z, Tsuda T and Moriguchi T (2002). Anthocyanin biosynthetic genes are coordinately expressed during red coloration in apple skin. *Plant Physiology and Biochemistry*, 40, 955-962.

Hu M, Chen J, Li ZY, Au L, Hartland GV, Li X, Marquez M and Xia Y (2006). Gold nanostructures: engineering their plasmonic properties for biomedical applications. *Chemical Society Reviews*, 35, 1084-1094.

Huang W, Zhang S, Qin G, Wenquan L and Wu J (2012). Isolation and determination of major anthocyanin pigments in the pericarp of *P. communis* L. cv. 'Red Du Comices' and their association with antioxidant activity. *African Journal of Agricultural Research*, 7, 3772-3780.

Human JP (2013). Breeding blush pears (*pyrus communis* L.) in South Africa. *Acta horticulture*, 976, 383-388.

Hupkens P, Boxma H and Dokter J (1995). Tannic acid as a topical agent in burns: historical considerations and implications for new developments. *Burns*, 21, 1, 57-61.

Jahangirian H, Lemraski EG, Webster TJ, Rafiee-Moghaddam R and Abdollahi Y (2017). A review of drug delivery systems based on nanotechnology and green chemistry: green nanomedicine. *International Journal of Nanomedicine*, 12, 2957-2978.

Jain S, Hirst DG and O' Sullivan JM (2012). Gold nanoparticles as novel agents for cancer therapy. *The British Journal of Radiology*, 85, 101-113.

Jana NR, Gearheart L and Murphy CJ (2001). Evidence for seed-mediated nucleation in the chemical reduction of gold salts to gold nanoparticles. *Chemistry of Materials*, 13, 2313-2322.

Jin S and Sato N (2003). Benzoquinone, the substance essential for antibacterial activity in aqueous extracts from succulent young shoots of the pear *Pyrus* spp. *Phytochemistry*, 62, 101-107.

Jolly PR (1993). Release of the pear cultivar – Flamingo Information Bulletin Number 625, Fruit and Fruit Technology Research Institute, Stellenbosch.

Kasthuri J, Kathiravan K and Rajendiran N (2009). Phyllanthin-assisted biosynthesis of silver and gold nanoparticles: a novel biological approach. *Journal of Nanoparticle Research*, 11, 1075–1085.

Khan I, Saeed K and Khan I (2017). Nanoparticles: properties, applications and toxicities. *Arabian Journal of Chemistry*.

Kiran, Garg V, Dhiman A, Dutt R and Ranga S (2018). The genus *Pyrus*: An update. *The Pharma Innovation Journal*, 7, 2, 143-145.

Kolniak-Ostek J (2016). Chemical composition and antioxidant capacity of different anatomical parts of pear (*Pyrus communis* L.). *Food Chemistry*, 203, 491-497.

Kong J, Chia L, Goh N, Chia T and Brouillard R (2003). Analysis and biological activities of anthocyanins. *Phytochemistry* 63, 923-933.

Krishnaswamy K, Vali H and Orsat V (2014). Value-adding to grape waste: Green synthesis of gold nanoparticles. *Journal of Food Engineering*. 142, 210-220.

Kumar B, Smita K, Cumbal L and Debut A (2017). Green synthesis of silver nanoparticles using Andean blackberry fruit extract. *Saudi Journal of Biological Sciences*, 24, 45-50.

Kumar KM, Mandal BK, Sinha M and Krishnakumar V (2012). *Terminalia chebula* mediated green and rapid synthesis of gold nanoparticles. *Spectrochimica Acta Part A* 86, 490-494.

Kumar S, Aaron J and Sokolov K (2008). Directional conjugation of antibodies to nanoparticles for synthesis of multiplexed optical contrast with both delivery and targeting moieties. *Nature Protocols*, 3, 314-320.

Kumar SSD, Mahesh A, Antoniraj MG, Rathore HS, Houreld NN and Kandasamy R (2018). Cellular imaging and folate receptor targeting delivery of gum kondagogu capped gold nanoparticles in cancer cells. *International Journal of Biological Macromolecules*, 109, 220-230.

Kumar VG, Gokavarapu SD, eswari A, Dhas TS, Karthick V, Kapadia Z, Shrestha T, Barathy IA, Roy A and Sinha S (2011). Facile green synthesis of gold nanoparticles using leaf extract of antidiabetic potent *Cassia auriculata*. *Colloids and Surfaces B: Biointerfaces*, 87, 159-163.

Kundu S, Peng L and Liang H (2008). A new route to obtain high-yield multiple-shaped gold nanoparticles in aqueous solution using microwave irradiation. *Inorganic Chemistry*, 47, 14, 6344-6352.

Leiva A, Saldias C, Quezada C, Toro-Labbé A, Espinoza-Beltrán FJ, Urzúa M, Gargallo L and Radic D (2009). Gold-copolymer nanoparticles: poly ([epsilon]-caprolactone)/poly (N-vinyl-2-pyrrolidone) biodegradable triblock copolymer as stabiliser and reductant. *European Polymer Journal*, 45, 11, 3035-3042.

Li X, Wang T, Zhou B, Gao W, Cao J and Huang L (2016). Chemical composition and antioxidant and anti-inflammatory potential of peels and flesh from 10 different pear varieties (*Pyrus* spp.). *Food Chemistry*, 203, 491-497.

Li L, Ban ZJ, Li XH, Wu M, Wang, AL, Jiang YQ and Jiang YL (2012). Differential expression of anthocyanin biosynthetic genes and transcription factor *PcMYB10* in pears (*Pyrus communis* L.). *PLoS ONE*, 7, 9.

Lin PC, Lin S, Wang PC and Sridhar R (2014). Techniques for physicochemical characterization of nanomaterials. *Biotechnology Advances*, 32, 711-726.

Link S and El-Sayed MA (1999). Size and temperature dependence of the plasmon absorption of colloidal gold nanoparticles. *The Journal of Physical Chemistry B*, 103, 4212-4217.

Linseisen J, Rohrmann S, Miller AB, Bueno-de-Mesquita HB, Büchner FL, Vineis P, Agudo A, Gram IT, Janson L, Krogh V, Overvad K, Rasmuson T, Schulz M, Pischon T, Kaaks R, Nieters A, Allen NE, Key TJ, Bingham S, Khaw KT, Amiano P, Barricarte A, Martinez C, Navarro C, Quirós R, Clavel-Chapelon F, Boutron-Ruault MC, Touvier M, Peeters PH, Berglund G, Hallmans G, Lund E, Palli D, Panico S, Tumino R, Tjønneland A, Olsen A, Trichopoulou A, Trichopoulos D, Autier P, Boffetta P, Slimani N and Riboli E (2007). Fruit and vegetable consumption and lung cancer risk: updated information from the European Prospective Investigation into Cancer and Nutrition. *International Journal of Cancer*, 121, 5, 1103-1114.

Liu WT (2006). Nanoparticles and their biological and environmental applications. *Journal of Bioscience and Bioengineering*, 102, 1, 1-7.

Massard C, Dubois C, Raspal V, Daumar P, Sibaud Y, Mounetou E, Bamdad M and Awitor OK (2018). Cytotoxicity study of gold nanoparticles on the basal-like triple-negative HCC-1937 breast cancer cell line. *Journal of Biomaterials and Nanobiotechnology*, 9, 13-25.

Mink PJ, Scrafford CG, Barraji LM, Harnack L, Hong CP, Nettleton JA and Jacobs DR (2007). Flavonoid intake and cardiovascular disease mortality: a prospective study in postmenopausal women. *The American Journal of Clinical Nutrition*, 85, 895-909.

Mittal AK, Chisti Y and Bannerjee UC (2013). Synthesis of metallic nanoparticles using plant extracts. *Biotechnology Advances* 31. 346-356.

Mohamed MM, Fouad SA, Elshoky HA, Mohammed GM and Salaheldin TA (2017). Antibacterial effect of gold nanoparticles against *Corynebacterium pseudotuberculosis*. *International Journal of Veterinary Science and Medicine*, 5, 1, 23-29.

Mountrichas G, Pispas S and Kamitsos E (2014). Effect of temperature on the direct synthesis of gold nanoparticles mediated by poly (dimethylaminoethyl methacrylate) Homopolymer. *The Journal of Physical Chemistry C*, 118, 22754–22759.

Mukherjee S, B V, Prashanthi S, Bangal PR, Sreedhar B and Patra C (2013). Potential therapeutic and diagnostic applications of one-step *in situ* biosynthesized gold nanoconjugates (2-in-1 system) in cancer treatment. *RSC Advances*, 3, 2318-2329.

Muraki I, Imamura F, Manson JE, Hu FB, Willett WC, van Dam RM and Sun Q (2013). Fruit consumption and risk of type 2 diabetes: results from three prospective longitudinal cohort studies. *BMJ*, 347.

Nadeem M, Abbasi BH, Younas M, Ahmad W and Khan T (2017). A review of the green syntheses and antimicrobial applications of gold nanoparticles. *Green Chemistry Letters and Reviews*, 10, 4, 216-227.

Nayak S, Sajankila SP and Rao CV (2018). Green synthesis of gold nanoparticles from banana pith extract and its evaluation of antibacterial activity and catalytic reduction of malachite green dye. *Journal of Microbiology, Biotechnology and Food Sciences*, 6, 641-645.

Naz S, Siddiqi R, Ahmad S, Rasool SA and Sayeed SA (2007). Antibacterial activity directed isolation of compounds from *Punica granatum*. *Journal of Food Science*, 72, 341-345.

Nethi SK, Mukherjee S, Veeriah V, Barui AK, Chatterjee S and Patra CR (2014). Bioconjugated gold nanoparticles accelerate the growth of new blood vessels through redox signalling. *Chemical Communications*, 50, 14367-14370.

Noruzi M (2015). Biosynthesis of gold nanoparticles using plant extracts. *Bioprocess and Biosystems Engineering*, 38, 1-14.

Olenic L, Crisan M, Vulcu A, Berghian-Grosan C, Crisan D and Chiorean I (2016). Green nanomaterials for psoriatic lesions. *Nanomaterials and Regenerative Medicine*, 18, 477-508.

Oren-Shamir M (2009). Does anthocyanin degradation play a significant role in determining pigment concentration in plants? *Plant Science*, 177, 310-316.

Oueslati MH, Tahar LB and Harrath AH (2018). Catalytic, antioxidant and anticancer activities of gold nanoparticles synthesized by kaempferol glucoside from *Lotus leguminosae*. *Arabian Journal of Chemistry*, 2018.

Öztürk A, Demirsoy L, Demirsoy H, Asan A and Gül O (2015). Phenolic compounds and chemical characteristics of pears (*Pyrus communis* L.). *International Journal of Food Properties*, 18, 3, 536-546.

Pandey S, Oza G, Mewada A and Sharon M (2012). Green synthesis of highly stable gold nanoparticles using *Momordica charantia* as nano fabricator. *Archives of Applied Science Research*, 4, 1135–1141.

Parida UK, Bindhani BK and Nayak P (2011). Green synthesis and characterization of gold nanoparticles using onion (*Allium cepa*) extract. *World Journal of Nano Science and Engineering*, 1, 93–98.

Parle M and Arzoo (2016). Why is pear so dear. *International Journal of Research in Ayurveda and Pharmacy*, 7, 108-113.

Pérez ZEJ, Mathiyalagan R, Markus J, Kim Y-J, Kang HM, Abbai R, Seo KH, Wang D, Soshnikova V and Yang DC (2017). Ginseng-berry-mediated gold and silver nanoparticle synthesis and evaluation of their in vitro antioxidant, antimicrobial, and cytotoxicity effects on human dermal fibroblast and murine melanoma skin cell lines. *International Journal of Nanomedicine*, 12, 709-723.

Philip D (2010). Rapid green synthesis of spherical gold nanoparticles using *Mangifera indica* leaf. *Spectrochimica Acta Part A* 77, 807-810.

Phull AR, Abbas Q, Ali A, Raza H, Kim S J, Zia M and Haq I (2016). Antioxidant, cytotoxic and antimicrobial activities of green synthesized silver nanoparticles from crude extract of *Bergenia ciliate*. *Future Journal of Pharmaceutical Sciences*, 2, 31-36.

Qureyshi S, Niazi K and Usman M (2016). Silver nanoparticles mediated through green route using pyrus seed extract. *Journal of Basic and Applied Chemistry*, 6, 1-7.

Raghunandan D, Bedre MD, Basavaraja S, Sawle B, Manjunath SY and Venkataraman A (2010). Rapid biosynthesis of irregular shaped gold nanoparticles from macerated aqueous extracellular dried clove buds (*Syzygium aromaticum*) solution. *Colloids and Surfaces B: Biointerfaces*, 79, 1, 235-240.

Reiland H and Slavin J (2015). Systematic review of pears and health. *Food and Nutrition*, 50, 6, 301-305.

Sadeghi B (2015). *Zizyphus mauritiana* extract-mediated green and rapid synthesis of gold nanoparticles and its antibacterial activity. *Journal of Nanostructure in Chemistry*, 5, 265-273.

Sahoo SK, Parveen S and Panda JJ (2007). The present and future of nanotechnology in human health care. *Nanomedicine*, 3, 1, 20-31.

Sanvicens N and Marco MP (2008). Multifunctional nanoparticles – properties and prospects for their use in human medicine. *Trends in Biotechnology*, 26, 8, 18-26.

Sarpooshi HR, Haddadi M, Siavoshi M and Borghabani R (2017). Wound healing with Vitamin C. *Translational Biomedicine*, 8, 4, 139.

Seigneuric R, Markey L, Nuyten DSA, Dubernet C, Evelo CTA, Finot E and Garrido C (2010). From nanotechnology to nanomedicine: applications to cancer research. *Current Molecular Medicine*, 10, 640-652.

Sengani M, Grumezescu AM and Rajeswari VD (2017). Recent trends and methodologies in gold nanoparticle synthesis – A prospective review on drug delivery aspect. *OpenNano* 2, 37-46.

Senthilkumar S, Kashinath L, Ashok M and Rajendran A (2017). Antibacterial properties and mechanism of gold nanoparticles obtained from *Pergularia Daemia* leaf extract. *Journal of Nanomedicine Research*, 6, 1, 00146.

Septiani NL, Yulianto B, Iqbal M and Nugraha (2017). Synthesis of zinc oxide nanoparticles using anthocyanin as a capping agent. *Material Science and Engineering*, 202.

Sett A, Gadewar M, Sharma P, Deka M and Bora U (2016). Green synthesis of gold nanoparticles using aqueous extract of *Dillenia indica*. *Advances in Natural Sciences: Nanoscience and Nanotechnology*, 7.

Shah M, Badwaik V, Kherde Y, Waghvani HK, Modi T, Aguilar ZP, Rogers H, Hamilton W, Marutharaj T, Webb C, Lawrenz MB and Dakshinamurthy R (2014). Gold nanoparticles: various methods of synthesis and antibacterial applications. *Frontiers in Bioscience*, 19, 1320-1344.

Shamaila S, Zafar N, Riaz S, Sharif R, Nazir J and Naseem S (2016). Gold nanoparticles: and efficient antimicrobial agent against enteric bacterial human pathogen. *Nanomaterials*, 6.

Sharma S and Rao TVR (2015). Xanthan gum based edible coating enriched with cinnamic acid prevents brownish and extends the shelf-life of fresh-cut pears. *LWT – Food Science and Technology*, 62, 791-800.

Sheny and Philip (2011). Phytosynthesis of Au, Ag and Au-Ag bimetallic nanoparticles using aqueous extract and dried leaf of *Anacardium occidentale*. *Spectrochimica Acta Part A: Molecular and Biomolecular Spectroscopy*, 79, 1, 254-262.

Silva GJ, Souza TM, Barbieri RL and de Oliveira AC (2014). Origin, domestication, and dispersing of pear (*Pyrus* spp.). *Advances in Agriculture*, 2014, 38-70.

Singh C, Sharma V, Naik PK, Khandel V and Singh H (2011). A green biogenic approach for synthesis of gold and silver nanoparticles using *zingiber officinale*. *Digest Journal of Nanomaterials and Biostructures*, 6, 535-542.

Singh P, Kim Y, Zhang D and Yang D (2016). Biological synthesis of nanoparticles from plants and microorganisms. *Trends in Biotechnology*, 34, 7, 588-599.

Song JY, Jang H-K and Kim BS (2009). Biological synthesis of gold nanoparticles using *Magnolia Kobus* and *Diopyros kaki* leaf extracts. *Process Biochemistry*, 44, 1133-1138.

Sperling RA, Gil PR, Zhang F, Zanella M and Parak WJ (2008). Biological applications of gold nanoparticles. *Chemical Society Reviews*, 37, 1896-1908.

Steyn WJ, Holcroft DM, Wand SJE and Jacobs G (2004). Anthocyanin degradation in detached pome fruit with reference to preharvest red colour loss and pigmentation patterns of blushed and fully red pears. *Journal of the American Society for Horticultural Science*, 129, 1, 13-19.

Sujitha MV and Kannan S (2013). Green synthesis of gold nanoparticles using citrus fruits (Citrus limon, Citrus reticulate and Citrus sinensis) aqueous extract and its characterization. *Spectrochimica Acta Part A: Molecular and Biomolecular Spectroscopy*, 102, 15-23.

Süntar I, Koca U, Keleş H and Akkol EK (2011). Wound healing activity of *Rubus sanctus* schreber (Rosaceae): preclinical study in animal models. *Evidence-Based Complementary and Alternative Medicine*, 137, 1-7.

Thakor AS, Jokerst J, Zavaleta C, Massoud TF and Gambhir SS (2011). Gold nanoparticles: a revival in precious metal administration to patients. *Nano Letters*, 11, 10, 4029-4036.

Thanh NTK, Maclean N and Mahiddine S (2014). Mechanisms of nucleation and growth of nanoparticles in solution. *Chemical Reviews*, 114, 7610-7630.

Thomas LA, Sehata MJ, du Preez MG, Rees JG and Ndimba BK (2010). Establishment of proteome spot profiles and comparative analysis of the red and green phenotypes of 'Bon Rouge' pear (*Pyrus communis* L.) leaves. *African Journal of Biotechnology*, 9, 4334-4341.

Tsuda T, Horio F, Uchida K, Aoki H and Osawa T (2003). Dietary cyaniding 3-O- β -D-glucose-rich purple corn color prevents obesity and ameliorates hyperglycemia in mice. *American Society for Nutritional Sciences*, 2125-2130.

Tsuzuki T (2009). Commercial scale production of inorganic nanoparticles. *International Journal of Nanotechnology (IJNT)*, 6.

Turkevich J, Stevenson PC and Hillier J (1951). A study of the nucleation and growth processes in the synthesis of colloidal gold. *Discussions of the Faraday Society*, 11, 55–75.

Vijayakumar S and Ganesan S (2012). *In vitro* cytotoxicity assay on gold nanoparticles with different stabilizing agents. *Journal of Nanomaterials*, 2012.

Vijayakumar S, Vaseeharan B, Malaikozhundan B, Gopi N, Ekambaram P, Pachaiappan R, Velusamy P, Murugan K, Benelli G, Suresh Kumar R and Suriyanarayanamoorthy M (2017). Therapeutic effects of gold nanoparticles synthesized using *Musa paradisiaca* peel extract against multiple antibiotic resistant *Enterococcus faecalis* biofilms and human lung cancer cells (A549). *Microbial Pathogenesis*, 102, 173–183.

Xin Lee K, Shameli K, Miyake M, Kuwano N, Bt Ahmad Khairudin NB, Bt Mohamad SE and Yew YP (2016). Green synthesis of gold nanoparticles using aqueous extract of *Garcinia mangostana* fruit peels. *Journal of Nanomaterials*, 2016, 1–7.

Xue H, Shi T, Wang F, Zhou H, Yang J, Wang L, Wang S, Su Y, Zhang Z, Qiao Y and Li X (2017). Interval mapping for red/green skin color in Asian pears using a modified QTL-sequence method. *Horticulture Research*, 4.

Yang Y, Yao G, Zheng D, Zhang S, Wang C, Zhang M and Wu J (2015). Expression differences of anthocyanin biosynthesis genes reveal regulation patterns for red pear coloration. *Plant Cell Reports*, 34, 189-198.

Yin R, Li T, Tian JX, Xi P and Liu RH (2018). Ursolic acid, a potential anticancer compound for breast cancer therapy. *Critical Review in Food Science and Nutrition*, 58, 4, 568-574.

Wang ZL (2001). Characterisation of nanophase materials. *Particle & Particles Systems Characterization*, 18, 142-165.

Wang J, Zhang G, Li Q, Jiang H, Liu C, Amatore C and Wang X (2013). *In vivo* self-bio-imaging of tumors through *in situ* biosynthesized fluorescent gold nanoclusters. *Scientific Reports*, 3, 1157.

Wang Z, Meng D, Wang A, Li T, Jiang S, Cong P and Li T (2013). The methylation of the *PcMYB10* promoter is associated with green-skinned sport in max red Bartlett pear. *Plant Physiology*, 162, 885-896.

Zhou Y, Kong Y, Kundu S, Cirillo JD and Liang H (2012). Antibacterial activities of gold and silver nanoparticles against *Escherichia coli* and bacillus Calmette-Guérin. *Journal of Nanobiotechnology*, 10, 1-9.

Zhu J, Kónya Z, Puentes V, Kiricsi I, Miao CX, Ager J, Alivisatos A and Somorjai G (2003). Encapsulation of metal (Au, Ag, Pt) nanoparticles into the mesoporous SBA-15 structure. *Langmuir*, 19, 4396–4401.

